University of Nevada

Reno

STRUCTURAL, TECTONIC AND QUATERNARY STUDY OF THE EASTERN MADELINE PLAINS, CALIFORNIA AND SOUTHWESTERN SMOKE CREEK DESERT, NEVADA

A Thesis submitted in partial fulfillment
of the requirement for the degree of
Master of Science in Geology

by

Rodney J. Weick

December 1990

The thesis of Rodney J. Weick is approved:

Thesis Advisor

Department Chairman

Dean, Graduate School

University of Nevada

Reno

December 1990

ABSTRACT

A structural, tectonic and Quaternary study of the eastern Madeline Plains (MP) and southwestern Smoke Creek Desert (SCD) in northeastern California and northwestern Nevada indicates that: 1) the Likely fault zone (LFZ) may be the northeastern limit of the Walker Lane (WL), 2) the WL appears to step right to the LFZ in the eastern Honey Lake Valley (HLV)/southwestern SCD area of California and Nevada, 3) a structural block defined by the Honey Lake Fault (HLF) and the northern extension of the WL on the west, easternmost HLV/southwestern SCD on the south, and the LFZ, Dry Valley-Smoke Creek Ranch fault zone (DV-SCRFZ) and the Bonham Ranch fault zone (BRFZ) on the east may be migrating toward the northwest, and 4) eastern HLV and southwestern SCD may be a young pull-apart basin forming along the trailing edge of the northwest migrating block.

Pluvial deposits of <5,000 years have been displaced along the LFZ in eastern MP. Pluvial deposits of <12,000 years have been displaced along the right-oblique-slip DV-SCRFZ and BRFZ in southwestern SCD. Fault scarp profiles along the BRFZ show two tectonic events in the past 12,000 years; the most recent occurred about 290 ± 70 years B.P. This event resulted in about 40 km of surface rupture length and a maximum of 2.9 m of vertical displacement. Surface magnitudes of M_s 7.0 and M_s 7.3 for the 290 ± 70 years B.P. event were estimated using the regression curves, respectively, of Slemmons and others (1989) and Bonilla and others (1984).

TABLE OF CONTENTS

	Page
ABSTRACT	i
ACKNOWLEDGEMENTS	viii
INTRODUCTION	1
Geographic Location and Setting of Study Area	3
Human Activity	5
Topographic Coverage	5
Physiographic Setting	6
Literature Search and Previous Work	6
Remote Sensing Imagery and Aerial Photography	8
Field Mapping	10
STRATIGRAPHY	12
Mesozoic Stratigraphy	12
Tertiary volcanic and volcaniclastic rocks	14
Dacites plugs, flows, and flow breccias (Trd)	14
High Rock sequence (Tts)	15
Upper Miocene and Pliocene basalts (Tba)	21
Quaternary Stratigraphy	26
Quaternary basalts (Qba)	26
Pre-Lake Lahonton sediments (Qpl, Qpg)	28
Alluvial fan deposits	29
Older alluvial fans (Qf1, Qf1-2)	33
Intermediate alluvial fans (Qf2, Qf2-3)	34

Young alluvial fans (Qf3) 35

Landslide deposits (Qls) 35

Lake Lahonton and Post-Lake Lahonton deposits (Ql) 36

Playa deposits (Qp) 42

Alluvium (Qalo, Qal) 44

Talus deposits (Qt) 42

Eolian deposits (Qsd, Qes) 44

STRUCTURAL AND TECTONIC ANALYSIS 46

Quaternary Faults 46

Madeline Plains area 46

Likely fault zone 47

Normal faults 52

Smoke Creek Valley area 55

Smoke Creek Desert area 57

Dry Valley - Smoke Creek Valley fault zone 57

Bonham Ranch fault zone 60

Recency of Faulting 65

Lake Lahonton stratigraphy and chronologies 66

Fault scarp profiling 71

Radiometric age dates 80

Tectonic Analysis 86

CONCLUSIONS 109

REFERENCES 113

APPENDIX A FAULT SCARP PROFILES 127

LIST OF TABLES

Table		Page
1	Summary of carbon sample age dates	83
2	Diffusion parameters	85

LIST OF FIGURES AND PLATES

Figure		Page
1	Map showing the regional topography and geographic boundaries of the study area in northeastern California and northwestern Nevada	4
2	Photograph showing metacarbonate outcrop at the mouth of Thomas Canyon in T29N, R19E, Sec. 19 of the Dry Valley area in Smoke Creek Desert	13
3	Photograph showing pyroclastic rocks the High Rock sequence (Tts) in T29N, R19E, Sec. 25 near Thomas Canyon in the Dry Valley area of Smoke Creek Desert	17
4	Photograph showing diatomaceous and tuffaceous sediments of the High Rock Sequence in the Smoke Creek Reservoir spillway	19
5	Photograph of diatomaceous beds of the High Rock sequence (Tts) west of T32N, R20E, Sec. 31 in Smoke Creek Desert	20
6	Photograph of Miocene lacustrine sediments correlative to the High Rock Sequence (Tts) of Bonham (1969)	22
7	Photograph of a typical stratovolcano (Observation Peak) and upper Miocene-Pliocene basalts (Tba)	23
8	Typical Upper Miocene-Pliocene basalt fissure dikes showing columnar jointing and radial pattern at top of the dike	24

9	Photograph showing Quaternary basalt flows in Smoke Creek Valley	27
10	Photograph showing a pre-Lake Lahonton fanglomerate deposit (Qpl) in Smoke Creek Desert	30
11	Pleistocene pedisediments (Qpg) cap pre-Lake Lahonton deposits (Qpl) north of Smoke Creek	31
12	Pedisediments on a ballena in west-central Smoke Creek Desert north of Smoke Creek	32
13	Trego Hot Springs (THS) and Wono (W) tephra layers crop out in Sehoo Alloformation lacustrine silt and clay deposits near the playa margin in southwestern Smoke Creek Desert	39
14	Fallon Alloformation Disconformably overlies Sehoo Alloformation Lake Clays near Smoke Creek	41
15	Typical playa deposits (Qpa) in southwestern Smoke Creek Desert	43
16	Low sun angle aerial photograph showing the trace of Fault D and E of the Likely fault zone in Holocene Fallon Alloformation equivalent deposits in eastern Madeline Plains	51
17	Mosaic of low sun angle aerial photographs that show Fault Zone G which borders the eastern margin of Madeline Plains	54
18	Low sun angle aerial photograph mosaic that shows the Smoke Creek fault zone (SCFZ) in Miocene-Pliocene basalt flows in central Smoke Creek	57
19	Overview of southwestern Smoke Creek Desert (SCD) and Dry Valley (DV), Nevada	59
20	Several parallel to subparallel fault splays of the Bonham Ranch fault zone (BRFZ) displace uppermost Pleistocene and Holocene Lake Lahonton sediments (Ql) and Tertiary basalts (Tba)	61
21	Schematic diagram showing the Quaternary stratigraphy, pluvial cycles and chronology of Lake Lahonton	68

22	Distribution of the major pluvial lakes during the Late Pleistocene pluvial maximum	70
23	Photograph showing a typical Bonham Ranch fault zone scarp in Smoke Creek Desert	73
24	Comparison of linear regression best-fit lines of alluvial fans, gravelly sands and lake clays cut by faults in Smoke Creek Desert	78
25	Graben infill deposits at the toe of the BRFZ fault scarp in T30N, R19E, Sec. 15 exposed in a channel cut	81
26	Simplified map showing the western termination of the Basin and Range Province by strike-slip faults	87
27	Diagrammatic sketch illustrating the spatial relationship of the Likely fault zone and the Walker Lane in northwestern Nevada and northeastern California	90
28	Generalized area of the northern extension of the Walker Lane Belt in northeastern California	93
29	Simplified fault map of southwestern Smoke Creek Desert, Nevada and Madeline Plains, California	95
30	Space shuttle SIR-A imagery of Pyramid Lake, Nevada and southern Honey Lake Valley, Nevada and California delineating the Warm Springs fault and Pyramid Lake fault of the Walker Lane	97
31	Generalized geologic map of the vicinity of Nevada Line 8	102
32	Modified schematic representation of COCORP interpretations of Nevada Line 8	103
33	Geologic map of U.S. Geological Survey seismic refraction lines in northeastern California	104
34	Geologic cross section along the east-west seismic refraction line in northeastern California	105

Plates

1	Geologic Maps of the Madeline Plains, California, and Smoke Creek Desert Region of Northeastern California and Northwestern Nevada	In Pocket
2 and 3	Geologic map of a Portion of Smoke Creek and southwestern Smoke Creek Desert, Nevada	In Pocket
4 and 5	Geologic map of a portion of southwestern Smoke Creek Desert, Nevada	In Pocket

ACKNOWLEDGEMENTS

I would like to take this opportunity to thank the members of my thesis committee Dr. R. A. Schweickert, Dr. F. F. Peterson, and committee chairman Dr. D. B. Slemmons, under whose support and guidance this thesis was completed. Partial research funding was provided by grants from Sigma Xi, Chevron USA, and the Mackay School of Mines. The staff of the Susanville, California, BLM office provided maps and aerial photographic coverage of the study area. I thank Leighton and Associates, Inc. for funding the radiocarbon age dates and providing support and time away from work to complete the thesis. I appreciate and thank E. J. Hanford (Bell) and R. A. Whitney for their field assistance. Discussions with T. L. T. Grose of the Colorado School of Mines, R. A. Whitney of Leighton and Associates, Inc., and E. J. Hanford (Bell) of Science Applications International Corporation improved my understanding of Late Cenozoic tectonics, regional geology and Quaternary geology of the northern segment of the Walker Lane in northwestern Nevada and northeastern California. Most importantly, I thank my wife, Jeani Crichlow, whose patience, support, and inspiration made this study possible.

INTRODUCTION

The Likely fault zone (LFZ) is a major structural feature in northeastern California that shows right-slip displacement of Tertiary volcanic units and Quaternary lake deposits. Data for the LFZ has mostly been limited to regional and reconnaissance investigations (Gay and Aune, 1958; Lydon et al., 1960; Iwamura and Hill, 1961). Gay and Aune (1958) and Lydon et al. (1960) mapped the LFZ from near Ambrose Siding, California, (T42N, R15E) to the northern border of eastern Madeline Plains (T35N, R15E). Iwamura and Hill (1961) projected the fault zone across Madeline Plains to Observation Peak. The mapped and projected length of the LFZ is approximately 100 kilometers (km). Regional and reconnaissance studies by Dodge (1980), Dodge and Grose (1980), and Bell and Slemmons (1982) suggested that the LFZ may extend southeastward into Smoke Creek Desert (SCD), Nevada.

As part of the right-slip tectonic system that includes the Walker Lane, which terminates the western margin of the Basin and Range Province, the LFZ is recognized as a major structural feature (Lawrence, 1976; Wright, 1976; Stewart, 1983). The purpose and objectives of this study are to provide geologic evidence for the postulated southeastward extension of the LFZ (Dodge, 1978; Bell, 1981; Bell and Slemmons, 1982)

and to evaluate the tectonic relationship between the Likely and Walker Lane fault zones. The criteria to achieve these objectives are:

1. Define the southern limit of the LFZ.
2. Evaluate the character and activity of faulting in the region between the presently mapped limits of the LFZ and Smoke Creek Desert.
3. Define and evaluate the tectonic activity along the western margin of Smoke Creek Desert and its relationship to the LFZ.
4. Interpret the relationship between the LFZ and the Walker Lane, as well as its role in the right-slip tectonic system that terminates the western margin of the Basin and Range.

To accomplish the objectives of this study, the following tasks were performed:

1. Compile pertinent published and unpublished literature and evaluate the data presented in these publications.
2. Interpret and analyze stereoscopic aerial photography, including low-sun angle (LSA) photography that covered a portion of the study area.
3. Interpret remote sensing imagery of the study area.

4. Map faults of the study area and ground check the geologic units and geomorphic features observed on the aerial photographs and remote sensing imagery.
5. Compile geologic maps at scales of 1:62,500 and 1:24,000 of the study area, incorporating previous geologic mapping by others and the work of this study.

Geographic Location and Setting of Study Area

The study area is 3,538 square km (1,340 square miles) within northeastern California and northwestern Nevada (Figure 1). Access to the east Madeline Plains area and Smoke Creek, north of Smoke Creek Reservoir, is from U.S. Highway 395 at Ravendale and Termo, California. The primary access roads in east Madeline Plains are paved and unpaved roads of good quality. All other roads, except for the road to Dodge Reservoir, are unpaved and generally poor to very poor quality.

The southwestern portion of Smoke Creek Desert and Smoke Creek Valley south of Smoke Creek Reservoir are accessed by unpaved, well-maintained roads from Gerlach and Sutcliffe, Nevada. The area is accessible from U.S. Highway 395 through Wendel, California. The unpaved road between Madeline Plains and Smoke Creek Desert is no longer through-going to Smoke Creek Reservoir. Except for the primary access roads, road conditions generally require four-wheel drive vehicles. Most of Madeline Plains and portions of Smoke Creek Desert are in

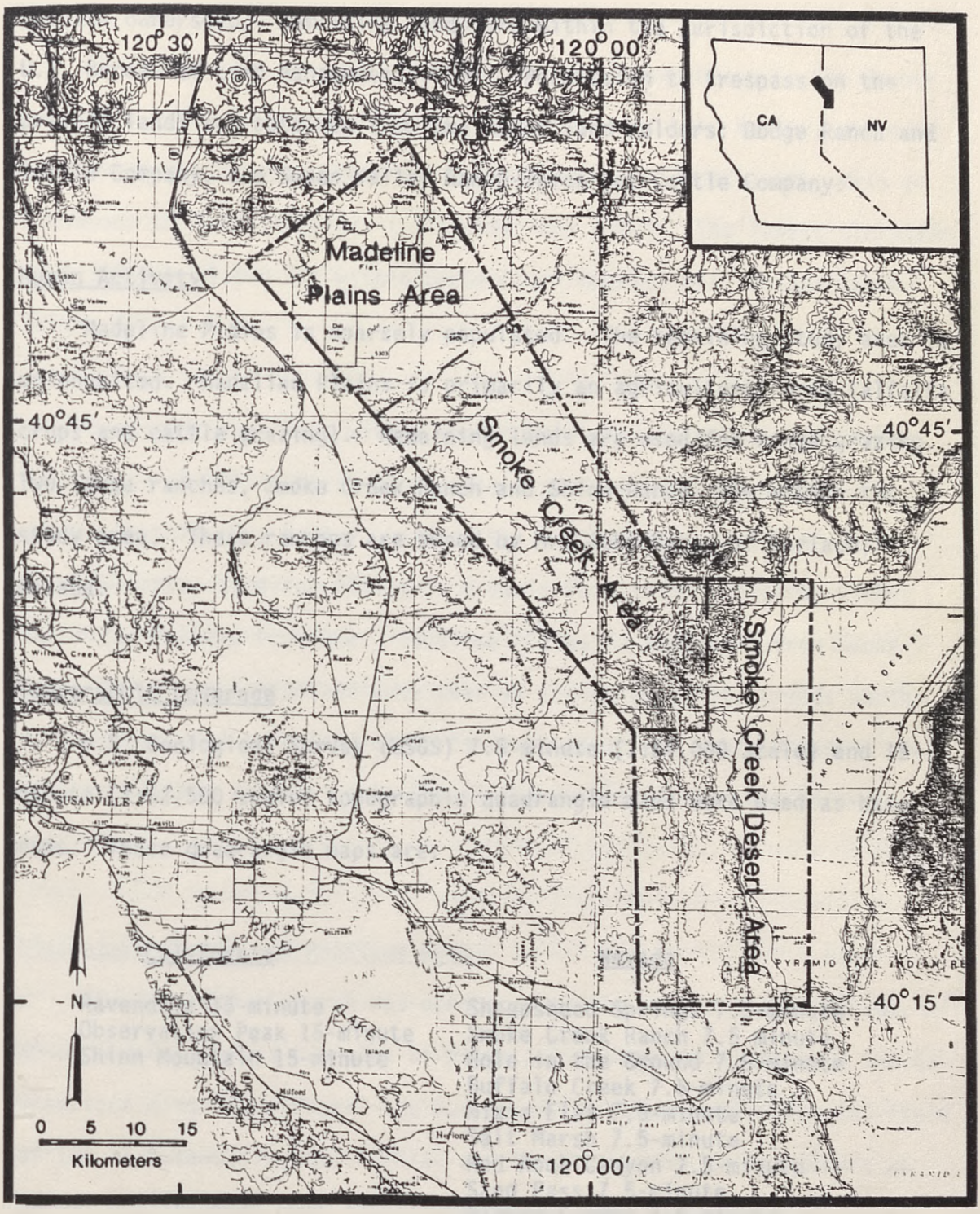

Figure 1. Map showing the regional topography and geographic boundaries of the study area in northeastern California and northwestern Nevada.

private ownership. Remaining lands are within the jurisdiction of the U.S. Bureau of Land Management (BLM). Permission to trespass on the private lands was obtained from the major land holders: Dodge Ranch and Cattle Company, and Susan Valley Ranch-Three Dot Cattle Company.

Human Activity

Madeline Plains is sparsely populated. The remaining study area is uninhabited. Madeline Plains is primarily an agricultural area (alfalfa crops and cattle grazing). Remaining lands are used for range grazing. Two large ranches, Smoke Creek Ranch and Shinn Ranch, are within the study area. These ranches are owned by Mr. John Casey of Gerlach, Nevada.

Topographic Coverage

U.S. Geological Survey (USGS) 7.5-minute (1:24,000 scale) and 15-minute (1:62,500 scale) topographic quadrangle maps were used as base maps. These quadrangle maps are:

California	Nevada
Ravendale 15-minute	Sheepshead Springs 7.5-minute
Observation Peak 15-minute	Smoke Creek Ranch 7.5 minute
Shinn Mountain 15-minute	Hole in the Ground 7.5-minute
	Buffalo Creek 7.5-minute
	Mixie Flat 7.5-minute
	Salt Marsh 7.5-minute
	Red Rock Canyon 7.5-minute
	Sand Pass 7.5-minute
	Parker Canyon 7.5-minute

Physiographic Setting

The study area is bounded on the north and northeast by the Warner Mountains, west by stratovolcanos, south by Honey Lake Valley, and east by Smoke Creek Desert. Observation Peak is the highest point, with an elevation of 2,427.4 meters (m) (7,964 feet (ft)). The lowest elevation is 1,182.6 m (3,880 ft) within Smoke Creek Desert, near Bonham Ranch (Plate 5).

The study area lies within the Modoc Plateau and Basin and Range provinces. A tilted horst block with a smaller internal horst and graben feature (Dry Valley) borders the southwestern margin of Smoke Creek Desert. Madeline Plains is a basin that trends westerly within the Modoc Plateau Province. Madeline Plains is separated from Smoke Creek Desert by a highland area that is tilted westerly, trends north-to northwest and comprised of Tertiary volcanic and volcanoclastic rocks (Figure 1) that appears to be the southern extension of the Warner Mountains.

Literature Search and Previous Work

The literature search was conducted at the University of Nevada, Reno, the California Division of Mines and Geology in Sacramento and San Francisco district offices, the Bureau of Land Management district field office in Susanville, California, and the University of California at Irvine, California. The literature review continued throughout the

course of the study. Pertinent new publications were incorporated into the study.

Most literature relating to northeastern California and northwestern Nevada discusses petrology and chronology to the extensive sequence of volcanic rocks. Literature pertaining to the tectonics of the region is limited. Research of active faults within this study region were by Bonham (1969), Wallace (1977, 1978a, 1978b), Dodge (1978), Dodge and Grose (1980), Bell (1981), Roberts and Grose (1982), and Bell and Slemmons (1982).

Published regional geologic maps of the study area and nearby regions are the California Division of Mines and Geology geologic maps at a scale of 1:250,000 prepared by Gay and Aune (1959), Lydon et al. (1960), California Department of Water Resources geologic map of the Madeline Plains (Hill et al., 1961), and the Nevada Bureau of Mines geologic map of Washoe County at a scale of 1:250,000 (Bonham, 1969). Dodge (1978) mapped a portion of west-central Smoke Creek Desert at a scale of 1:24,000. The geologic maps by Gay and Aune (1959), Lydon et al. (1960), and Bonham (1969) provides complete regional coverage of the study area. Regional geophysical and limited seismological data of Hill et al. (1961), Thompson and Burke (1974), Eaton et al. (1978), Mohler (1980), and Grose and McKee (1982) were used in this study. The northern portion of this study area in Smoke Creek Desert overlaps the area mapped by Dodge (1978) which was included in this study.

Remote Sensing Imagery and Aerial Photography

NASA, Skylab, LANDSAT, and Space Shuttle SIR-A imagery were used for mapping faults and lineaments within the study area. NASA and SIR-A provided black and white imagery of the study area. NASA imagery consisted of three frames with approximately 15 percent cloud cover. The thin cloud cover diffused detail over Smoke Creek. The SIR-A imagery consisted of two side-looking radar generated reflection strips. Each strip covered a ground surface width of 50 km. SIR-A imagery did not cover Madeline Plains. LANDSAT imagery consisted of pre-EDIPS and post-EDIPS color composites. EDIPS is a computer enhancing process that produces greater clarity. However, the post-EDIPS enhanced imagery only provided coverage of northeastern California, a portion of northern Nevada, and southern Oregon. The post-EDIPS imagery did not cover the Smoke Creek Desert portion of the study area. The pre-EDIPS enhanced imagery covered northeastern California and northwestern Nevada.

Conventional and low-sun angle aerial photographs were reviewed and analyzed to map the geology and geomorphic features of the study area. Aerial photography sources included the U. S. Geological Survey (USGS), the California Division of Mines and Geology (CDMG), the Bureau of Land Management (BLM), and the U.S. Department of Agriculture (USDA). These photographs provided black and white and color coverage of the entire study area at various scales. A low-sun angle (LSA) aerial photographic flight was flown as part of this study to obtain black and white photographs at an approximate scale of 1:18,000 to emphasize fault

scarps. The study area was mapped in detail from the aerial photographs and field mapped to check geology and geomorphic features observed on the photographs.

The LSA aerial photographs were taken under morning, low-sun angle conditions on October 2, 1982. Coverage was limited to the Madeline Plains and Smoke Creek Valley area. The aircraft was a turbocharged Cessna 206 with a 9-inch by 9-inch, in-cabin mounted K-17 military camera equipped with a 6-inch lens. The camera was actuated by an electrical switch and manually leveled. Frame intervals calculated for photographic scale, aircraft velocity, and 60 percent forelap were timed by an automatic resetting stopwatch. Photographs were taken on Kodak Tri-X (#2405) high speed black and white aerographic film. A total of 123 LSA prints of good to excellent quality were obtained. The LSA aerial photographs are in the archives at the Center for Neotectonic Studies, Mackay School of Mines, University of Nevada, Reno.

Color infrared (IR) photography consisted of positive transparency strips at a scale of approximately 1:34,000. Coverage was limited to the Madeline Plains area. Tonal changes observed on IR photographs facilitated identification of Quaternary geologic units and geomorphic features not readily visible on standard photographs.

Stereographic analysis of the aerial photography was made using a Wild ST-4 and an Abrams CB-1 stereoscope. Structural features, springs

and seeps, surficial deposits, and bedrock units were delineated on mylar overlays that were placed on alternate photographic frames. The observed features were then manually transferred to the base maps (Plates 1 to 5).

Remote sensing images were used to identify regional lineaments and structural trends. Prominent geologic features, i.e. faults, major joint patterns, and gross lithologic types were identified. These features were used as a guide for structural features on the aerial photography, and the compilation of a regional structural synthesis.

Field Mapping

Geologic field mapping consisted of ground verification of structural features and selected surficial deposits observed on the aerial photographs and images. Alluvial fan deposits, geomorphic feature identification, and terminology were adapted from Carr et al. (1978, 1979), Hooke (1965), Hoover (1981), Ritter (1978, 1979) and Peterson (1981). Other Quaternary deposits nomenclature were adapted from Morrison and Frye (1965) and Davis (1978a). Bedrock units were grouped and included Tertiary and Quaternary volcanic rocks consisting of basalt, rhyolite, and pyroclastic rocks. Bedrock types were field checked at selected sites. Petrographic identification was limited to hand samples examined with a 10-power hand lens. Detailed petrographic description of bedrock was not within the scope of this study; principal focus was the Quaternary geology and faults. Bedrock lithologies were

by Bonham (1969), Gay and Aune (1959), Lydon et al. (1960), and Dodge (1978).

Fault scarps were field checked by walking traces observed on photographs. Fault scarp profiles were measured at selected locations. Fault scarp profiling methods, analysis and terminology were adapted from methods of Bucknam and Anderson (1979) and Wallace (1977).

STRATIGRAPHY

Mesozoic Stratigraphy

Bonham (1969) and Dodge (1978) mapped Permo-Triassic metasedimentary and metavolcanic rocks, and Cretaceous granodioritic rocks north and east of the study area. Pre-Cenozoic rocks were mapped near Thomas Canyon (Plate 5) in R18E, T29N, Sec. 25. Pre-Cenozoic rocks have not been identified in the portion of the study area in northeastern California.

Outcrops of metasedimentary rocks occur at the mouth of Thomas Canyon and extend about 1,220 m (4,000 feet) south at the base of the bluff (Plate 5). At Thomas Canyon, the marble is gray to light-gray with near-white bands (Figure 2). Some cross-banding is present and appears to represent in-filled fractures. The marble is altered at the unconformable contact with an overlying ash-flow tuff breccia. Fold axes in the marble trend N50° to 60°W. Layering, in general, strikes N55°W and dips 85° north and south to vertical. However, folds are not expressed and appear to be absent in outcrops south of Thomas Canyon. In that area possible relict bedding strikes N15° to 20°W, with dips 45° to 50° east.

Triassic-Jurassic limestone and dolomite occur in the Fox Range (eastern boundary of Smoke Creek Desert) in the Nightingale sequence and within the Peavine sequence north of Reno, Nevada (Bonham, 1969). The

Figure 2. Photograph showing possible marble outcrop at the mouth of Thomas Canyon in T29N, R19E, Sec. 19 of the Dry Valley area in Smoke Creek Desert. Grose (personal comm.) has visually identified this outcrop as a Tertiary perlitic intrusive dome.

marble near Thomas Canyon is similar to Bonham's (1969) description of the Nightingale and Peavine sequences. Therefore, it is assumed the marbles within the study area are Triassic-Jurassic in age.

Grose (personal comm., 1990), based on his visual observations, suggests these marble rocks are exposures of an intrusive dome with flow bands. Therefore, Grose suggests a Tertiary age for these rocks.

Tertiary volcanic and volcaniclastic Rocks

Tertiary volcanic and volcaniclastic rocks are extensive throughout northeastern California and northwestern Nevada and comprise the Tertiary rocks within the study area. These rocks include basalts, andesitic basalts, andesites, rhyolites, and pyroclastic rocks, including ash-flow tuffs. Bonham (1969) mapped these volcanic and volcaniclastic rocks in the Smoke Creek Desert region as part of the Canyon Assemblage. Formational names were not assigned to these areally extensive rocks in Nevada (Bonham, 1969) and in northeastern California (Gay and Aune, 1959; Lydon and Others, 1960).

Dacite plugs, flows, and flow-breccias (Trd). Dacite flow-breccias of very limited areal extent and an isolated plug were mapped near Burro Mountain from the aerial photographs. These dacite rocks are located on the east flank of Burro Mountain in T31N, R19E, Sec. 21 and 22 (Plate 3) and were not field checked.

Dacitic rocks in the study area described by Bonham (1969) and Dodge (1978) have hornblende and plagioclase laths in a dense, light gray groundmass. Phenocryst laths average about 2 millimeters (mm) and occur as long as 6 mm. Phenocrysts of plagioclase, hornblende, alkali feldspars, and quartz average 4 to 6 mm in size. Dodge described the groundmass of the plug as variable in color from light gray to pink buff.

No formational name has been applied to these isolated dacitic rocks in the study area. Bonham (1969, p. 10) included dacite flows and breccia flows as part of the South Willow Formation, which he correlated with 31 Ma rocks in Hays Canyon (Bonham, 169, p. 12 and 131). Lithologic description of the dacite rocks within the study provided by Dodge (1978) are similar to the South Willow Formation and may be correlative. Dacite rocks in the study area appear to be the oldest Tertiary rocks.

<u>High Rock Sequence (Tts)</u>. Undifferentiated units of the upper Miocene to lower Pliocene High Rock sequence in the study area consist of ash-flow tuffs, air-fall tuffs, and fluviolacustrine deposits including diatomite and diatomaceous tuffs. Bonham (1969, p.15-20) described the High Rock sequence in the Smoke Creek Desert region as "... a moderately

thick sequence of ash-flow tuffs, tuffaceous fluviolacustrine deposits, and mafic tuffs and flows..." which typically has a "...marked angular unconformity..." with various older rocks, and is "...separated from overlying upper Miocene to Pliocene basalts by a disconformity." The bulk of the High Rock sequence, as described by Bonham, consists of ash-flow and ash-fall tuffs with abundant pumice lapilli "...locally constituting 90 percent or more of the tuff." The fluviolacustrine deposits are typically well-stratified tuffs and very thinly bedded diatomite and diatomaceous tuffs.

Rocks of the High Rock sequence crop out at three locations in the Smoke Creek Desert (Plates 2, 3, and 5) and within eastern Madeline Plains (Plate 1) where they were mapped as Miocene pyroclastic rocks by Lydon and others (1960). These rocks consist of ash-flow and ash-fall tuffs, and lacustrine tuffs and diatomite.

South of Thomas Canyon in T29N, R19E (Plate 5), rocks of the High Rock sequence occur at the base of the near-vertical bluffs (Figure 3). Three distinct units are exposed in the outcrop. The lower unit is a light to medium gray, massive to very crudely bedded, poorly sorted fluvial deposit. Clasts are subrounded to rounded and range in size from pebble to small boulder. Clasts are principally volcanic and occur

Figure 3. Photograph showing pyroclastic rocks of the High Rock sequence (Tts) in T29N, R19E, Sec. 25 near Thomas Canyon in the Dry Valley area of Smoke Creek Desert.

within a fine-grained tuffaceous sand matrix. The unit unconformably overlies Triassic-Jurassic marble rocks and is disconformably overlain by the middle and upper units of ash-flow tuff and air-fall tuff. The middle and upper units of the High Rock sequence near Thomas Canyon consist of light brown and gray to pink-gray ash-flow tuff and air-fall tuffs.

Clasts predominantly consist of pumice (visually 70 percent of clasts) and andesitic rocks. The maximum clast size observed was 15 cm. The ash-flow tuff is poorly sorted and stratified, that fines upward. Estimated thickness of the High Rock sequence near Thomas Canyon is 70 m. The units disconformably underlie upper Miocene to Pliocene basalts.

Very thinly bedded to laminated diatomite, intercalated with tephra, crops out in the Smoke Creek Reservoir spillway west of T32N, R19E, Sec. 31 (Plate 2 and Figure 4) and west of T32N, R20E, Sec. 31 in Smoke Creek Desert (Plate 3 and Figure 5). The exposed thickness of these units is 2.4 m and 3 m, respectively. Both outcrops are unconformably overlain by Lake Lahonton deltaic deposits.

Miocene pyroclastic rocks were mapped by Gay and Aune (1959) and Lydon and others (1960). These rocks crop out along the eastern margin of Madeline Plains and Dodge

Figure 4. Photograph showing diatomaceous and tuffaceous sediments of the High Rock sequence (Tts) exposed in the Smoke Creek Reservoir spillway. Other units are dam embankment fill (Fill) and Quaternary basalts (Qba). View is toward the northeast.

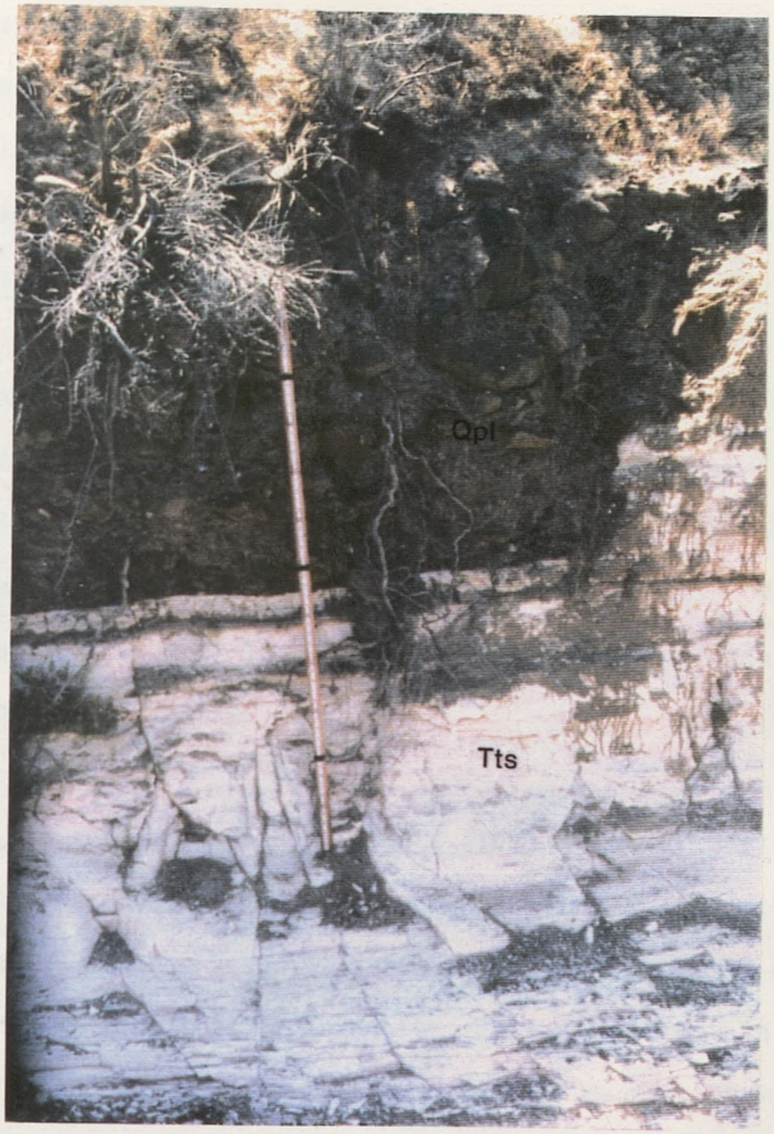

Figure 5. Photograph of diatomaceous beds of the High Rock sequence (Tts) west of T32N, R20E, Sec. 31 in Smoke Creek Desert. Pre-Lake Lahonton fanglomerate (Qpl) unconformably overlies the diatomaceous beds.

Reservoir. Lydon and others (1960) described these rocks as "...light colored hornblende and pyroxene andesite breccia, mudflow breccia, conglomerate, and tuff...solfatarized rhyolite tuff...pumiceous lapilli tuff, ash-beds, and diatomaceous beds in the Madeline Plains area." These Miocene pyroclastic rocks are correlative with and similar in description to the High Rock sequence of Bonham (1969). Figure 6 shows an outcrop of the High Rock sequence in Madeline Plains. Pumice and volcanic rock clasts shown in Figure 6 range up to 7.6 cm in size. Bedding is moderately defined and fines upward to well bedded silts. Cross-bedding is evident within some individual layers. Upper Miocene and Pliocene basalts disconformably overlie these rocks. Maximum exposed thickness of the High Rock Sequence in Madeline Plains is approximately 30 m.

Upper Miocene and Pliocene Basalts (Tba). Upper Miocene and Pliocene basalt flows erupted from numerous small shield volcanoes, central vents, and fissure dikes (Figures 7 and 8), and are the most areally extensive Tertiary unit within the study area. The basalts are commonly olivine rich, have diktytaxitic interiors and scoriaceous surfaces. Dodge (1978, p. 17) described these rocks as "...20 percent olivine, 10 percent olivine altered to iddingsite, 10 percent augite, and

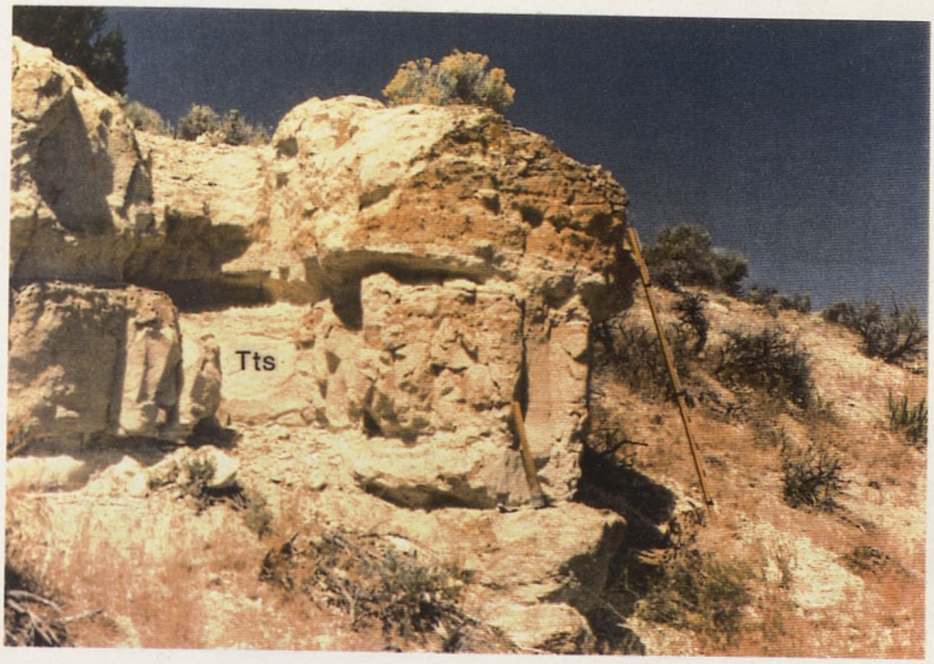

Figure 6. Photograph of Miocene lacustrine sediments correlative with the High Rock sequence (Tts) of Bonham (1969). The outcrop is located in T34N, R16E, SE¼ Sec. 24 of eastern Madeline Plains.

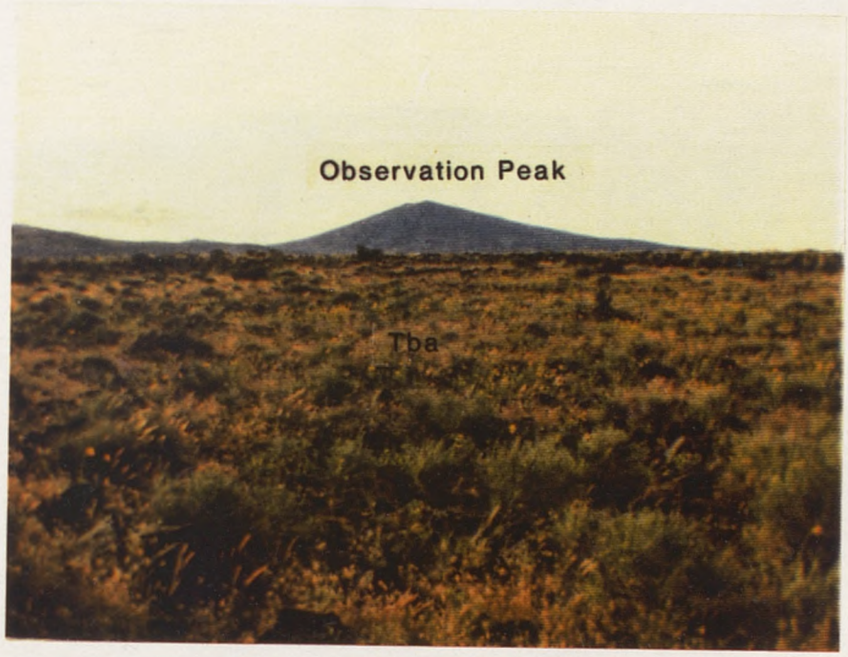

Figure 7. Photograph showing a typical stratovolcano (Observation Peak) and upper Miocene-Pliocene basalts (Tba).

Figure 8. Typical upper Miocene-Pliocene basaltic fissure dike showing columnar jointing and radial pattern at top of the dike. Several basalt dikes in Smoke Creek Valley have radial flow patterns and columnar jointing similar to this dike. View is to the southeast along the western margin of Smoke Creek Desert.

2 percent sphene, in a matrix of 40 percent plagioclase and 10 percent glass material."

These basalts have no formational name and are co-extensive with Tertiary basalts in northwestern Nevada, northeastern California, and southern Oregon. Lydon et al. (1960) mapped these volcanic flows as Pliocene basalts unconformably overlying Miocene pyroclastic rocks. Based on areal distribution, close proximity of numerous source areas, and lithologic similarities, the Pliocene basalts of Lydon et al. (1960) have been mapped as upper Miocene and Pliocene basalts (Tba) as described by Bonham.

A light tan to buff colored, nearly circular breccia pipe consisting of andesite and olivine basalt fragments intrudes upper Miocene and Pliocene basalts in T32N, R17E, sec. 13 near Smoke Creek Reservoir (Plate 2), east of T32N, R18E, sec. 34 (Plate 3), and in T31N, R19E, secs. 21 and 22 (Plate 3). Mineral fragments include plagioclase and biotite in an amorphous matrix. Basaltic dikes have subsequently intruded the pipe breccia in T31N, R19E, secs. 21 and 22.

Quaternary Stratigraphy

Quaternary stratigraphy and nomenclature were adapted from Lydon and others (1960), Morrison (1964), Bonham (1969), and Morrison and Davis (1984). Geomorphic nomenclature generally follows that of Peterson (1981), unless otherwise noted. Since there is a variation in nomenclature between Lydon et al. (1960) and Bonham (1969), Bonham's nomenclature was employed where lithologic and stratigraphic correlations could be made. The close proximity of Madeline Plains to late Pleistocene Lake Lahonton allows assumption that pluvial events were coeval. Therefore, upper Pleistocene units of Lake Lahonton that include the Sehoo and Fallon Alloformations of Morrison (1964; Morrison and Davis, 1984) have been correlated with similar deposits of Madeline Plains.

Mapped Quaternary units (Plates 1 through 5) consist of igneous olivine basalts (Qba), pre-Lake Lahonton sediments (Qpl and Qpg), alluvial fan deposits (Qf), undifferentiated upper Pleistocene Lake Lahonton deposits (Ql), and alluvium (Qal and Qals).

Quaternary basalts (Qba). Quaternary basalts comprised of several thick flows from a central vent in northeastern Smoke Creek Valley (Plates 1, 2 and 3) unconformably overlie upper Miocene and Pliocene basalts in Smoke Creek Valley (Figure 9). The Quaternary basalts are dark gray to gray, vesicular, and

Figure 9. Photograph showing Quaternary basalt flows (Qba) in central Smoke Creek Valley. Flows are nearly horizontal and unconformably overlie Miocene-Pliocene basalt flows (Tba). Pleistocene-Holocene lacustrine deposits of the Sehoo Alloformation (Ql) blanket the Quaternary basalt flows. Alluvial (Qal) and Sehoo deposits comprise the foreground. View is to the southwest.

diktytaxitic. Pale yellow olivine and plagioclase phenocrysts up to 3 mm in size are set in a dark gray groundmass. The upper and lower surfaces of the flows are scoriaceous. Columnar jointing within flows is moderately to well developed.

Megascopically, these basalts are similar to the 1.14 Ma McClellan Peak basalts Schilling, 1965, p. 65) and are equated by Bonham (1969) to the Lousetown Formation of Thompson and White (1964) which is 1.3 to 2.3 Ma (Bonham, 1969, p. 39 and 40). Therefore, the Quaternary basalts in the study area probably range in age from latest Pliocene to Pleistocene.

Pre-Lake Lahonton sediments. Pre-Lake Lahonton sediments typically occur as fan remnants, ballenas (Qpl), and pedisediments (Qpg) within the Smoke Creek Desert and lower Smoke Creek Valley. These sediments consist of subangular to subrounded basalt clasts in a light tan to buff and red-brown matrix of sand, silt, and clayey silt. Clasts vary in size from boulders to gravel, with the majority of clasts in the large cobble to gravel range. Near-surface and surface clasts typically have a caliche coating which acts as a cementing agent in moderately indurated soils of this unit.

Bedding within the fan remnants and ballenas is variable, ranging from thickly to thinly bedded, poorly to moderately consolidated sand and gravel, with minor intercalated tuffaceous sand (Figure 10). Observed bedding dips 6° to 9° southwest. Assuming the units were originally deposited as beds with dips of 3° to 4° northeast (toward Smoke Creek Desert basin), pre-Lake Lahonton deposits appear to be tectonically backtilted 10° to 13°.

Pedisediment deposits (Qpg) occur on geomorphic surfaces formed on the fan remnants, ballenas, and locally on erosional surfaces developed upon upper Miocene and Pliocene basalts (Figure 11). Clasts at the surface of pedisediments have two distinct sizes about 3 centimeters (cm) and 10 to 15 cm (Figure 12). These surface clasts are typically angular to subangular . Boulders within the pedisediment are areally limited in distribution and range in size about 25 to 33 cm. Most clasts exposed at surface have desert varnish. Westerly facing surfaces appear to be winnowed. Pedisediment matrix consists of a tan to buff silt that is caliche rich, and poorly to moderately indurated.

Alluvial fan deposits (Qf). Alluvial fans were grouped as oldest (Qf1), intermediate (Qf2), and youngest (Qf3). This grouping was based on geomorphology, stratigraphic relation to

Figure 10. Photograph showing a pre-Lake Lahonton fanglomerate deposit (Qpl) in Smoke Creek Desert. Channel cut in a relic fan provides cross-sectional view of poorly sorted, thickly bedded conglomerate with intercalated ash beds. Stadia rod is 1.8 m (6 feet). View is to the north.

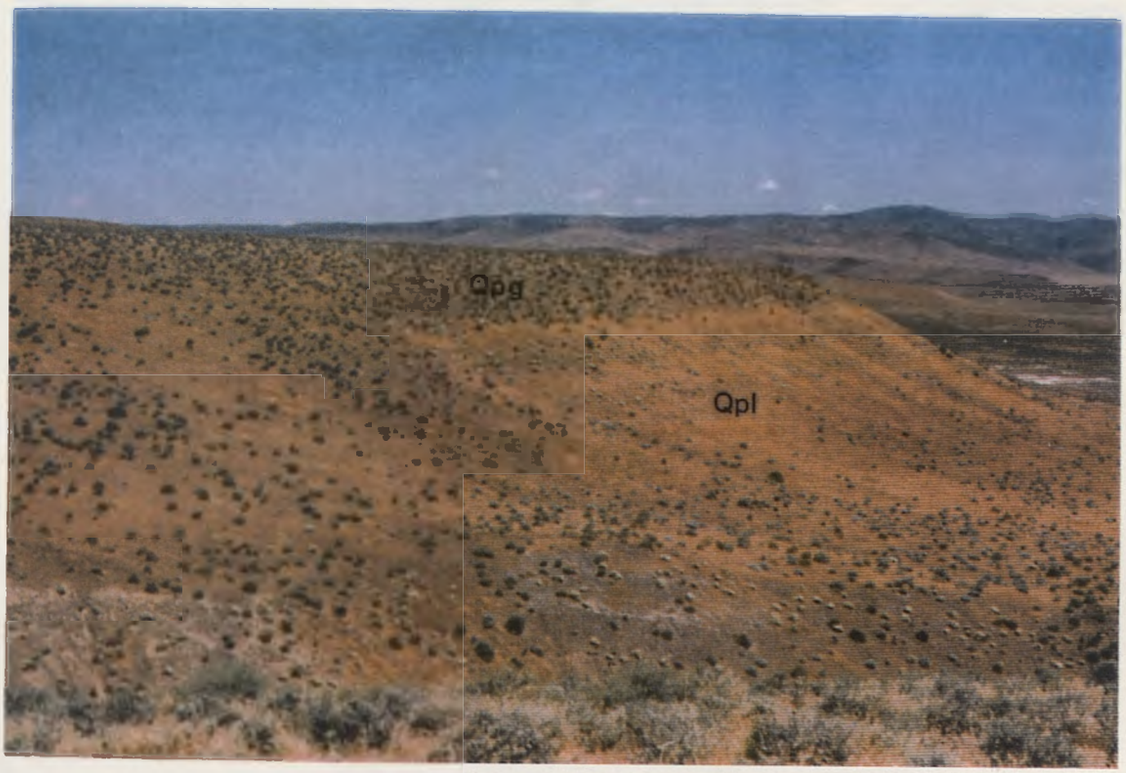

Figure 11. Pleistocene pedisediments (Qpg) cap pre-Lake Lahonton deposits (Qpl) north of Smoke Creek. View is to the east. Fox Range is in the background.

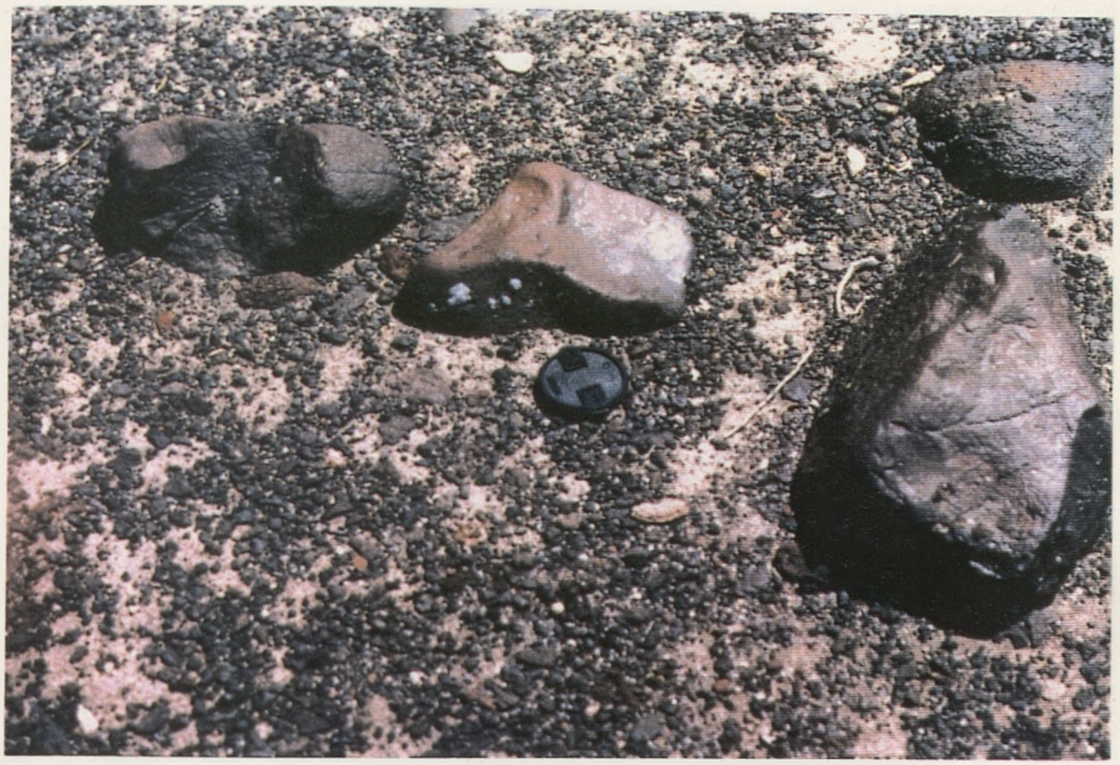

Figure 12. Pedisediments on a ballena in west-central Smoke Creek Desert north of Smoke Creek. Pedisediments in Smoke Creek Desert typically have three distinct grain sizes as illustrated in this photograph. Gravel average about 2.5 cm; cobbles average about 10-15 cm. Boulders are 25-35 cm. Matrix consists of fine sand, silt and caliche. Note the desert varnish and winnowed characteristic of the clasts.

Lake Lahonton sediments, and degree and type of fan surface dissection. Undifferentiated alluvial fan deposits (Qf) were mapped when grouping was not possible. In some cases, deposits were grouped together (Qf1-2 or Qf2-3) where individual classifications were uncertain. In general, alluvial fan deposits are composed of poorly sorted, angular to subrounded boulders to pebbles in a sand and silt matrix. Intercalated tuffaceous sand beds occur occasionally in older fan deposits (Qf1). Clasts consist of upper Miocene and Pliocene basalts. Clast size tends to decrease, sorting increases, and bedding becomes better defined with increasing distance from the fan apex. Bedding of older and intermediate fans tends to be tectonically backtilted. Most younger fans (Qf3) post-date morphologically young appearing faults. Young fans are smaller in areal extent than intermediate and older fans.

Older alluvial fans. Older alluvial fan deposits (Qf1) occur as erosional fan remnants and ballenas. On-fan surface drainage generally becomes subparallel. Relief is up to 6 m due to dissection by subparallel on-surface drainage channels. Contacts with intermediate and younger fan deposits generally occur along steep erosional side-slopes or are gradational at

the distal fan margins. Surface soils of older fan deposits are soft to moderately indurated.

Intermediate alluvial fans. Intermediate alluvial fans (Qf2) are similar to the older fans in texture, lithology and morphology. The deposits are typically poorly sorted. Channel backfill deposits are occasionally exposed in slopes of incised drainage. The drainage pattern is typically distributary and well defined. Dissection is typically less than 3 to 5 m (about 10 to 15 ft). Some drainage channels head on the fan surface. The constructional surfaces of the intermediate fans are slightly to moderately weathered. Weak soils with caliche development extend to depths of 0.3 to 0.6 m (1 to 2 ft). A distinctive desert pavement is typical on the intermediate fan surfaces. The intermediate fans are intercalated with deposits of the Sehoo Alloformation in Smoke Creek Desert and equivalent deposits in Madeline Plains.

Where intermediate fans could not be clearly distinguished from older fans, the alluvial fans were identified as older-intermediate alluvial fans (Qf1-2).

Younger alluvial fans. Young alluvial fans (Qf3) occur at the mouth of lesser canyons and drainage, and the nickpoints of faulted drainage. Young alluvial fan deposits are typically "tear drop" in shape. These fans are areally less extensive than intermediate alluvial fan deposits. Younger alluvial fan deposits are poorly sorted (boulders to silt) and have a distinct lack of bedding. Sorting is slightly better toward the distal margins. Fan surfaces lack defined drainage and dissection. Where drainage can be found, they are tributary, radiating from the fan apex. No drainage were found to head on the younger fan surfaces. Younger fan deposits are unconsolidated and unweathered, lacking in soil development.

Where younger and intermediate alluvial fans could not be clearly distinguished, they were identified as intermediate-young alluvial fans (Qf2-3).

Landslide deposits (Qls). Landslides are common in northern Washoe County, Nevada (Bonham, 1969, p. 41). They typically occur on the tectonically oversteepened volcanic range fronts. Large landslide complexes were mapped from aerial photographs and field verified at four locations within the Smoke Creek and Smoke Creek Desert regions (Plates 1, 3, and 5). The landslides consist of several slide blocks within each slide mass. Backtilted slide blocks suggest rotational failure

surfaces. Debris is chaotic and consists of basalt and tuffaceous rocks. All landslides within the study area are faulted.

The landslide failure mechanism appears related to erosional undermining of the tuffs and sedimentary rocks beneath the basalt (Bonham, 1969, p. 41). As these landslides are cut by faults and occur on tectonically oversteepened slopes, they may also be tectonically controlled.

Landslides in the study area are unconformably overlain by upper Pleistocene Lake Lahonton deposits. For older landslides in Washoe County, thorough weathering and decay occurs to depths of 6 m (20 ft) or more (Thompson and White, 1964). Bonham (1969, p. 42) suggested the degree of weathering of landslides is equivalent to the degreee of weathering associated with Sherwin age glacial deposits.

Lake Lahonton and post-Lake Lahonton lacustrine deposits (Ql). Lacustrine deposits of Pleistocene Lake Lahonton have been identified by Morrison (1964), Morrison and Frye (1965), and Davis (1978a). Dodge (1980, p. 22) classified lacustrine deposits between 1,335 m (4,380 feet) and 1,204 m (3,950 ft) as "Sehoo" and those deposits below about elevation 1,204 m (3,950 ft) as "Fallon" in the Smoke Creek Desert region. The

contact elevation between Sehoo and Fallon Alloformations is based on: 1) Fallon deposits are "post-Lake Lahonton", Holocene in age and are found below approximately 1,204 m (3,950 ft) as defined by Morrison and Frye (1965, p. 19), 2) the Sehoo deposits contain the youngest deposits of late Pleistocene Lake Lahonton (Morrison and Frye, 1965: Davis, 1982a), and 3) the last high stand of Lake Lahonton was about elevation 1332 m, before isostatic rebound (Morrison and Frye, 1965; Davis, 1982a). In the Madeline Plains region, lacustrine deposits equivalent to the Sehoo and Fallon Alloformations were mapped below approximate elevation 1,707 m (5,600 ft) and 1,637 m (5,380 ft), respectively. Madeline Plains and Smoke Creek Desert are former Pleistocene pluvial lakes separated by a tilted block of upper Miocene-Pliocene age volcanic and volcaniclastic rocks. These pluvial lakes are presumed coeval as discussed under the Recency of Faulting section, and have not contained significant amounts of water since the mid-Holocene "Fallon" highstand of Lake Lahonton (Morrison, 1965, Morrison and Frye, 1965; Davis, 1978a and 1982a).

The Sehoo and Fallon Alloformations are shown as undifferentiated Lake Lahonton deposits on Plates 1 through 5 (map symbol Ql). The Sehoo deposits primarily consist of near shore and beach sand and gravel, shallow lake sand and silt,

and deeper lake clay. Gravels consist of subangular to well rounded cobbles to pebbles. The matrix sand is poorly to moderately indurated. Sand deposits are poorly sorted. Gravel represent deltaic and long shore drift deposits. Brown to green-gray lacustrine clay and silt are found in erosional gullies cut into the playa margins and low hills created within the playa by deflation.

The Fallon Alloformation disconformably overlies the Sehoo. It typically consists of intermixed sand and silt with scattered gravel layers. The unit within the study area is typically undergoing deflation. The exposed thickness of the Fallon Alloformation (Figure 13) is about 1 to 2 m in a deeply incised gully near the distal outflow of Smoke Creek (Plate 4). The Fallon Alloformation was deposited within the last 5,000 years (Morrison and Frye, 1965). The last lake maximum occurred about 100 years ago (Dodge, 1980), but did not reach the elevation of the "Fallon" high stand of Morrison and Frye (1964).

Four tephra beds are exposed in lacustrine clays of the Sehoo Alloformation. Samples were collected from each tephra bed. Sample locations are shown on Plates 3, 4, and 5. Davis (1988, personal comm.) petrographically classified the tephras as (oldest to youngest) Mount Saint Helens "C" (Marble Bluff)\

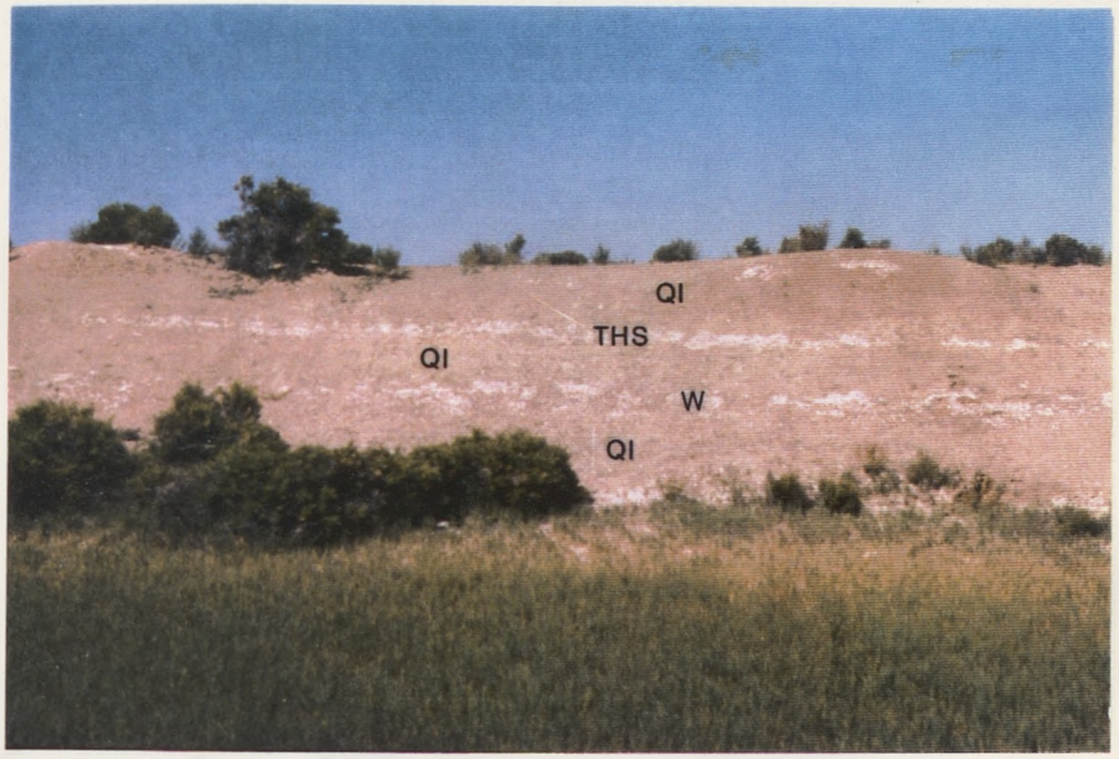

caption for Figure 14, p. 41

Figure 13. Fallon Alloformation sand and silt deposits (Fallon) disconformably overlie Sehoo Alloformation lacustrine silt and clay deposits (Sehoo). The marker bed near the drainage bottom is the Trego Hot Springs tephra (THS). View is to the west. Outcrop is south of Smoke Creek in T30N, R19E, Sec. 15.

tephra, Timber Lake tephra, Wono tephra, and Trego Hot Springs tephra.

Mount Saint Helen "C" Tephra. The Mount Saint Helens "C",about 35,000 years in age (Davis, 1985), contains abundant hornblende with lesser amounts of biotite phenocrysts. Biotite phenocrysts typically adhere to the glass shards. Mount Saint Helens "C" is most likely the Marble Bluff tephra (Davis, 1985, p. 41).

Timber Lake Tephra. Petrographically, the Timber Lake tephra bed consists of poorly sorted glass shards with sparse hypersthene and augite phenocrysts and opaque minerals. The Timber Lake tephra is about 25,000 to 29,000 years in age (Davis, 1978a).

Wono Tephra. Wono tephra about 1.5 m stratigraphically lower than the Trego Hot Springs layer in Lake Lahonton clays (Figures 13 and 14). Wono tephra contained hypersthene and scattered hornblende phenocryst. Thickness varies between 5 and 7 cm. The Wono is about 24,800 years in age (Davis, 1978a; Valastro and others, 1978).

Caption for Figure 13, p. 39.

Figure 14. Trego Hot Springs (THS) and Wono (W) tephra layers crop out in lacustrine silt and clay deposits of the Sehoo Alloformation near the playa margin in southwestern Smoke Creek Desert (east of T30N, R19E, Sec. 12). View is to the southwest. The Wono is about 24,800 years in age (Davis, 1978a; Valastro and others, 1978).

Trego Hot Springs Tephra. Trego Hot Springs tephra, about 23,400 years in age (Verosub, et. al., 1978; Davis, 1983), contains scattered phenocrysts of hornblende and occasional hypersthene and augite phenocrysts, and few opaque minerals. Thickness averages about 1 to 2 cm.

Playa deposits (Qpa). Playa deposits consist of brown clays with evaporite salts (Figure 15). Sand and silt occurs along the playa margins. The deposits disconformably overlie the Fallon Alloformation and locally unconformably overlie the Sehoo Alloformation. Playa deposits have intensely desiccated surfaces during dry periods. However, they are very moist to saturated below the desiccated crust. A 3 to 7 cm crust of white, puffy evaporite salts typically develop at the playa edge.

Alluvium (Qal, Qalo). Alluvium in major drainage consists of gravel, sand and silt with locally derived large angular boulders to pebbles. These deposits are light brown to tan, lensoidal, cross-bedded and unconsolidated. Thickness near the mouth of Smoke Creek varies from less than 1 meter to about 5 m. Undifferentiated alluvium (Qal) is considered post-Lake Lahonton (Holocene in age) and is undergoing active deposition during periods of high rainfall and where streams

a.

b.

Figure 15. Typical playa deposits (Qpa) in southwestern Smoke Creek Desert. Desiccated, barren clay surfaces (a) and disseminated evaporite deposits (b, white band) are common. The elevated surface at the playa margin (b) is a scarp along the Bonham Ranch fault zone (BRFZ). The low hill in the background is Quaternary basalt within the playa floor east of T30N, R19E, Sec. 13 (Plate 4). Views are to the east (a) with the Fox Range in the distant background and to the west (b).

are perennial. Older alluvium (Qalo) occurs in terraces formed as a result of tectonic activity. The most prominent alluvial terraces are near the mouth of Smoke Creek (Plate 3).

Talus deposits (Qt). Chaotic, angular talus debris accumulates at the base of moderately steep to steep slopes. Talus consists of poorly sorted, large boulders to cobbles of volcanic rocks derived from adjacent tectonically formed steep slopes. Talus deposits below about 1,335 m (4,380 ft) are intercalated with well rounded gravel of Lake Lahonton longshore deposits, indicative of deposition during and post-Lake Lahonton high stand.

Large angular boulders, up to 3 m across, occur well downslope of the tectonically formed steep volcanic rock slopes in southwestern Smoke Creek Desert. These large boulders are similar in distal position to boulders tectonically displaced in Dixie Valley (Whitney, 1988, personal comm.).

Eolian deposits (Qsd, Qes). Active eolian processes are depositing predominantly fine grained sand and silt as sand dunes (Qsd) and unconsolidated eolian sand (Qes). Active sand dunes are forming barchanoid ridges up to 5 m in height in the

southeastern portion of Madeline Plains and the southern portion of Smoke Creek Desert (Plates 1 and 5). Sand dune deposits consist of well sorted, light brown to tan, fine grained sands. Sparse to moderately established vegetation tends to stabilize the dunes. Dune orientation in the Madeline Plains and Smoke Creek Desert indicates dominant westerly and southwesterly wind directions, respectively.

Eolian sand (Qes) occurs as thin, well-sorted sand and silt sheets which form a veneer on the basalt flows and Quaternary deposits in eastern Madeline Plains and southern Smoke Creek Desert. Eolian deposits in Madeline Plains were largely derived from littoral and bottom deposits of Madeline Plains. In the southwestern Smoke Creek Desert, these deposits apparently originated from Honey Lake Valley as well as southernmost Smoke Creek Desert. Active deflation in southern Smoke Creek Desert has formed a hummocky topography of sand mounds that are anchored by vegetation.

STRUCTURAL AND TECTONIC ANALYSIS

Quaternary Faults

Faults first mapped on aerial photographs were identified as Quaternary faults in the field when they displaced Pleistocene. Relative fault displacement ages were determined in the field by displacement of upper Pleistocene and Holocene pluvial deposits in the Madeline Plains and Smoke Creek Desert. Lineaments mapped on aerial photographs in the Smoke Creek Valley occur within the Miocene-Pliocene volcanic rocks, except for a fault scarp in upper Pliocene-Quaternary basalt flows south of Smoke Creek Reservoir in T31N, R18E, Sec. 6 and 7 and T32N, R18E, Sec. 31 (Plate 3).

Madeline Plains Area: Faults in the eastern Madeline Plains area form the southern terminus of the Likely fault zone. These faults trend about N35°W, and several normal-slip faults trend north to northeast at about 45 degrees to the Likely fault zone. These normal-slip faults are along the eastern margin of Madeline Plains east of the likely fault zone, and extend to Surprise Valley in northeastern California.

The estimated age of fault scarps mapped in Madeline Plains is based on the presumption that Madeline Plains was a Pleistocene pluvial lake coeval with Lake Lahonton and that

its time-straigraphic relationships are synchronous with Lake Lahonton as discussed in the Recency of Faulting section. The highstand elevation of 1,667 m (5,470 ft) in Madeline Plains is considered coeval with the uppermost Pleistocene (12,000-year) highstand of Lake Lahonton. The shoreline features at elevation 1,637 m (5,370 ft) in Madeline Plains is considered coeval with the mid-Holocene (5,000-year) pluvial maximum of Lake Lahonton.

Likely Fault Zone (LFZ): The LFZ has right-oblique displacement. Up to 1.5 km of right-slip displacement was suggested by Lydon and others (1960). Geomorphic evidence for right-slip faulting includes aligned springs, linear valleys, a sag pond, apparent right-lateral offset drainage and rhomboidal depressions. A normal-slip component of displacement is indicated by the steep escarpment of volcanic rocks along the LFZ. The presence of a normal-slip component is consistent with faults that trend about N35°W in the Honey Lake-Eagle Lake-Medicine Lake Highlands area of northeastern California (Robert and Grose, 1982; Grose, 1986).

The LFZ exhibits left-stepping, right-oblique-slip displacement within Madeline Plains. Faults A through E (Plate 1) are individual faults of the LFZ that displace upper Pleistocene and Holocene pluvial deposits in eastern Madeline

Plains. These faults appear as distinct lineaments on the aerial photographs. During field mapping, these faults were observed to be consistent with the mapping of Gay and Aune (1959) and Lydon and others (1960). Hill and others (1961) extended Fault A across Madeline Plains and indicated normal displacement.

The age of fault displacements is based on the presumption that pluvial deposits of Madeline Plains are coeval with the pluvial deposits of Lake Lahonton as discussed in the Recency of Faulting section. As such, the ages of the Sehoo and Fallon Alloformations (about 12,000 and 5,000 years B.P.) (Morrison and Frye, 1965; Davis, 1978a and 1982a; Morrison and Davis, 1984) of Lake Lahonton were used to determine relative age of faults within Madeline Plains.

Fault A has two distinct, left-stepping, en echelon lineaments (Plate 1). Skeleton Flats (T36N, R14E, Sec. 21) may represent a rhomboidal depression where Fault A appears to step to the left. A depression on Juniper Ridge (T35N, R14E, Sec. 14) along Fault A appears to be a sag pond. A scarp along Fault A, as observed on aerial photographs and in volcanic rocks, appears to have normal-slip component of displacement (down to the east). Based on these geomorphic features, right oblique-slip displacement is inferred for

Fault A. No evidence of offset of Sehoo (Morrison and Frye, 1965; Davis, 1978a and 1982a) equivalent pluvial deposits was observed on the aerial photographs or during field mapping. Therefore, the last tectonic activity on Fault A probably predates the last high stand of Lake Lahonton (about 12,000 years ago) (Davis, 1978a and 1982a) and the recurrence interval or return time is greater than 12,000 years.

Fault B is marked by a well-defined lineament and aligned springs (Plate 1). Apparent offset of drainage indicates right-slip displacement of approximately 150 m in the Maiden Flat area (T36N, R14E, Sec. 6). A poorly defined vegetation lineament observed on the low-sun angle aerial photographs extends approximately 800 m into Madeline Plains lake deposits that are considered equivalent to the Holocene Fallon Alloformation of Lake Lahonton. Shoreline features observed on these photographs do not appear to be displaced along the vegetation lineament. The fault is inferred to be mainly right-slip from its parallel alignment with Fault A and possible connection to the right-lateral fault of T36N, R14E, Section 36.

Fault C (Plate 1) is marked by aligned springs, well-defined linear drainages and an apparent offset drainage. A rhomboidal depression near Ethecopar Springs (T36N, R14E, Sec.

14) indicates a possible left-step between Faults B and C. Apparent offset of drainages in T36N, R14E, Sec. 23, 24, and T35N, R14E, Sec. 25 indicates approximately 300 m of right-slip displacement. Well-defined scarps within the volcanic rocks indicate a normal-slip component. Three lineaments in Sehoo-equivalent gravel at the southern terminus of Fault C were observed on the low-sun angle aerial photographs. No evidence of these splays was found during field mapping. Accordingly, the recurrence interval is inferred to be greater then 12,000 years.

Faults D and E are defined by linear drainages that extend from near Long Spring (T36N, R14E, Sec. 36) southeastward through Brin Marr Ranch in Madeline Plains (T35N, R14E, Sec. 4). Fault E splays from Fault D near T35N, R15E, Sec. 10, and terminates near T34N, R15E, Sec. 32. A shallow depression (T35N, R15E, Sec. 13 and 14 and R15E, T34N, sec 23, 24, 25, and 30) with an obvious tonal change (Figure 16) appears to represent a post-Fallon (Holocene) sag depression formed between Faults D and E (Figure 16 and Plate 1). Faults D and E are coincident with inferred faults of Hill and others (1961) that cross Madeline Plains. Fault D

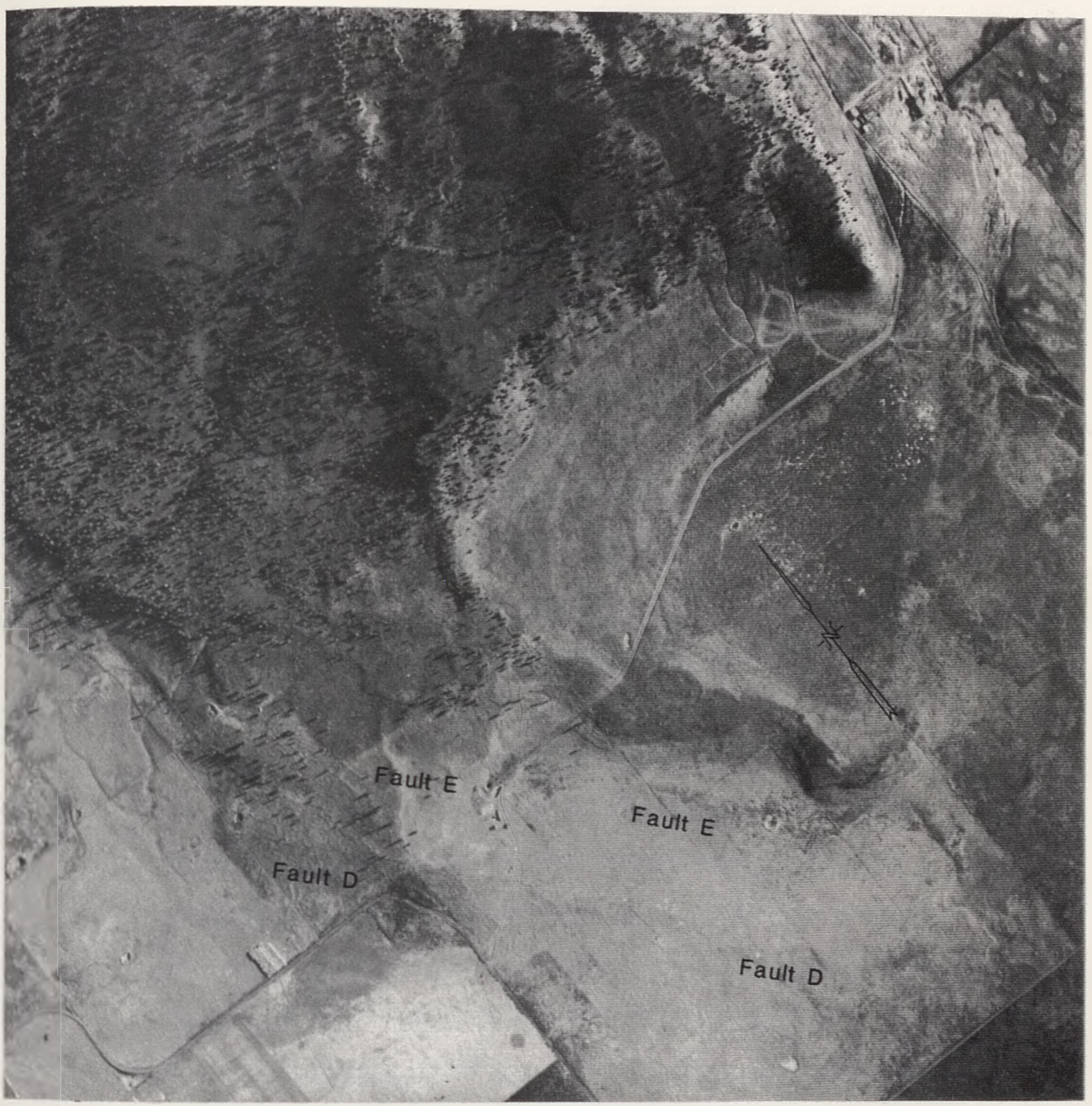

Figure 16. Low sun angle aerial photograph showing trace of Faults D and E of the Likely fault zone in deposits equivalent to the Holocene Fallon Alloformation in eastern Madeline Plains. North is toward the upper left corner of the photograph.

extends across Madeline Plains and terminates on the eastern flank of Observation Peak. Fault D appears to represent the southern termination of the LFZ. The recurrence interval is approximately less than 12,000 years.

Normal-Slip Faults: Two normal-slip fault zones (Faults F and G, Plate 1), mapped and ground verified along the eastern margin of Madeline Plains trend generally about 45 degrees to the LFZ. These faults form high, well defined scarps in Miocene-Pliocene volcanic rocks. Fault zone F appears to displace pluvial sediments and shoreline features coeval with the Sehoo and Fallon Alloformations. Fault zone G does not appear to displace deposits equivalent to the Fallon Alloformation.

Fault zone F is marked by high, arcuate, west dipping scarps on the east flank of Cold Springs Valley, which is indicative of normal-slip displacement. Fault zone F occurs predominantly in volcanic rocks and extends into easternmost Madeline Plains. Deposits equivalent to the Fallon Alloformation appear faulted near T35, R15E, Sec. 6 and 31 (Plate 1). Evidence for Holocene faulting consisted of subtle topographic breaks indicative of low height normal-slip scarps and vegetational lineaments that extend about 1.2 km into Madeline Plains. Ground verification was not possible as

these features were under water during the field investigations.

Fault zone G appears to dip west and has normal-slip displacement. Fault G extends across the southern Warner Mountains from Surprise Valley into eastern Madeline Plains. The fault zone bends southward and trends along the eastern margin of Madeline Plains (Figure 17 and Plate 1). Fault zone G terminates near Buckhorn Canyon in T35N, R17E, Sec. 35. Deposits equivalent to the Sehoo Alloformation are cut by Fault G (Figure 17). Alluvial deposits are not offset at the fault zone. Eolian deposits blanket the fault scarps in southeasternmost Madeline Plains. Fault scarp morphology (Profiles 27, 28 and 29, Appendix A) suggests two tectonic events with total displacement of approximately 1.7 m (Figure 17) post-dating the Lake Lahonton equivalent high stand (12,000 years ago) . The lack of evidence of fault scarps across the alluviated canyons may be explained by post-faulting erosion. This would suggest that the tectonic events are of pre-Fallon age (5,000 years ago). Apparent offsets of drainage that cross the fault zone suggest a Pleistocene left-slip component of up to 100 m. However, alluvial deposits in T35N, R16E, sec. 25 and 26.

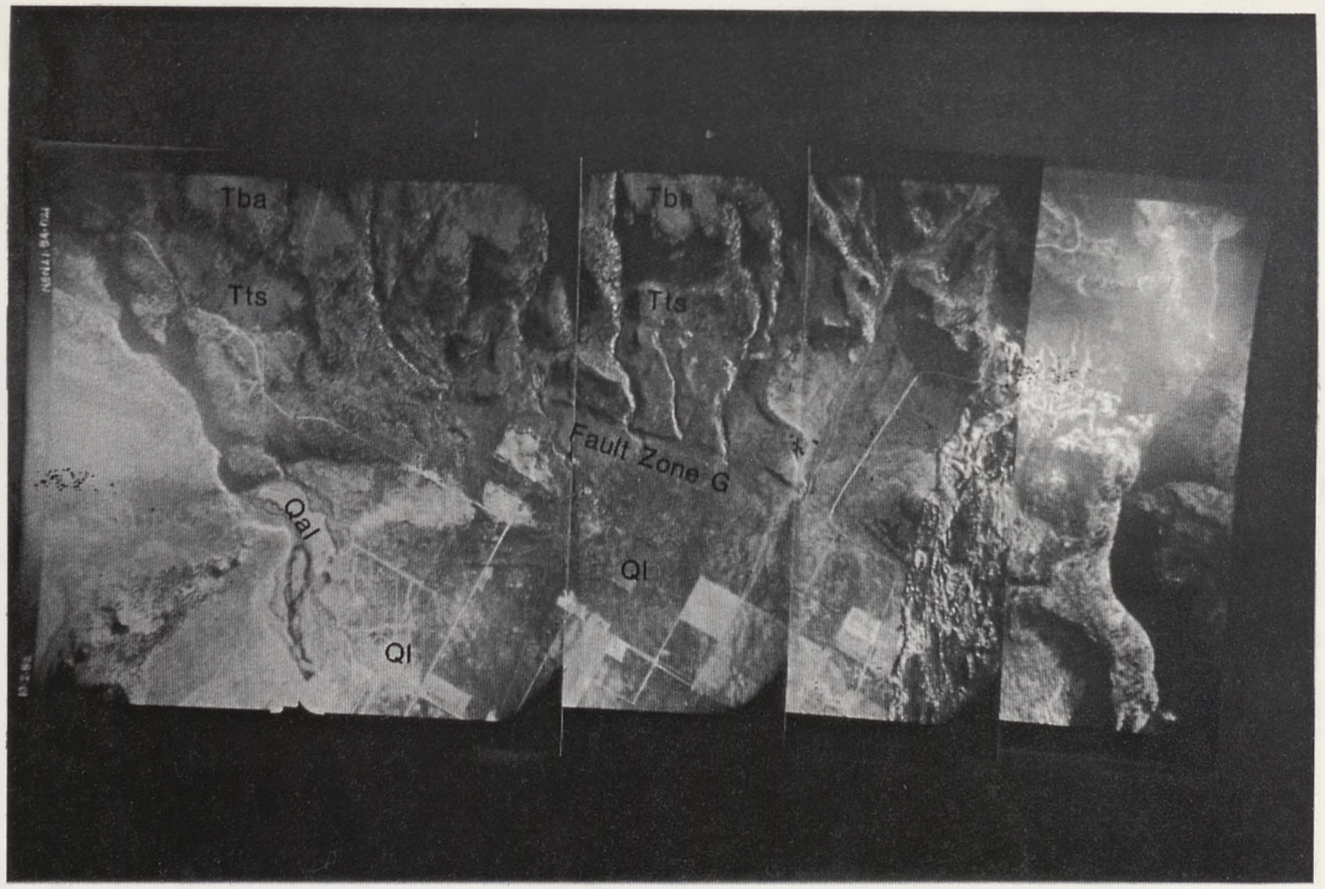

Figure 17. Mosaic of low sun angle aerial photographs that show Fault Zone G which borders the eastern margin of Madeline Plains. The fault scarp is about 1.7 m in vertical height. Sand dunes blanket the scarps in the lower right portion of the photograph. Drainage offsets indicate an apparent left-slip displacement of about 100 m. North is toward the upper left corner.

are not displaced by Fault G. These alluvial deposits overlie the deposits equivalent to the Fallon Alloformation and are younger than 5,000 years. Therefore, the recurrence interval is greater than 5,000 years.

Normal-slip faults bounding the eastern margin of Madeline Plains are tectonically active as defined in Slemmons (1977, 1981) and Slemmons and dePolo (1986a, 1986b). Geomorphic data indicates Holocene activity for Fault Zone F and at least late Pleistocene activity for Fault Zone G.

Smoke Creek Valley Area

A broad fault zone approximately 2 km wide and 5 km long that consists of several "lineaments" was mapped northeast of Smoke Creek Reservoir in T32N, R17E, Sec. 8 through 20, 25 through 28, and 33 through 36 (Plates 1 and 2). This fault zone was observed on low-sun angle and normal aerial photographs, and is informally named the Smoke Creek fault zone (SCFZ). It is characterized by generally parallel faults that have an older, weathered appearance indicative of a mature fault zone (Figure 18) entirely within Miocene-Pliocene volcanic rocks. A graben-like geomorphic feature and a spring alignment mark the western limit of this fault zone. Apparent right-slip displacement may be inferred from drainage patterns within the fault zone. The SCFZ aligns with Fault D of the

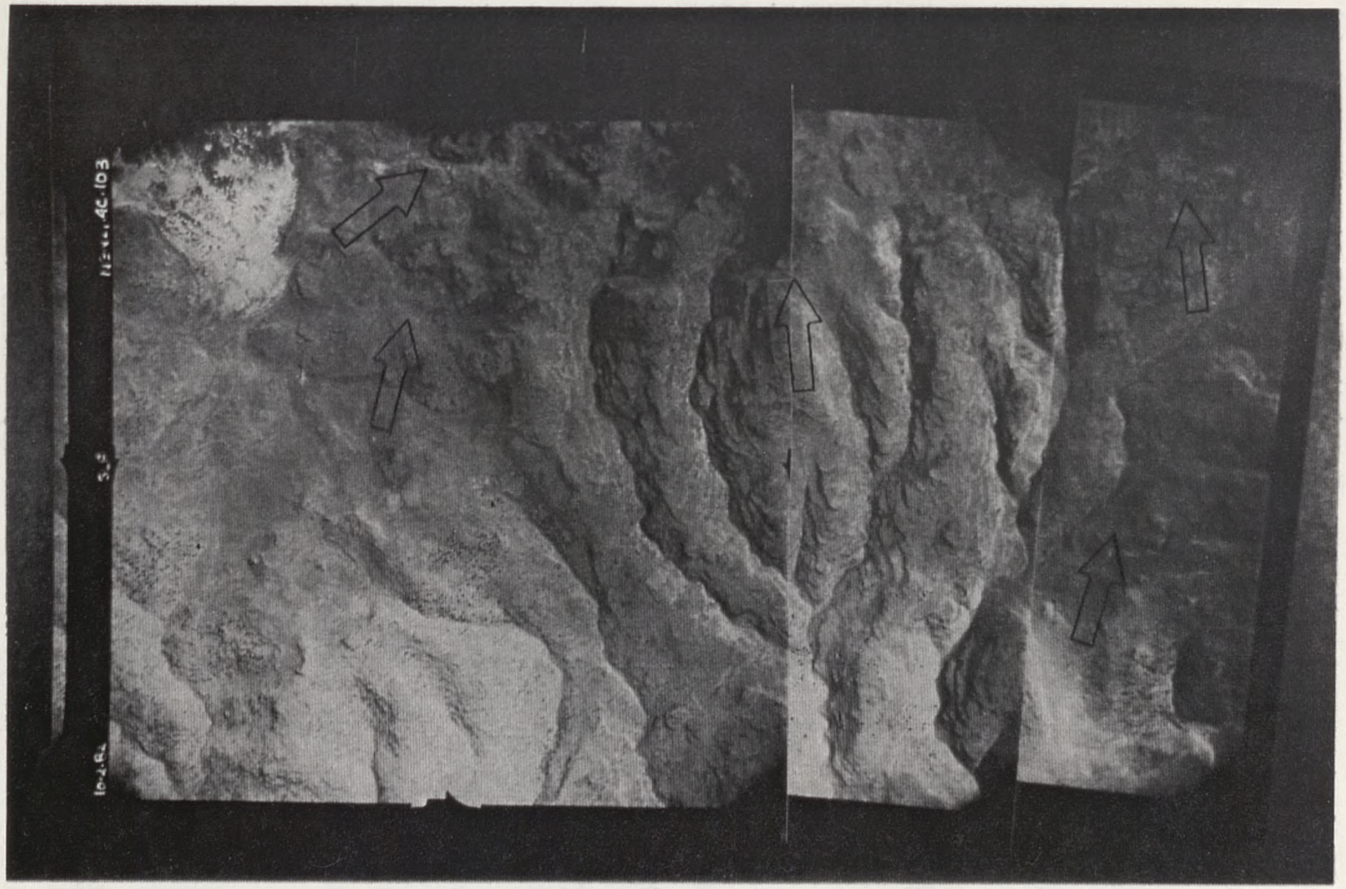

Figure 18. Low sun angle aerial photograph mosaic that shows the Smoke Creek fault zone (SCFZ) in Miocene-Pliocene basalt flows (Tba) in central Smoke Creek Valley. The faults within the fault zone (arrows) have a weathered, mature appearance. Width of the SCFZ is approximately 2 km.

LFZ. Since the fault zone does not displace Quaternary Pleistocene deposits and has an older, weathered appearance, an upper Pliocene age for last surface rupture is likely.

A well-defined normal fault bounds the western margin of the SCV area. This fault terminates northwest of Smoke Creek Reservoir and extends southeast to south along the Tertiary basaltic range front of Dry Valley. It is considered the northern portion of the informally named Dry Valley - Smoke Creek fault zone.

Smoke Creek Desert Area

The Smoke Creek Desert (SCD) area of this study encompasses southwestern Smoke Creek Desert and Dry Valley (Plates 2 through 5). Quaternary faults within the area were previously mapped by Bonham (1969) and Dodge (1978). This study defines two major fault zones bounding the western margin of Dry Valley and Smoke Creek Desert. These two fault zones are herein informally named the Dry Valley-Smoke Creek Ranch and Bonham Ranch fault zones.

Dry Valley-Smoke Creek Ranch Fault Zone. The Dry Valley-Smoke Creek Ranch fault zone (DV-SCRFZ) originally was mapped by Bonham (1969). It is marked by a steep escarpment along the western margin of Dry Valley and the southwestern margin of Smoke Creek Valley, and by well-defined scarps in pluvial

sediments within Dry Valley. Bonham (1969) terminated the DV-SCRFZ near Flannigan, Nevada (T27N, R19E, Sec. 18), in easternmost Honey Lake Valley southwest of Smoke Creek Desert. Total fault length is approximately 50 km (31 miles). Displacement is predominantly normal-slip. Minimum vertical displacement, based on the height of the volcanic escarpment along the western margin of Dry Valley, is approximately 460 m (1,500 ft) since the termination of Miocene-Pliocene volcanism. Minimum cumulative latest Pleistocene-Holocene displacement is approximately 2 m (Profiles 1 and 2, Appendix A).

In southern Dry Valley, The DV-SCRFZ consists of several subparallel faults across the valley. Apparent offsets of alluvial fans in the southern Dry Valley (Plate 5) indicate a right-slip component of displacement. The DV-SCRFZ steps left to the normal-slip faults which form the steep escarpment at the western margin of Dry Valley (Figure 19).

In Smoke Creek Valley, southwest of Smoke Creek Reservoir, the DV-SCRFZ scarp in upper Pliocene-Quaternary basalts is about 60 m (200 ft), down to the northeast. Fault scarps in the Sehoo Alloformation in southern Dry Valley are up to 1 meter in vertical height. Although Dry Valley is above the Fallon Alloformation datum of 1,204 m (3,950 feet),

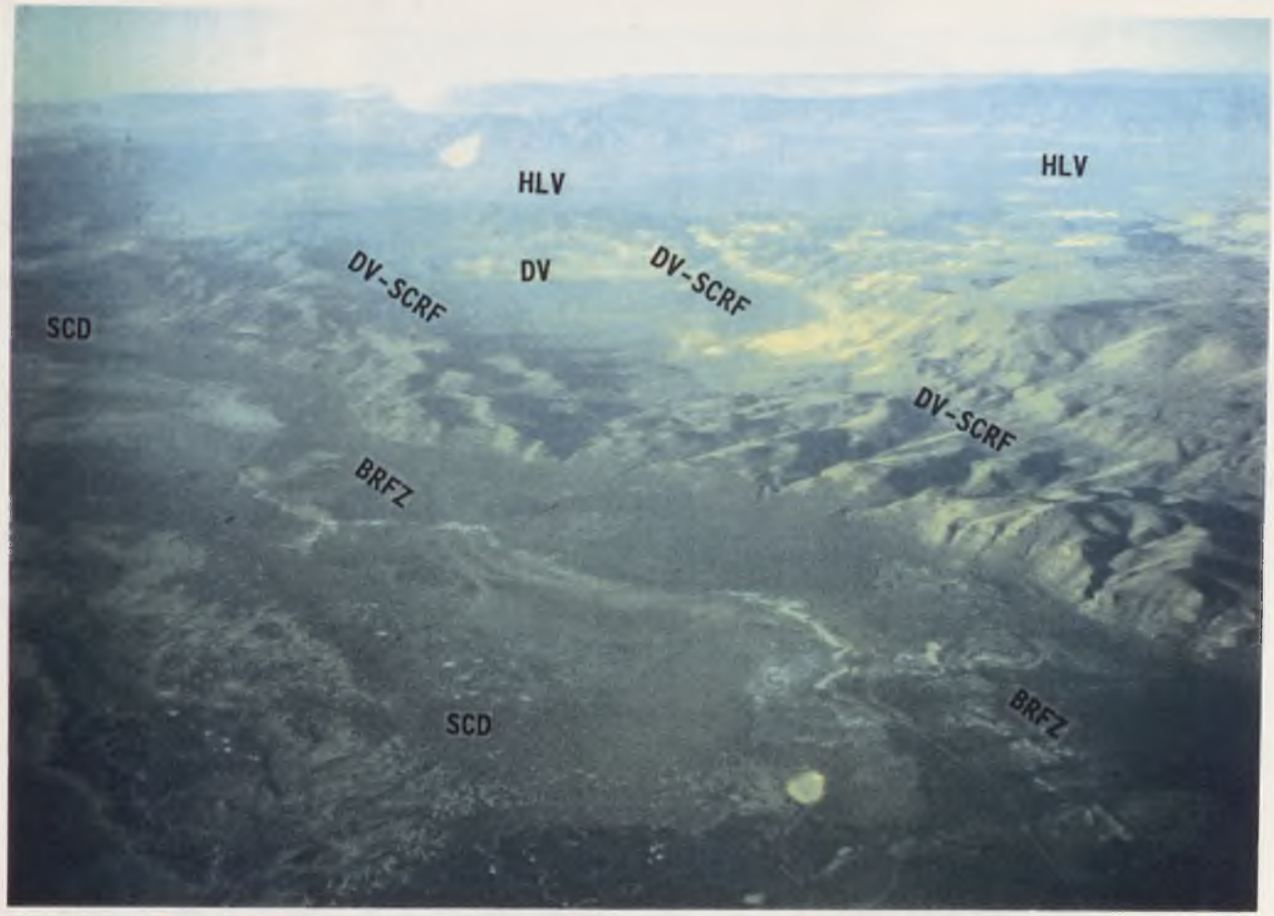

Figure 19. Overview of southwestern Smoke Creek Desert (SCD) and Dry Valley (DV), Nevada. Eastern Honey Lake Valley (HLV) is visible in the background. The Dry Valley-Smoke Creek Desert (DV-SCRFZ) and Bonham Ranch (BRFZ) fault zones are delineated. The DV-SCRFZ steps left in Dry Valley to the east-facing escarpment. View is toward the south.

fault scarp slope angles in pluvial sediments (Profile 1 and 2, Appendix A) suggest that displacement occurred within the past 2,000 years and was probably concurrent with last faulting event along the Bonham Ranch fault zone.

Bonham Ranch Fault Zone (BRFZ): Several parallel to subparallel faults that extend from the range front into the Smoke Creek Desert playa (Figure 20) are herein informally named the Bonham Ranch fault zone (BRFZ). The mapped limits of the BRFZ extend from approximately 12 km (7.5 miles) north of Buffalo Creek (Plate 2) in T33N, R20E, Sec. 18 to about 3.3 km (2 miles) south of Bonham Ranch in T28N, R19E, Sec. 24 (Plate 5). The width of the BRFZ varies from less than 2 km to approximately 9 km. The BRFZ within the study area includes previously mapped faults of Bonham (1969) and Dodge (1980). The total mapped length of the BRFZ in Smoke Creek Desert is about 48 km (30 mi). Faults mapped by Bonham (1969) in the Terrace Hills south of Sand Pass may be a continuation of the BRFZ to a point near the Needle Rocks at the north end of Pyramid Lake, Nevada. The total length of the BRFZ may be about 68 km (42 miles), including the Terrace Hills-Needle Rocks segment.

The faults within the BRFZ south of Buckbrush Springs in T29N, R19E, sec. 10 (Plate 5) are less sinuous in trend. This

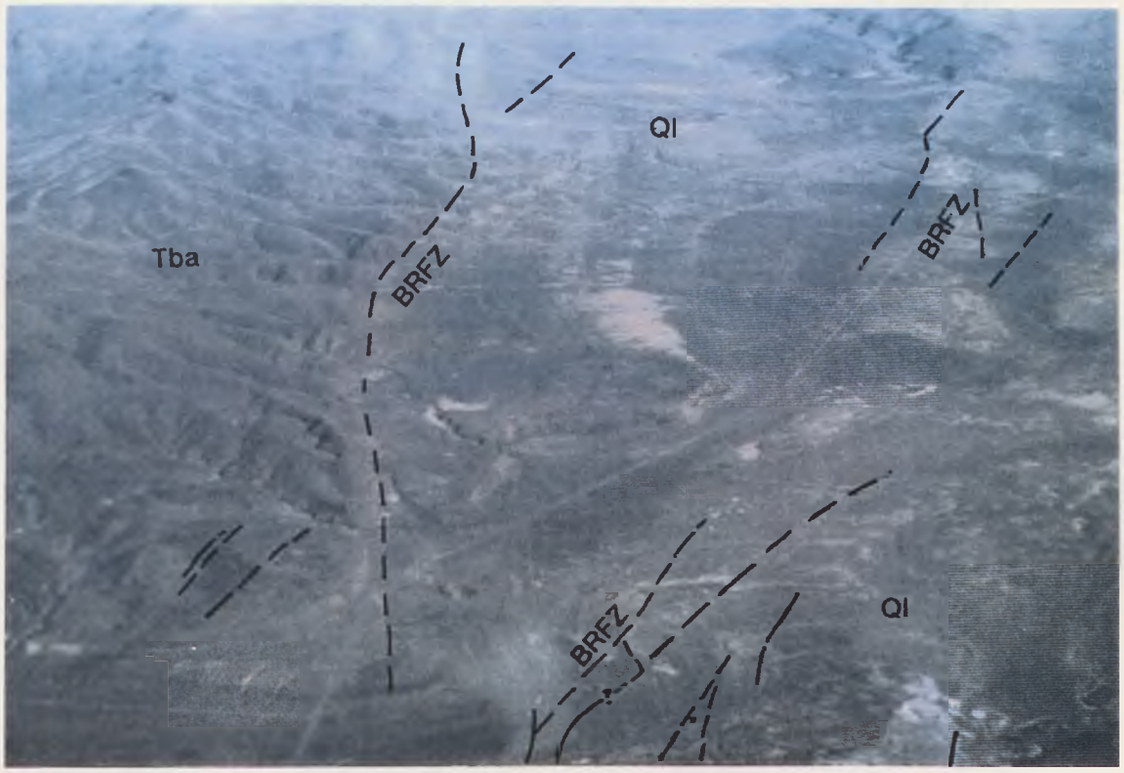

Figure 20. Several parallel to subparallel fault splays of the Bonham Ranch fault zone (BRFZ) displace upper Pleistocene and Holocene Lake Lahonton sediments (Ql) and Tertiary basalts (Tba). The BRFZ extends eastward into Smoke Creek Desert (SCD). View is toward the north.

apparent lack of sinuosity in the southernmost portion of the BRFZ may represent a more dominant strike-slip component. The faults mapped in the Terrace Hills (Bonham, 1969) are linear and the Terrace Hills terrain is indicative of strike-slip faulting. East-west faults mapped at the southern end of Smoke Creek Desert (Bonham, 1969) may represent a left-step transition from the right-slip faults of the Terrace Hills (Slemmons, personal communication, 1989; Whitney, personal communication, 1989) to the BRFZ.

The BRFZ is comprised of three main faults in the vicinity of Smoke Creek (Plates 3 and 4) that exhibit right-oblique-slip displacement, where the normal-slip component is down to the east. The normal-slip component on faults that displace upper Pleistocene Sehoo Alloformation and Holocene Fallon Alloformation varies from less than 0.5 m to about 4.5 m. Profiles 4, 5, 7, and 8 (Appendix A) were measured across fault scarps of the BRFZ (Plate 4) that displace the Sehoo and Fallon Alloformations. From these profiles, a vertical displacement of 4.5 m (15 ft) and 2 m (7 ft) of the Sehoo and Fallon deposits, respectively, was determined.

North of Bonham Ranch (Plate 5), the sinuosity of the BRFZ clearly reflects normal-slip displacement with younger faults occurring toward the playa. South of Bonham Ranch, the

faults are much less sinuous. This lack of sinuosity may suggest a strike-slip component along the southern portion of the BRFZ. East-West faults mapped at the southern end of Smoke Creek Desert (Bonham, 1969; Whitney, personal comm., 1989) may represent a left-step transition from the Terrace Hills-Needle Rock faults to the BRFZ.

Faults observed in the range front escarpment have east dips up to 70 degrees. Faults observed in deltaic deposits about 610 m (2,000 ft) north of T32N, R19E, Sec. 1 (Plate 3) strike N5° to 15°W, dip 70° to 74°E and have striations that plunge 25° to 38°S, which is indicative of right-oblique-slip displacement.

In T30N, R18E, NW1/4 Sec. 15 (Plate 4), eolian sands are juxtaposed against Sehoo Alloformation lake clays by a high angle reverse fault. Near-surface reverse faults occur in unconsolidated sediments overlying a bedrock normal-slip fault. From model experiments using a glass-walled fault test box, Lade and others (1984a) demonstrated that multiple failure surfaces, including reverse failure surfaces, form as primary and secondary ruptures in unconsolidated sediments over a bedrock dip-slip fault. Further, near-surface reverse faults were observed in alluvial deposits overlying the normal-slip bedrock fault activated by the earthquake of

August 17, 1959, at Hebgen Lake, Montana, and in trenches overlying normal-slip faults at Point Conception, California (Lade and others, 1984b).

Faults of the BRFZ cut "Sehoo" and "Fallon" shoreline features. Age approximations by fault scarp profiling methods indicate the last surface rupture to be about 700 to 800 years in age. Carbon samples collected from the base of the fault scarp about 415 m northeast of Profile 7 (Plate 4) yield a minimum age for surface rupture of 290 ± 70 years ago. This age dating technique is discussed in detail under "Recency of Faulting."

Fault scarps of the BRFZ that displace Holocene Fallon Alloformation in the central portion of the fault zone (Plates 3 and 4), have the maximum scarp heights. Profiling of these fault scarps show that most of these scarps were formed by a single tectonic event. Therefore, it is presumed that the earthquake of about 290 ± 70 years ago formed these scarps that have a total length of Holocene surface rupture is 40 km (25 mi).

Slemmons and others (1989) and Bonilla and others (1984) developed surface magnitude (Ms) regressions using worldwide seismic data. Using a surface rupture length of 40 km, and

amaximum vertical displacement of 2.9 m for a single event (Profile 26, Appendix A and Plate 4), the estimated magnitude is Ms 7.0 (Slemmons and others, 1989). Based on regressions of Bonilla and others (1984), the 290 ± 70 seismic event had an Ms of 7.3.

Profiles 3, 4, 5, 7, and 30 (Plates 4 and 5, and Appendix A) show at least two episodes of fault surface rupture with a maximum total vertical displacement of 3.5 m. These events offset deposits of the Fallon Alloformation that have an upper age limit of about 5,000 years. This would yield a maximum recurrence interval of about 4,700 years and a minimum slip rate of about 0.5 m per 1,000 years.

Recency of Faulting

The recency of fault surface rupture and tectonic activity was evaluated using three dating techniques: 1) Lake Lahonton stratigraphy and chronologies, 2) fault scarp profiling methods, and 3) radiometric age dates. The Lake Lahonton stratigraphic units mapped in the Smoke Creek Desert portion of the study area were based on Morrison's (1964) stratigraphy as revised by Davis (1978a) and Morrison and Davis (1984). Stratigraphic age controls were derived from Lake Lahonton chronologies suggested by Davis (1982a). Methodology for profiling fault scarps was adapted from Wallace (1977) and Bucknam and Anderson (1979). Nash's (1984) SLOPEAGE (Version 1) and Hank and others (1984) diffusion models

were applied to selected scarp profiles to approximate the age of the scarps. These ages were compared to the dated Black Rock Fault scarps (Dodge and Grose, 1980) that displaced similar sediments in the Black Rock Desert, Nevada. Carbon samples were collected at the base of a BRFZ fault scarp. The radiometric age dates that were yielded from the samples provided a minimum age for the fault scarps.

Lake Lahonton stratigraphy and chronologies. Time-stratigraphic relationships and chronologies of Smoke Creek Desert and Madeline Plains provide the basis to assess relative ages of fault scarps. These relationships and chronologies were derived for Lake Lahonton by Morrison and Frye (1965) and Davis (1978a, 1982a). The two youngest lacustrine deposits are the Sehoo and Fallon Alloformations of latest Pleistocene and mid-Holocene ages, respectively (Morrison, 1965; Morrison and Frye, 1965; Davis, 1978a). Detailed descriptions of the alloformations are provided in detail by Morrison and Frye (1965) and Davis (1977 and 1978a). The Sehoo and Fallon Alloformations are areally extensive within the Smoke Creek Desert portion of the study area.

The upper member of the Sehoo Alloformation represents deposits of the last major highstand of Lake Lahonton during the latest Pleistocene (about 12,000 years ago). Subsequent to latest Pleistocene-early Holocene Sehoo deposition, the

subaerial Turupah Alloformation, Toyeh Soil, and Fallon Alloformation were deposited (Figure 21), based on Morrison's (1964) stratigraphic framework in the Carson Desert. The last major highstand provides a key datum to determine relative ages of faults. This datum is defined by prominent shoreline features at elevation 1,335 m (4,380 ft) in Smoke Creek Desert.

The deposits of the Fallon Alloformation represent a mid-Holocene Lake Lahonton maximum. In the Carson Desert region and the Pyramid Lake basin, the mid-Holocene maximum is placed at 1,190 m (3,904 ft) (Morrison, 1964; Morrison and Frye, 1965). Davis (1978a) also suggests that the elevation of the mid-Holocene maximum in the Black Rock Desert is at 1,190 m. Based on the stratigraphic sequence developed by Morrison and Frye (1965) and revised by Davis (1978a), the deposits of the Fallon Alloformation represent the mid-Holocene Lake Lahonton highstand and overlie the upper unit of the upper Pleistocene Sehoo Alloformation (Figure 21).

In west-central Smoke Creek Desert, Dodge (1980) used the stratigraphic correlations of Morrison and Frye (1965) and Davis (1978a) and defined the mid-Holocene highstand at elevation 1,204 m (3,950 ft), coincident with the contact of the Sehoo and Fallon Alloformations. To be consistent with

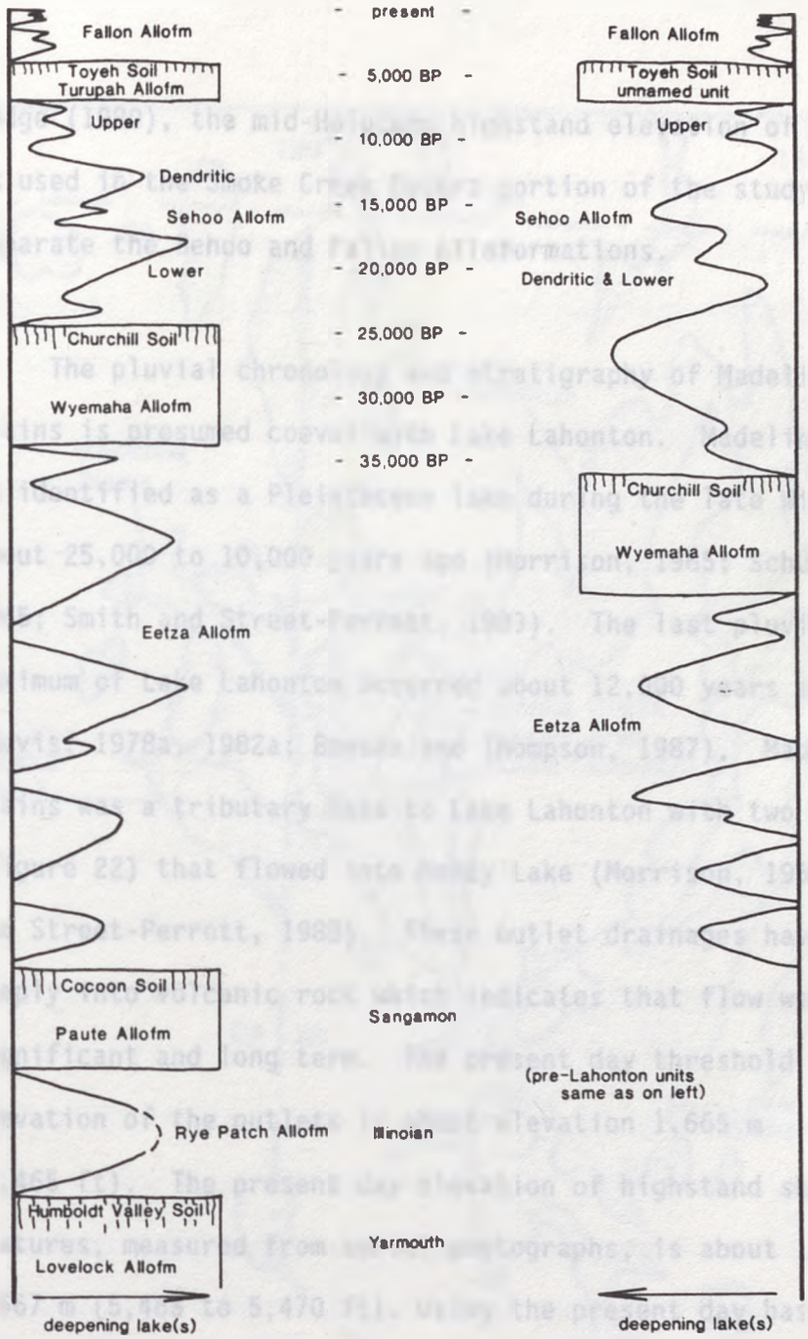

Figure 21. Schematic diagram showing the Quaternary stratigraphy, pluvial cycles and chronology of Lake Lahonton. Left column is Morrison's (1964) interpretation (Morrison and Frye, 1965). The right column is Davis' (1978a) revisions to Morrison's interpretations. Solid bars indicate subaerial deposition. Uneven vertical lines represent soil horizons. Modified from Davis (1978a) and includes Morrison and Davis (1984) nomenclature.

Dodge (1980), the mid-Holocene highstand elevation of 1,204 m is used in the Smoke Creek Desert portion of the study area to separate the Sehoo and Fallon Alloformations.

The pluvial chronology and stratigraphy of Madeline Plains is presumed coeval with Lake Lahonton. Madeline Plains is identified as a Pleistocene lake during the late Wisconsin, about 25,000 to 10,000 years ago (Morrison, 1965; Schumm, 1965; Smith and Street-Perrott, 1983). The last pluvial maximum of Lake Lahonton occurred about 12,000 years ago (Davis, 1978a, 1982a; Benson and Thompson, 1987). Madeline Plains was a tributary lake to Lake Lahonton with two outlets (Figure 22) that flowed into Honey Lake (Morrison, 1965; Smith and Street-Perrott, 1983). These outlet drainages have cut deeply into volcanic rock which indicates that flow was significant and long term. The present day threshold elevation of the outlets is about elevation 1,665 m (5,465 ft). The present day elevation of highstand shoreline features, measured from aerial photographs, is about 1,665 to 1,667 m (5,465 to 5,470 ft). Using the present day basin elevation of Madeline Plains, the water depth during the pluvial maximum was at least 53 m (175 ft). Therefore, Madeline Plains was a significant pluvial lake in northeastern California during the upper Pleistocene that was a tributary to Lake Lahonton.

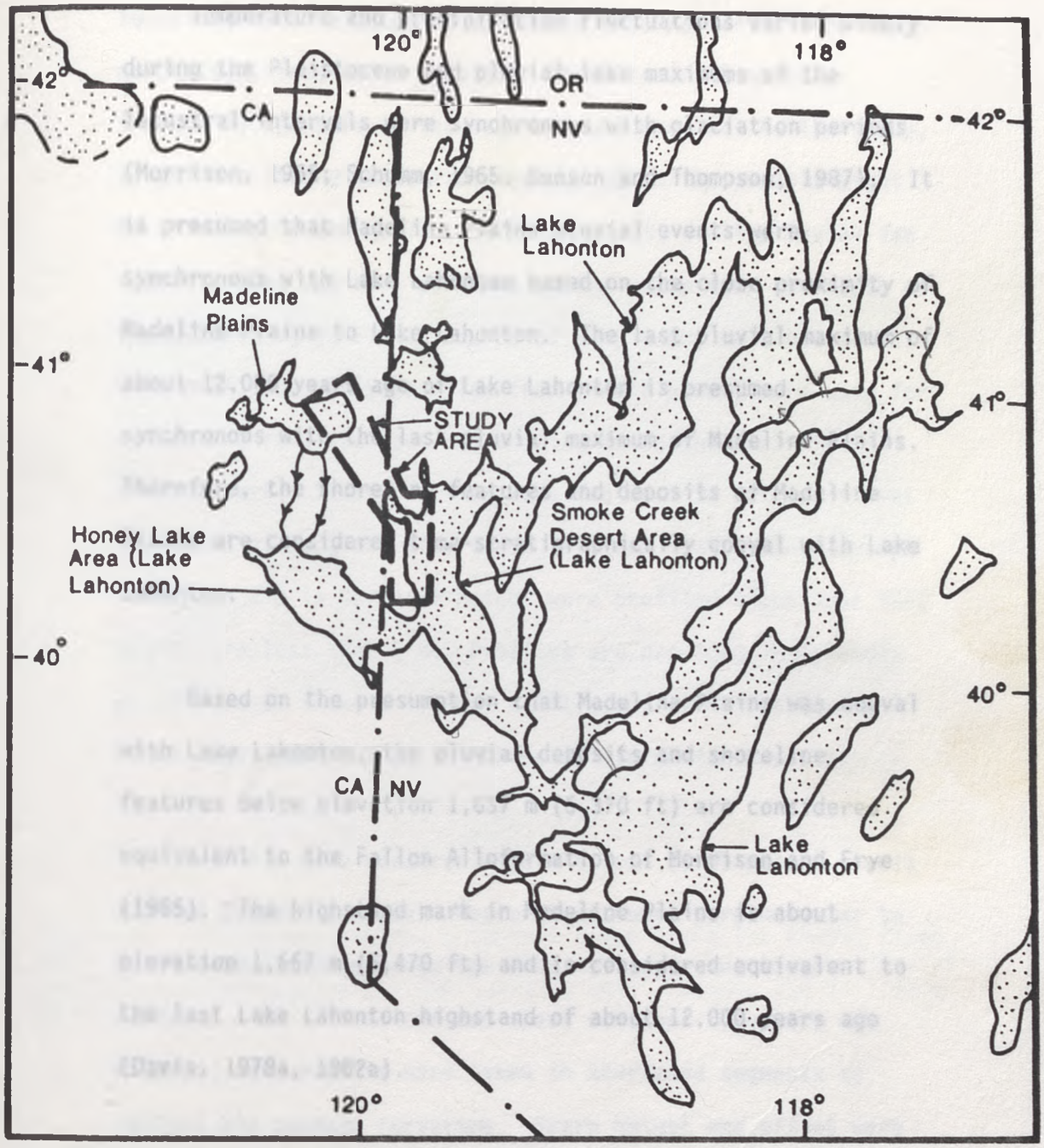

Figure 22. Distribution of the major pluvial lakes during the late Pleistocene pluvial maximum. Madeline Plains is located northwest of Lake Lahonton. Compiled from Morrison and Frye (1965), Snyder and others (1964), Morrison (1965), Flint (1971), Menard (1974) and Davis (1983).

Temperature and precipitation fluctuations varied widely during the Pleistocene and pluvial lake maximums of the lacustral intervals were synchronous with glaciation periods (Morrison, 1965; Schumm, 1965; Benson and Thompson, 1987). It is presumed that Madeline Plains pluvial events were synchronous with Lake Lahonton based on the close proximity of Madeline Plains to Lake Lahonton. The last pluvial maximum of about 12,000 years ago of Lake Lahonton is presumed synchronous with the last pluvial maximum of Madeline Plains. Therefore, the shoreline features and deposits of Madeline Plains are considered time-stratigraphically coeval with Lake Lahonton.

Based on the presumption that Madeline Plains was coeval with Lake Lahonton, the pluvial deposits and shoreline features below elevation 1,637 m (5,370 ft) are considered equivalent to the Fallon Alloformation of Morrison and Frye (1965). The highstand mark in Madeline Plains is about elevation 1,667 m (5,470 ft) and is considered equivalent to the last Lake Lahonton highstand of about 12,000 years ago (Davis, 1978a, 1982a).

Fault Scarp Profiling. Fault scarps in eastern Madeline Plains, Dry Valley and southwestern Smoke Creek Desert areas were measured in the field and profiles prepared. The profile

locations were selected to eliminate external effects on scarp morphology, insofar as possible. Such external effects include 1) channels at the base of, and parallel to the scarp, 2) gullies that dissect fault scarps where the profile might be affected by the gully side slope and 3) small alluvial fan deposits that may bury portions of the scarp near the mouth of the dissecting gullies. Scarps of single and multiple events were profiled. Only profiles from single events were used for estimating relative ages of faulting in southwestern Smoke Creek Desert. Scarp profiles were measured in materials that consisted of fanglomerate, sand, silt and clay. Fault scarps less than 2 m in vertical height were profiled since most BRFZ scarps are less than 2 m. Profiles are provided in Appendix A. Figure 23 shows a typical fault scarp along the Bonham Ranch fault zone (BRFZ) in Fallon Alloformation deposits.

Profiles were measured with a 6-foot (1.85-meter) stadia rod and Brunton compass. Measurements were perpendicular to fault scarps and included the original upper and lower surfaces. At inflections and where constant curvature was evident, measurements were taken in shortened segments to reflect the average curvature. Scarp height and offset were determined from the profile plot and diffusion equation models of Nash (1980, 1984) and Hank and others (1984).

Figure 23. Photograph showing a typical scarp along the Bonham Ranch fault zone in Smoke Creek Desert. The fault displaces sandy silts of the Fallon Alloformation (<5,000 years in age). Stadia rod is 1.85 m (6 ft).

A total of 33 fault scarp profiles were measured in Madeline Plains, Dry Valley and southwestern Smoke Creek Desert. Profiles showing single seismic events were selected to determine approximate age dates. The scarp materials were visually classified in the field. In the Smoke Creek Desert, single event fault scarps of the BRFZ displace Sehoo and Fallon Alloformational deposits that consist of sandy fanglomerate, sand, silt and clay. The SLOPEAGE (Version 1) model of Nash (1980, 1984) is limited in application to cohesionless deposits. The diffusion model of Hanks and others (1984) was applied to fine grained deposits. Approximate ages were determined by applying the diffusion equation model of Nash (1980, 1984) to the measured profiles.

Nash's (1980, 1984) model is derived from the equation used in heat flow analysis. The diffusion equation represents a first-order, mathematical approximation to erosional evaluation of nondisecting alluvial terrains (Hank and others, 1984). The topographic equivalent of thermal diffusivity is a single parameter, k, which incorporates the specific erosional processes of the soil type and climatic conditions. The parameter, k, of Hanks and others (1984) is equivalent to Nash's (1980, 1984) parameter, c. This parameter is considered as mass diffusivity expressed in units of square

meters per 1,000 years or kiloannum ($m^2/10^3$ years or m^2/ka). Nash (1984) simplified the equation to:

$$c = ct/t_d, \qquad (1)$$

where c is the mass diffusivity coefficient, a function of climate and material; ct is the product of the coefficient and time derived from the scarp profile, and t_d is the approximate age of the scarp. The value ct can be calculated using the scarp slope angle (Θ_s) and the far-field or original topographic surface angle (Θ_f) by equations (2) and (3):

$$\tan \Theta_s = \frac{9}{(\pi ct)^{\frac{1}{2}}} + b, \qquad (2)$$

where b represents the original topographic slope and :

$$b = \tan \Theta_f \qquad (3)$$

Hanks and others (1984) showed the geometric relation of the scarp height as:

$$H = \frac{a}{1 - \frac{\tan\theta_f}{\tan\theta_s}}$$

From equation (4), a nonlinear relationship can exist between 2H and 2a (scarp offset) whenever $\tan \Theta_s$ is comparable to $\tan \Theta_f$. It is 2a that determines the scarp modification, not 2H (Hanks and others, 1984). The relationship of these fault

scarp parameters from Hanks and others (1984) is provided below:

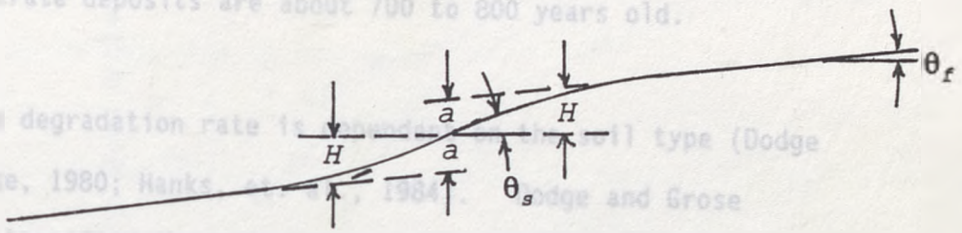

Fig. 1 of Hanks and Others (1984). The geometry of a fault scarp, mostly after Bucknam and Anderson (1979). In this study, we refer to 2a as the scarp offset and 2H as the scarp height. In the presence of nonzero θ_f, these amplitude measurements are not the same (see equation (11); and θ_s and θ_f are, respectively, the scarp slope angle and the far-field slope angle; the tangents of these angles are the scarp slope $\partial_u/\partial_x|_{x=0}$ and the far-field slope b, respectively.

If the value of c is known, the approximate scarp age (t_d) can be determined. For Lake Lahonton shoreline scarps cut into cohesionless gravelly alluvial fan deposits on the west flank of the Stillwater Range, the approximated c value is 1.1 + 0.5 $m^2/10^3$ years (Hanks and Wallace, 1985). Hecker (1985) determined c to be 1.3 $m^2/10^3$ years based on a larger data base of Lake Lahonton shoreline scarps. For the study area, the c values for Lake Lahonton were averaged (c = 1.2 $m^2/10^3$ years) to determine the approximate age of BRFZ scarps in cohesionless deposits. The ct product, scarp

height and offset were calculated using Nash's (1980) SLOPEAGE (Version 1) program. Based on this analysis, the ages of single tectonic event BRFZ scarps that displace alluvial fanglomerate deposits are about 700 to 800 years old.

The degradation rate is dependent on the soil type (Dodge and Grose, 1980; Hanks, et. al., 1984). Dodge and Grose (1980) classified the soil types along the Black Rock Fault (BRF) into three categories: 1) alluvial gravel, 2) lake gravel, and 3) lake clay. The fault scarps are approximately 1,400 years in age based on radiometric carbon dates. However, Dodge and Grose (1980) demonstrated that scarps in lake gravel and clay deposits degrade at a greater rate than scarps composed of alluvial gravel.

The relationship of scarp slope angle, scarp height and soil type for the BRFZ, BRF (Dodge and Grose, 1980) and Fish Springs (Bucknam and Anderson, 1979) is shown in Figure 24. The linear regression lines for Smoke Creek Desert are based on a limited data base. From the regression lines shown in Figure 24, the Smoke Creek Desert fault scarps are interpreted to contain a higher percentage of fine sediments, have initial slopes less than fault scarps in the Black Rock Desert and

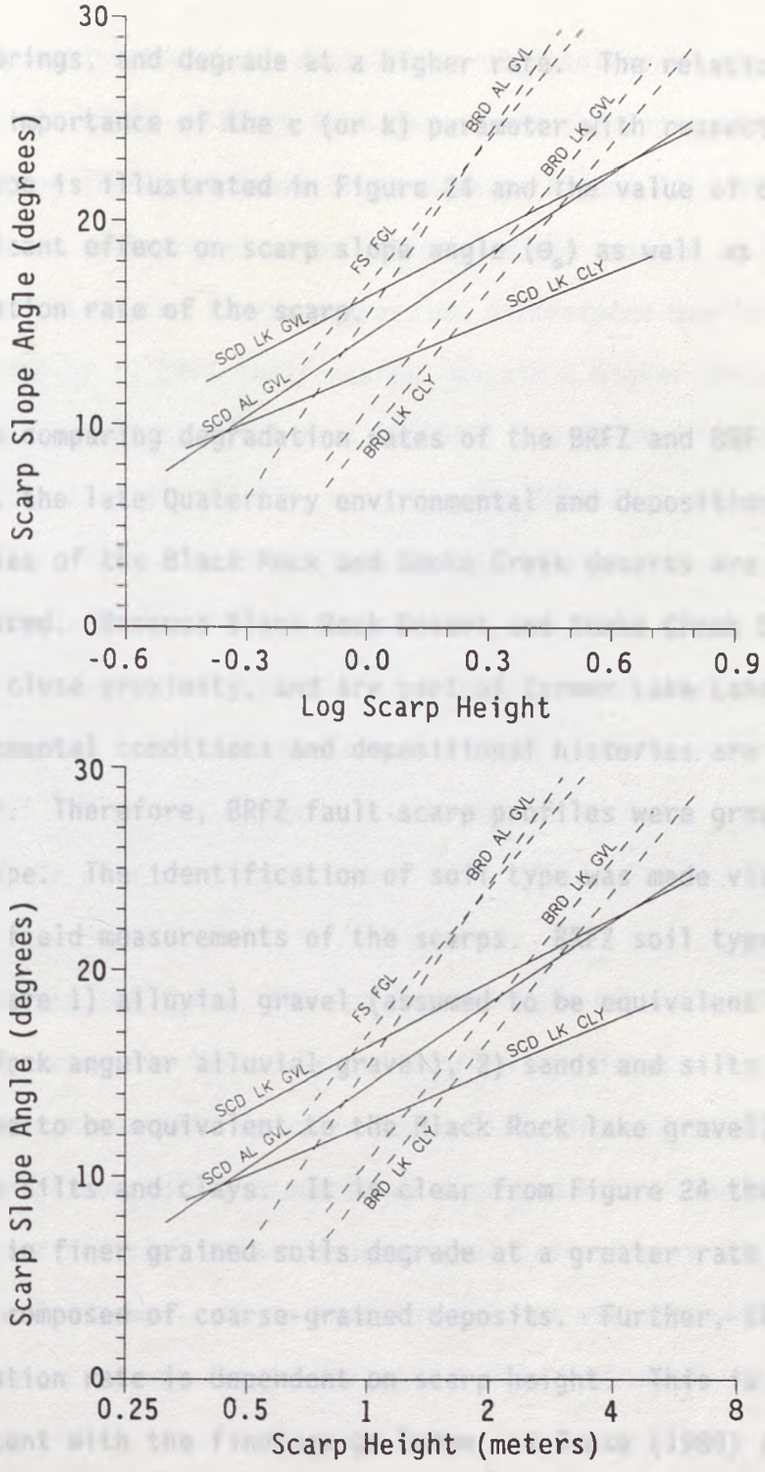

Figure 24. Comparison of linear regression best-fit lines of alluvial gravels/fan deposits (AL GVL), lake gravels/gravelly sands (LK GVL), fanglomerates (FGL), and lake clays (CLY) cut by faults in Smoke Creek Desert (SCD), Black Rock Desert, Nevada (BRD (Dodge and Grose, 1980)) and Fish Springs, Utah (FS (Bucknam and Anderson, 1979)).

Fish Springs, and degrade at a higher rate. The relationship of the importance of the c (or k) parameter with respect to soil type is illustrated in Figure 24 and the value of c has a significant effect on scarp slope angle (Θ_s) as well as the degradation rate of the scarp.

In comparing degradation rates of the BRFZ and BRF scarps, the late Quaternary environmental and depositional histories of the Black Rock and Smoke Creek deserts are considered. Because Black Rock Desert and Smoke Creek Desert are in close proximity, and are part of former Lake Lahonton, environmental conditions and depositional histories are similar. Therefore, BRFZ fault scarp profiles were grouped by soil type. The identification of soil type was made visually during field measurements of the scarps. BRFZ soil types groups are 1) alluvial gravel (assumed to be equivalent to the Black Rock angular alluvial gravel), 2) sands and silts (assumed to be equivalent to the Black Rock lake gravel), and 3) lake silts and clays. It is clear from Figure 24 that scarps in finer grained soils degrade at a greater rate than scarps composed of coarse-grained deposits. Further, the degradation rate is dependent on scarp height. This is consistent with the findings of Dodge and Grose (1980) and Hanks (1984).

Comparing the scarp degradation regressions of the Black Rock Fault (BRF) of Black Rock Desert and the Bonham Ranch fault zone (BRFZ) of Smoke Creek Desert (Figure 24), BRFZ scarps are interpreted to be younger and to degrade at a greater rate. The linear regression differences may be explained by 1) BRFZ fault scarps contain a higher percentage of fine-grained material than the BRF, and 2) BRFZ scarps are typically less than 2 m in height. The BRFZ faults are generally within the more distal parts of alluvial fans where the lithology becomes finer textured (Peterson, 1981). Scarps of 1 m or less in height tend to degrade faster than scarps greater than 1 m (Hanks and others, 1984). Since scarps on the BRFZ are generally about 1 m in height or less, they tend to degrade at a more rapid rate.

Radiometric age dates. The approximate ages of the BRFZ single event scarps were tested by radiocarbon age dates. A channel cut through the BRFZ scarp in T30N, R19E, Sec. 15 (Plate 4) exposed graben infill deposits of sand and silty sand that contained charcoal within depositional beds (Figure 25). Profile 7 (Appendix A) is near the channel exposure and shows that the scarp was formed during a single earthquake event.

Carbon samples were collected from the graben infill deposits at the locations shown on Figure 25. The samples

Figure 25. Graben infill deposits at the toe of the BRFZ fault scarp in T30N, R19E, Sec. 15 exposed in a channel cut. Charcoal sample locations are shown in a lensoidal sandy silt deposit. Radiometric C^{14} age dates from samples C38131 and C38132 are 290 ± 60 years and 290 ± 70 years B.P., respectively. Stadia rod is 1.85 m (6 ft). View is to the south.

C38131 = carbon sample location
A = lower carbon bed
B = cracks in deltaic deposits
Unit 1 = antesol
Unit 2 = poorly cemented eolian sand
Unit 3 = graben infill
Unit 3A = sand lens
Unit 4 = channel deposit
Unit 5 = Older eolian deposits
Unit 5A = sand lens
Unit 6 = cross-bedded sand
Unit 7 = red-brown coarse sand
Unit 8 = Bank slough and debris from cleaning exposure

were wrapped in aluminum foil, placed in plastic bags and shipped to Beta Analytical, Inc., Coral Gables, Florida, for radiometric C^{14} age dates. At Beta Analytical, Inc., the samples were pre-treated by examining for rootlets, then given a hot acid wash to eliminate carbonates. The samples were repeated rinsed to neutrality and subsequently given a hot alkali soaking to remove humic acids. The process was repeated with the hot acid wash and rinses to neutrality.

Carbon samples C38131 and C38132 yielded radiometric age dates of 290 ± 60 and 290 ± 70 years B.P., respectively. Table 1 provides a summary of the mass, counting time and age date for each sample. These C^{14} age dates represent minimum ages for the fault scarp and are the same order of magnitude as the approximated ages using Nash's (1980) method, which verified the applicability of scarp morphology profiling methods in this area.

The Dry Valley - Smoke Creek Ranch fault zone (DV-SCRFZ) is above the 1204 m (3950 feet) Fallon Alloformation datum and displaces Sehoo Alloformation sediments. The DV-SCRFZ profiles (Appendix A, Profiles 1 and 2) are on scarps near the valley floor and offset sand and silt deposits. The scarps are approximately 1 m in height, and have a maximum height of 2.9 m for a single event. These scarps have a high degradation rate, and the scarp morphology resembles that of older

TABLE 1

SUMMARY OF CARBON SAMPLE AGE DATES

	Sample C38131	Sample C38132
Mass (in grams)		
Initial	4.2	3.7
Dry pre-treated	2.7	1.8
Suitable C extracted	1.7	0.8
Counting Time (minutes)	1,300	2,700
C^{14} Age (years B.P. ± 1σ)	290 ± 60	290 ± 70

These dates analyzed by Beta Analytical, Inc. (Coral Gables, Florida) are reported as RCYBP (radiocarbon years before 1950 A.D.). By international convention, the half-life of radiocarbon is taken as 5,568 years and 95% of the activity of the National Bureau of Standards Oxalic Acid (original batch) used as the modern standard. The quoted counting errors are from the counting of modern standard, background, and sample being analyzed. They represent one standard deviation statistics (68% probability), based on the random nature of the radioactive disintegration process. Also, by international convention, no corrections were made for DeVries effect, reservoir effect, or isotope fractionation in nature.

faults. The DV-SCRFZ fault scarp morphology depicted on Profiles 1 and 2 (Appendix A) is similar to the BRFZ scarps composed of similar deposits. The ct value determined for Profile 1 (Plate 5) using SLOPEAGE (Nash 1980, 1984) and Hank and others, (1984) is 11.08 m^2 and 11.2 m^2, respectively. Using the c value of 87.9 m^2/ka determined from Profile 14 of a like soil, the estimated age by scarp profiling methods is 1,200 years. The DV-SCRFZ faults near the valley floor in Dry Valley have equivalent ages as the BRFZ and may have formed during the last BRFZ earthquake. In Smoke Creek Valley, the DV-SCRFZ displaces Quaternary-Tertiary basalts. However, data are inconclusive for evidence of more recent displacements.

The fault zone mapped in the north-central portion of Smoke Creek Valley (Plate 1) displaces volcanic rocks of upper Miocene and Pliocene age. The faults show subdued geomorphologic features in volcanic bedrock and lack well defined scarps. Based on geomorphic expression, it is unlikely that Quaternary tectonic activity resulting in surface displacement was younger than early Pleistocene.

For the faults in Madeline Plains, the diffusion models were applied to Profile 27 of Fault G in eastern Madeline Plains and time-stratigraphic correlations were applied to faults of the Likely fault zone (LFZ). Profile 27 of Fault G best fits the selection criteria

defined by Nash (1984). Diffusion parameters determined for Profile 27 are shown in Table 2:

TABLE 2

DIFFUSION PARAMETERS

Original surface angle Θ_s	Scarp slope angle Θ_f	Scarp offset m	ct m^2	c m^2/ka
7°	12°	0.96-1.0	9.17-9.38	87.9

From these parameters, the estimated age of the scarp on Fault G at Profile 27 is 10,500 ± 100 years.

Based on aerial photographic interpretations and field mapping, Fallon Alloformation equivalent deposits below elevation 1,637 m (5,370 ft) are displaced by the LFZ. This indicates tectonic activity along the southern portion of the LFZ since mid-Holocene (less than 5,000 years ago). Data is insufficient to evaluate recurrence intervals or whether more than one tectonic events have occurred within the last 5,000 years for the southern portion of the LFZ.

Tectonic Analysis

Late Cenozoic right-slip faults mark the western margin of the northern Basin and Range Province. These faults occur in three general zones of deformation: southern, central and northern. The southern and central zones include the Walker Lane Belt as defined by Stewart (1988) and illustrated in Figure 26. The southern zone in southeastern California and southern Nevada is a diffuse zone of north - northeast trending left-slip and normal faults, which include the Garlock and Lake Mead fault systems and northwest trending right-slip faults that include the Las Vegas and Death Valley/Furnace Creek fault zones (Burchfiel and Davis, 1973; Wernicke and others, 1982; Stewart, 1983 and 1988).

The central zone (Walker Lane) is a northwest trending, right-slip deformational zone up to 50 km wide (Ferguson and Muller, 1949; Nielsen, 1965; Shawe, 1965, Bonham and Slemmons, 1968; Bell, 1983; Stewart, 1983), which includes right-slip and conjugate left-slip faults in east-central California and west-central Nevada (Nielsen 1965; Wright, 1976; Bell and Slemmons, 1979; Slemmons and others, 1979; Bell, 1981; Molinari, 1983).

The northern zone in northeastern California and south-central Oregon consists of several right-stepping, right-slip faults which including the northern Walker Lane segment (Stewart, 1988), the Likely, Mount Mc Laughlin, Eugene-Denio, and Brothers fault zones (Donath, 1962; Pease, 1969; Lawrence, 1976; Wright, 1976; Roberts and Grose, 1982;

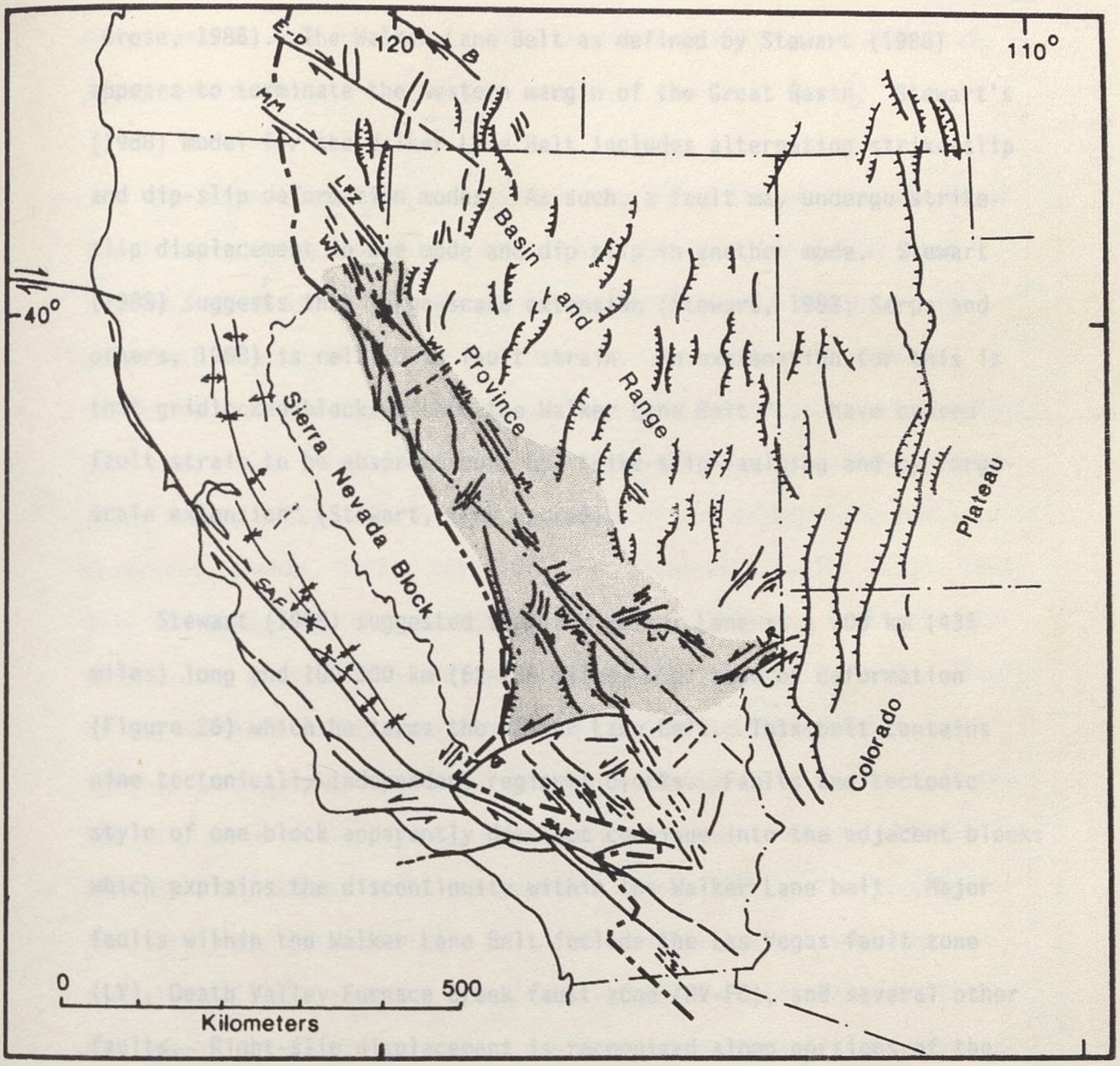

Figure 26. Simplified map showing the western termination of the Basin and Range Province by strike-slip faults (Pease, 1969; Lawrence, 1976; Wright, 1976) and the Walker Lane Belt (Stippled area) of Stewart (1988). Dashed line is approximate western boundary of the Basin and Range. Fault zone symbols are: B = Brothers; E-D = Eugene-Denio; MM = Mount Mc Laughlin; LFZ = Likely; WL = Walker Lane; DV/FC = Death Valley/Furnace Creek; LV = Las Vegas; G = Garlock; SAF = San Andreas. Modified from Wright (1976) and Stewart (1988).

Grose, 1986). The Walker Lane Belt as defined by Stewart (1988) appears to terminate the western margin of the Great Basin. Stewart's (1988) model for the Walker Lane Belt includes alternating strike-slip and dip-slip deformation modes. As such, a fault may undergo strike-slip displacement in one mode and dip-slip in another mode. Stewart (1988) suggests that large-scale extension (Stewart, 1983; Serpa and others, 1988) is related to fault strain. An explanation for this is that gridlocked blocks within the Walker Lane Belt "... have caused fault strain to be absorbed both by strike-slip faulting and by large-scale extension" (Stewart, 1988, p.705).

Stewart (1988) suggested that the Walker Lane is a 700 km (435 miles) long and 100-300 km (62-186 miles) wide zone of deformation (Figure 26) which he terms the Walker Lane Belt. This belt contains nine tectonically independent regional blocks. Faults and tectonic style of one block apparently does not continue into the adjacent blocks which explains the discontinuity within the Walker Lane belt. Major faults within the Walker Lane Belt include the Las Vegas fault zone (LV), Death Valley-Furnace Creek fault zone (DV-FC), and several other faults. Right-slip displacement is recognized along portions of the Walker Lane Belt (Shawe, 1965; Bonham and Slemmons, 1965; Hardyman and others, 1975; Molinari, 1983; Hamel, 1983; Bell, 1984). Stewart (1983) and Serpa and others (1988) suggested that the Death Valley-Furnace Creek faults are west dipping and terminate at a westward dipping

detachment surface, and that actual movement is extensional along the detachment surface.

The major structural deformation zone along the western margin of the Great basin is the Walker Lane Belt. The northern Walker Lane segment, which Stewart (1988) termed the Pyramid Lake Block, is the principal structural feature pertinent to this study. It extends northwest from the Carson Lineament (west-central Nevada) into the Honey Lake area of northeastern California (Bell and Slemmons, 1979;, Bell, 1984; Grose, 1986). The northern segment of the Walker Lane consists of divergent (Bonham, 1969), left-stepping, right-slip faults (Bell, 1984; Bell and Slemmons, 1979; Bonham and Slemmons, 1968) and right-oblique-slip faults (Grose, 1986, Vetter, 1984; Vetter and Ryall, 1983). Faults of the northern Walker Lane segment are the Pyramid Lake fault, Warm Springs fault, Honey Lake Fault and right-oblique-slip faults that trend N30-35°W north of Susanville, California (Bell and Slemmons, 1979; Bonham, 1969; Grose, 1986; Lemiszki and Brown, 1988). From regional seismicity and geomorphology, Bell (1984) suggested contemporaneous normal displacement on the Pyramid Lake fault. Fault plane solutions for recent seismicity indicate a contemporaneous normal-slip component within the northern Walker Lane segment (Vetter, 1984).

The Pyramid Lake fault trends about N50-55°W into Pyramid Lake where the Walker Lane steps left to the Warm Springs fault that trends about N60-65°W (Figure 27). These faults are separated by the Virginia

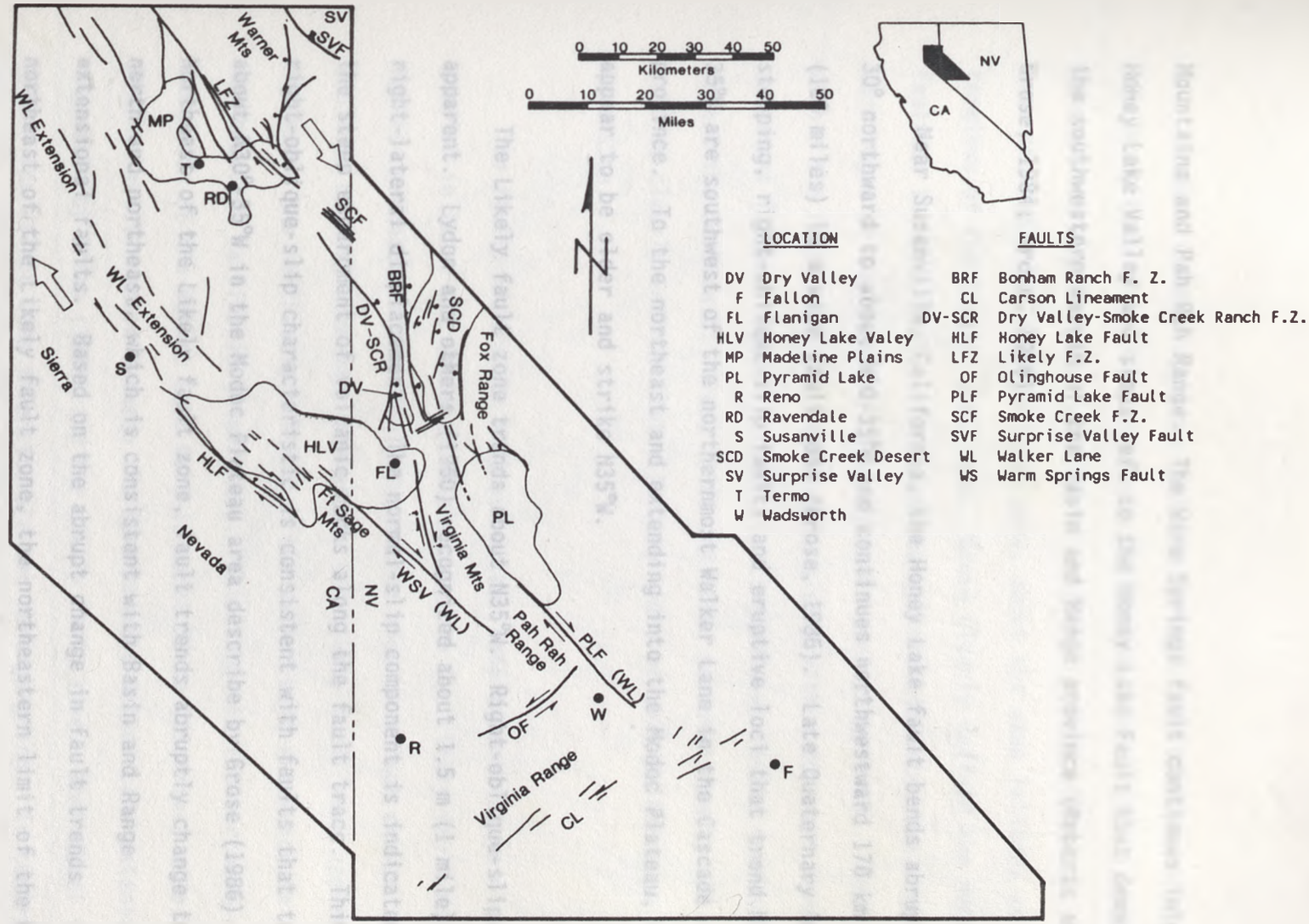

Figure 27. Diagrammatic sketch illustrating the spatial relationship of the Likely fault zone and the Walker Lane in northwestern Nevada and northeastern California. Faults were compiled from Gay and Aune (1959), Lydon and others (1960), Bonham (1969), Bell and Slemmons (1979, 1982), Bell, E. (1984), and Bell, J. (1986).

Mountains and Pah Rah Range. The Warm Springs fault continues into Honey Lake Valley and steps left to the Honey Lake Fault that demarks the southwestern margin of the Basin and Range province (Roberts and Grose, 1984; Grose, 1986).

Near Susanville, California, the Honey Lake fault bends abruptly 30° northward to about N30-35°W and continues northwestward 170 km (105 miles) in a wide fault zone (Grose, 1986). Late Quaternary left-stepping, right-oblique-slip faults and eruptive loci that trend N15-35°W are southwest of the northernmost Walker Lane in the Cascade province. To the northeast and extending into the Modoc Plateau, faults appear to be older and strike N35°W.

The Likely fault zone trends about N35°W. Right-oblique-slip is apparent. Lydon and others (1960) recognized about 1.5 m (1 mile) of right-lateral displacement. The normal-slip component is indicated by the steep escarpment of volcanic rocks along the fault trace. This right-oblique-slip characteristic is consistent with faults that trend about N30°-35°W in the Modoc Plateau area describe by Grose (1986). Northeast of the Likely fault zone, fault trends abruptly change to north and northeast, which is consistent with Basin and Range extensional faults. Based on the abrupt change in fault trends northeast of the Likely fault zone, the northeastern limit of the Walker Lane is placed at the Likely fault zone.

Stewart (1988) suggested that the Pyramid Lake block terminates in the Honey Lake area of northeastern California. Grose (1986), however, extended the Walker Lane as a 24-28 km (15-17 miles) wide fault zone into the Medicine Lake Highlands area, about the same latitude as the terminus of the Likely fault zone. Grose clearly defined the Honey Lake Fault as the southwestern limit of the Walker Lane extension, but is more vague in the Medicine Lake Highlands area (Figure 28). Faults within the fault zone are right-oblique-slip with a dominant normal-slip component (Grose, 1986). Further, spacing between faults increases toward the northeast. Grose (1986 and 1988, personal comm.) did not provide clearly defined limits for the width of this Walker Lane extension.

The faults within the northern Walker Lane extension are clearly similar in trend and sense of displacement to the Likely fault zone. Faults northeast of the Likely fault zone show an abrupt change in trend and mode of displacement. Therefore, the Likely fault zone appears to represent the northeastern limit of the Walker Lane extension in northeastern California (Figure 28). This suggests the northern extension of the Walker Lane belt is about 35 km (22 miles) wide. Dissimilarities exist between the northernmost Walker Lane extension as suggested by Grose (1986) and the Likely fault zone. Individual faults within the Walker Lane extension are not through-going. In contrast, the Likely fault zone is a well-defined, 104-km (65-mile) long continuous fault zone. Individual faults of the Walker Lane extension

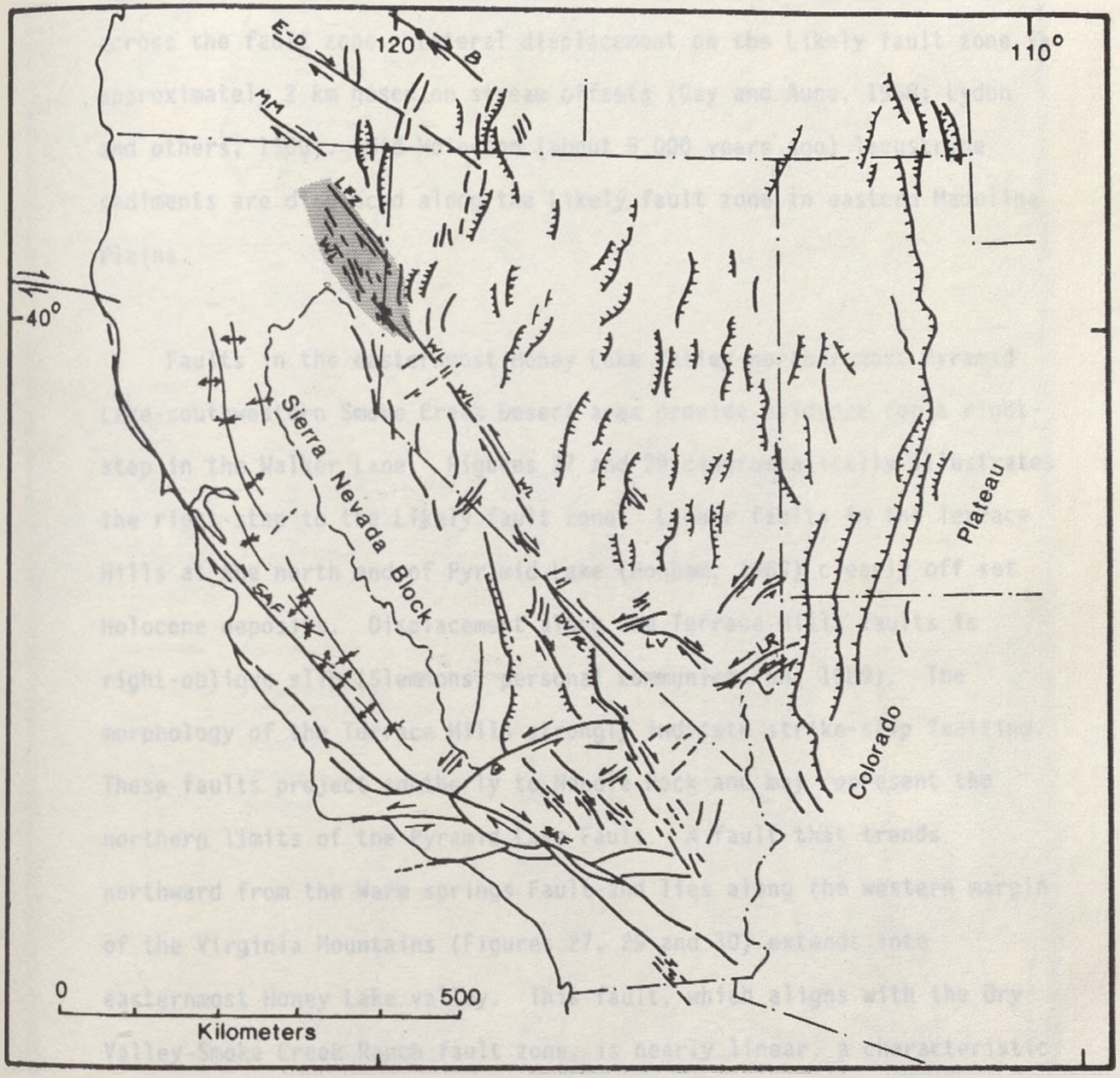

Figure 28. Generalized area of the northern extension of the Walker Lane Belt in northeastern California (shaded area). The Likely fault zone (LFZ) marks the northeastern limit of the Walker Lane Belt. The southwestern boundary is not clearly defined (Grose, personal comm., 1990).

lack significant lateral displacement (Grose, 1986, and personal communication, 1990). However, lateral displacement may be cumulative across the fault zone. Lateral displacement on the Likely fault zone is approximately 2 km based on stream offsets (Gay and Aune, 1958; Lydon and others, 1960). Mid-Holocene (about 5,000 years ago) lacustrine sediments are displaced along the Likely fault zone in eastern Madeline Plains.

Faults in the easternmost Honey Lake Valley-northernmost Pyramid Lake-southwestern Smoke Creek Desert area provide evidence for a right-step in the Walker Lane. Figures 27 and 29 diagrammatically illustrates the right-step to the Likely fault zone. Linear faults in the Terrace Hills at the north end of Pyramid Lake (Bonham, 1969) clearly off set Holocene deposits. Displacement along the Terrace Hills faults is right-oblique slip (Slemmons, personal communication, 1989). The morphology of the Terrace Hills strongly indicate strike-slip faulting. These faults project southerly to Needle Rock and may represent the northern limits of the Pyramid Lake Fault. A fault that trends northward from the Warm springs Fault and lies along the western margin of the Virginia Mountains (Figures 27, 29 and 30) extends into easternmost Honey Lake valley. This fault, which aligns with the Dry Valley-Smoke Creek Ranch fault zone, is nearly linear, a characteristic of strike-slip faults.

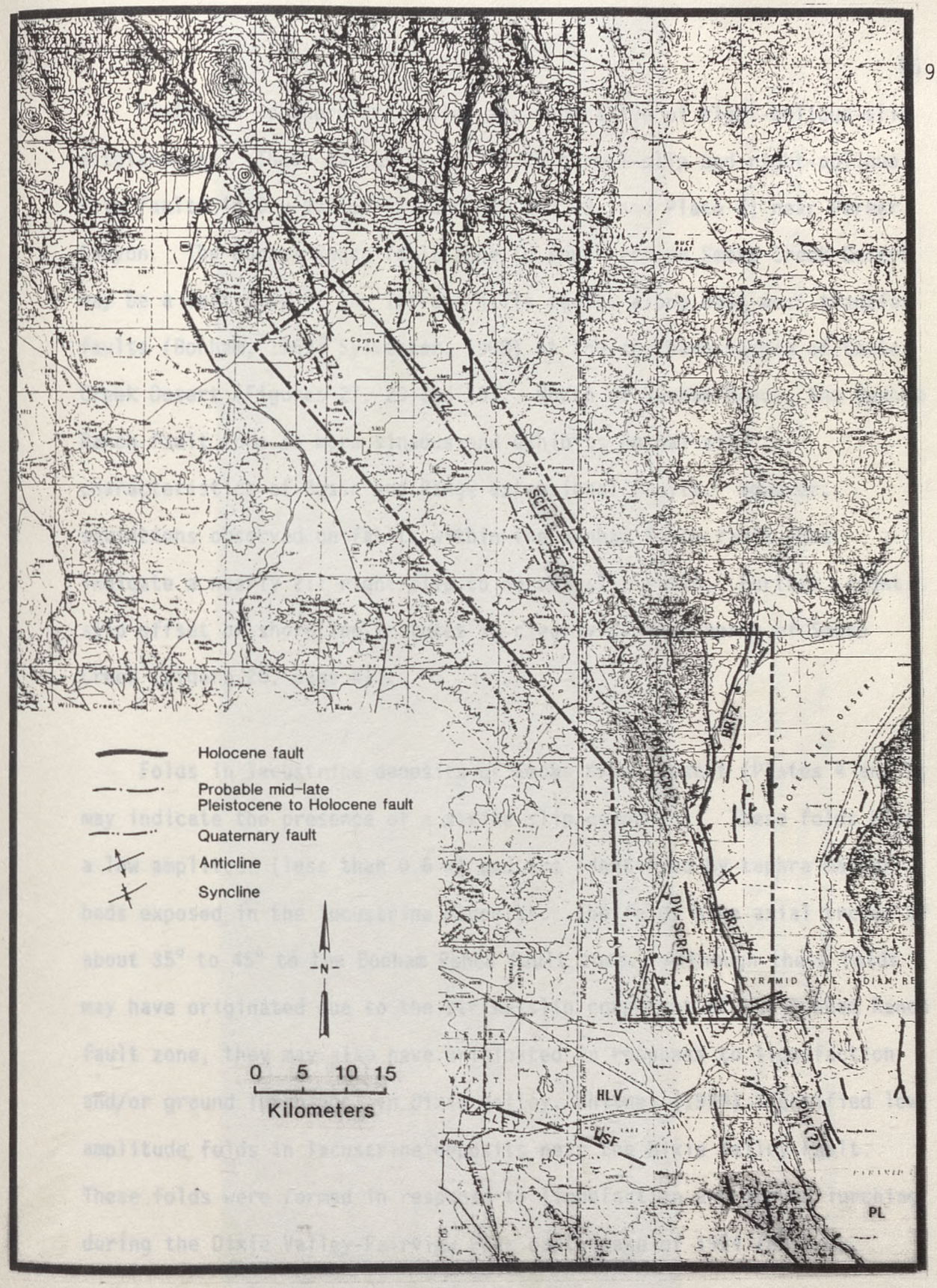

Figure 29. Simplified fault map of southwestern Smoke Creek Desert, Nevada and Madeline Plains, California. Bold Lines represent faults with evidence of Holocene displacement. Abbreviations for faults as shown on Figure 27.

Faults in southern Dry Valley are indicative of right-oblique-slip displacement. These faults step left to normal-slip and right-oblique-slip faults in Dry Valley (Figures 27 and 29, and Plate 4) near Parker Canyon. The Bonham Ranch fault zone in southwestern Smoke Creek Desert may be a left-step of the Terrace hills faults along east-west transfer faults (Bonham, 1969; Sylvester, 1988) at the southern margin of Smoke Creek Desert (Figures 27, 29 and 30). North of Bonham Ranch, the Bonham Ranch fault zone is more sinuous and exhibits normal-slip characteristics of Basin and Range extensional faults. However, striations observed on faults within the Bonham Ranch fault zone indicate a nearly 2:1 right-slip to normal-slip ratio. Further, right-slip offset of shoreline features is clearly evident north of Smoke Creek (Figure 20, page 61).

Folds in lacustrine deposits of Smoke Creek Desert (Plates 4 and 5) may indicate the presence of a strike-slip component. These folds have a low amplitude (less than 0.6 m) and are identified by tephra marker beds exposed in the lucustrine deposits. The folds have axial trends of about 35° to 45° to the Bonham Ranch fault zone. Although these folds may have originated due to the strike-slip component of the Bonham Ranch fault zone, they may also have originated in response to liquefaction and/or ground lurching. In Dixie Valley, Whitney (1978) identified low amplitude folds in lacustrine deposits near the Dixie Valley Fault. These folds were formed in response to liquefaction and ground lurching during the Dixie Valley-Fairview Peak earthquake of 1954 (Whitney,

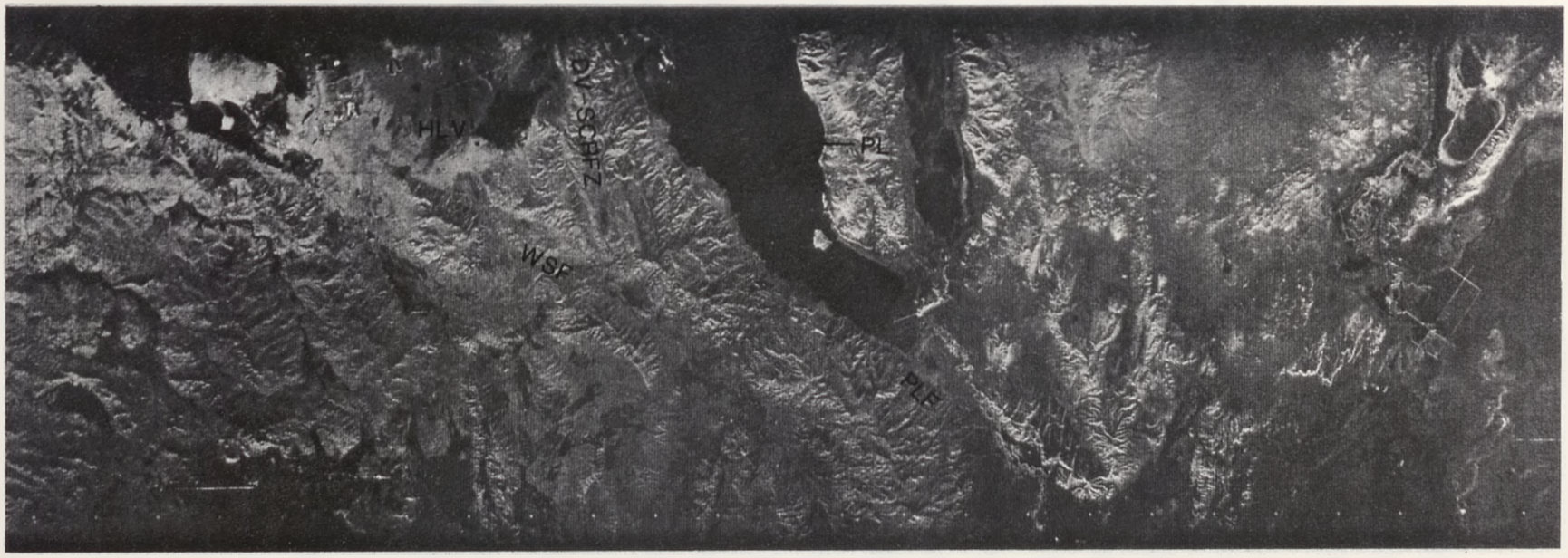

Figure 30. Space Shuttle SIR-A imagery of the Pyramid Lake, Nevada and southern Honey Lake Valley, California and Nevada delineating the Warm Springs fault (WSF) and Pyramid Lake fault (PELF) of the Walker Lane. The southern extension of the Dry Valley-Smoke Creek Ranch fault zone (DV-SCRFZ) may be the fault about 45°-50° from the Warm Springs fault.

1980). In Smoke Creek Desert, Whitney (personal communication, 1987) observed the folds and suggested a liquefaction and/or ground lurching origin based on their similarities to the folds in Dixie Valley.

Eastern Honey Lake Valley may be a pull-apart basin formed between the Warm Springs fault and the right-step to the Dry Valley-Smoke Creek Ranch fault zone (Figure 28). The Warm Springs fault diverges westward in eastern Honey Lake Valley from the trend of the Pyramid Lake Fault. A linear fault that trends about 45°-50°N of the Warm Springs fault, lies along the western margin of the Virginia Mountains and extends into easternmost Honey Lake Valley (Figures 27, 29 and 30), may be an extension of the Dry Valley-Smoke Creek Ranch fault zone.

In the northern Walker Lake block, the Walker Lane is presumed to step left from the Pyramid Lake Fault to the Warm Springs Fault and to the Honey Lake Fault (Figure 27), that Grose (1986) defines as the western limit of the Walker Lane. The right-slip faults in the Terrace Hills at the north end of Pyramid lake may be the northern terminus of the Pyramid Lake Fault and appear to step left to the Bonham ranch fault zone. Further, the Walker Lane may also step right along the linear fault that lies along the western edge of the Virginia Mountains to the Dry Valley-Smoke Creek Ranch fault zone (Figure 27, 29 and 30). The Dry Valley-Smoke Creek and the Bonham Ranch fault zones appear to step left to the Likely fault zone.

The block, defined by the Warm Springs Fault, the unnamed fault that lies along the western margin of the Virginia Mountains, the Honey Lake Fault and northern extension of the Walker Lane on the west, and the Dry Valley-Smoke Creek Ranch, Bonham Ranch and Likely fault zones on the east, may be migrating northwestward along several right-oblique-slip faults within the Walker Lane (Figure 27). Therefore, eastern Honey Lake Valley and southwestern Smoke Creek Desert may be young pull-apart basins formed along the trailing edge of the northwestward migrating block.

In the Smoke Creek Valley area, the Dry Valley-Smoke Creek Ranch fault zone bends abruptly to trend about N30°W. The fault zone is parallel to the Smoke Creek fault zone and Likely fault zone. The DV-SCRFZ is less sinuous in Smoke Creek Valley which indicates a strike-slip component. Smoke Creek Valley that trends N30°W and is deeply incised in Pliocene-Pleistocene basalt flows may well be fault controlled and represent the northwestward extension of the Dry Valley - Smoke Creek Ranch fault zone.

In summary, the Walker Lane steps left and right north of Pyramid Lake in the Honey Lake Valley and Smoke Creek Desert area. The Honey Lake Fault and northern extension of the Walker Lane denote the western limit of the Walker Lane. The Dry Valley-Smoke Creek Ranch and Bonham Ranch fault zones mark a right step in the Walker Lane to the Likely fault zone. Faults east of the Likely fault zone are divergent to the

Likely fault zone and are characteristic of Basin and Range extensional faults, whereas the Likely is parallel to the faults within the northern extension of the Walker Lane as described by Grose (1986). Therefore, the Likely fault zone marks the eastern limit of the Walker Lane, and the block bounded by eastern Honey Lake Valley to the south and the Walker lane limits as described above may be migrating northwestward along northwest trending right-oblique-slip faults. Eastern Honey Lake Valley and southwestern Smoke Creek Desert may be young pull-apart basins forming along the trailing edge of the block.

Regional strike-slip faults that are limited to the crust and separate regional tectonic domains are intraplate transform faults (Sylvester, 1988). The northern portion of the Walker Lane defined by Bell (1984) and Grose (1986), Likely fault zone and strike-slip faults in Oregon (Lawrence, 1976) separate domains of different tectonics. Seismic reflection and refraction interpretations (Knuepfer and others, 1987; Lemiszki and Brown, 1988) show that the Walker Lane and Likely fault zone are limited to the crust.

The COCORP and U.S. Geological Survey conducted a seismic reflection survey along the 40°N latitude in Nevada (Knuepfer and others, 1987) and a seismic refraction survey across the Klammath Mountains, Cascade Range, Modoc Plateau and Basin and Range provinces in northeastern California and northwestern Nevada (Fuis and others, 1988), respectively. The COCORP 40°N Latitude seismic reflection profile

crosses the Warm Springs and Pyramid Lake faults of the Walker Lane (Figures 31 and 32). Knuepfer and others (1987) interpret a mid-crustal detachment between 14 and 23 km (9 and 14 miles) beneath the Walker Lane in the Pyramid Lake region (Figure 32). This inferred detachment dips southwest. Moderate to steep faults that also dip southwest are projected to the surface at the Pyramid Lake Fault. These steep faults accommodate contemporaneous right-slip and normal displacements (Vetter, 1984; Vetter and Ryall, 1983; Lemiszki and Brown, 1988). The Warm Spring fault soles in an east dipping reflection (fault) that is terminated by the southwest dipping fault. Knuepfer and others (1987) interpret the basal surface of the Sierra Nevada batholith root at about 37 to 41 km (23 to 25 miles) in depth.

The U.S. Geological Survey east-west seismic refraction line (Fuis and others, 1988) crosses the Klammath Mountains, Cascade Range, Modoc Plateau, and extends into the Basin and Range province in northeastern California (Figure 33). The transect crosses the Likely fault zone at Shot Point 11. From the seismic refraction velocities, granitic and metamorphic basement rocks have been interpreted beneath the Modoc Plateau, which are generally consistent with basement rocks of the Sierra Nevada and other batholiths (Lynn and others, 1981; Fuis and others, 1988). These rocks may represent one or more magmatic arcs that have roots to about 35 to 40 km (22 to 25 miles). The depth of the granitic basement rock beneath the Modoc Plateau may to be at least 38 km (24 miles) (Lynn and others, 1981).

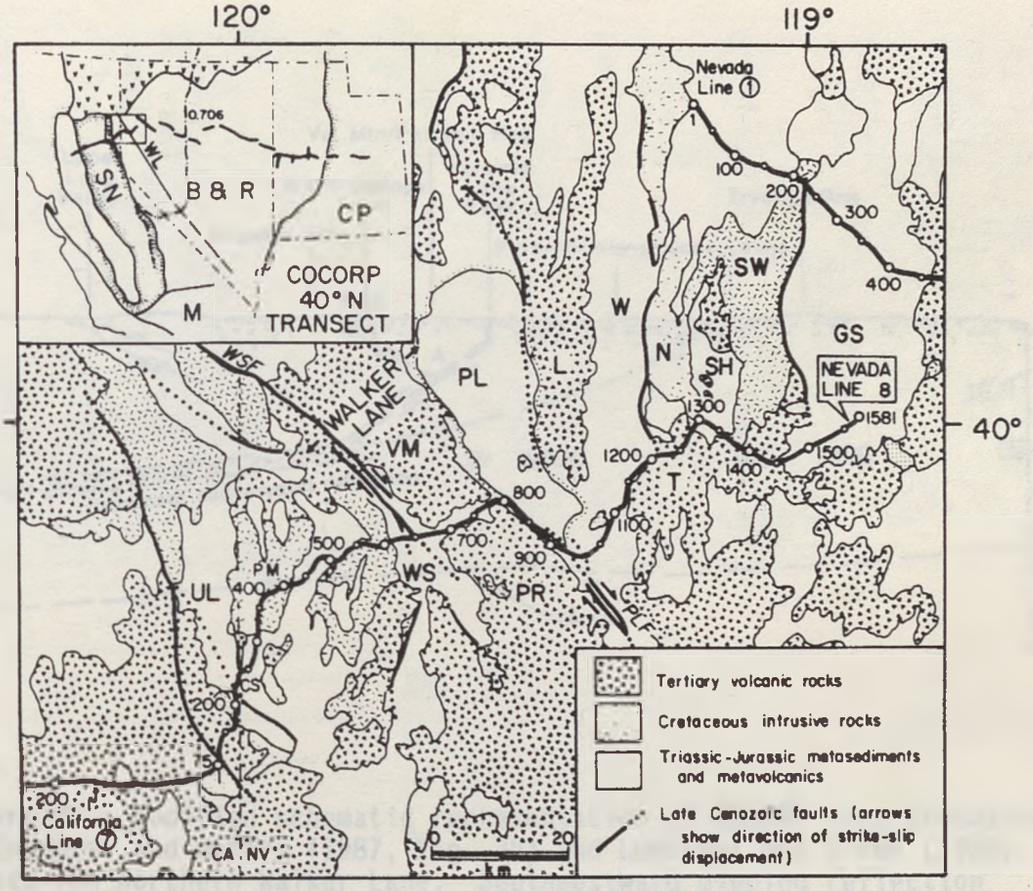

Figure 31. Generalized geologic map of the vicinity of Nevada Line 8, modified from Jennings (1977) and Stewart and Carlson (1978). Inset shows regional physiographic/tectonic provinces (SN, Sierra Nevada; B&R, Basin and Range; CP, Colorado Plateau; M, Mojave; WL, Walker Lane and 0.706 isotope ratio isopleth modified from Kistler and Peterman (1973). Faults of the Walker Lane are indicated by WSF (Warm Springs fault) and PELF (Pyramid Lake fault). UL, Upper Long Valley; CS, Cold Springs Valley; PM, Peterson Mountain; WS, Warm Springs Valley; VM, Virginia Mts.; PR, Pah Rah Range; PL, Pyramid Lake; L. Lake Range; W, Winnemucca Lake Valley; N, Nightingale Mts.; T, Truckee Range; SH, Sage Hen Valley; SW, Shawave Mts.; GS, Granite Springs Valley.

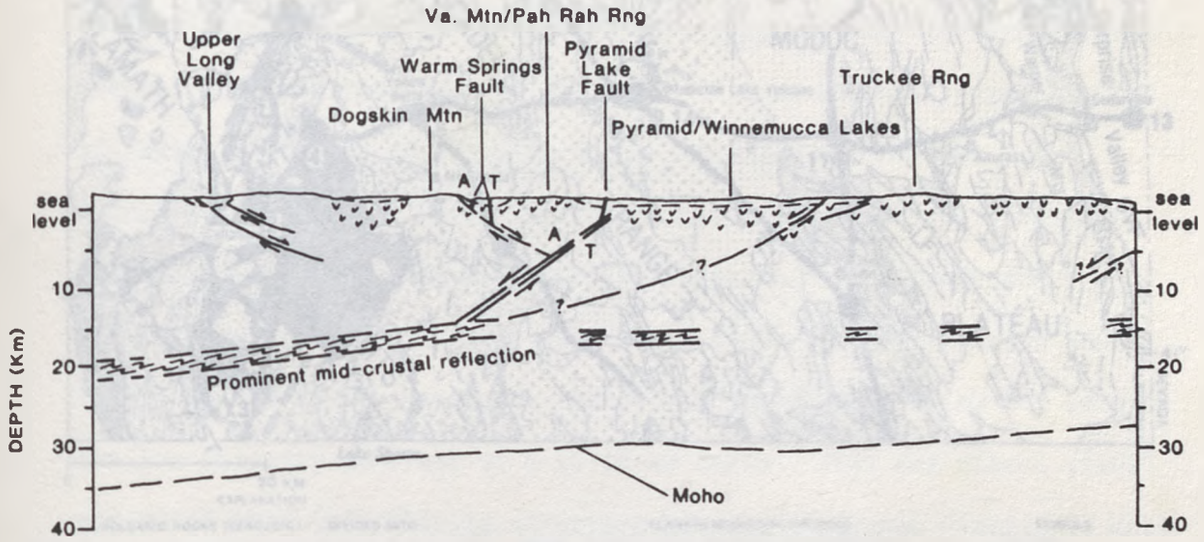

Figure 32. Modified schematic representation of COCORP interpretations by Knuepfer and others (1987, Fig. 2b) and Lemiszki and Brown (1988) across the northern Walker Lane. Southwestward dipping reflection surface projects to the surface trace of Pyramid Lake fault or into Pyramid Lake. This surface may be a detachment similar to the Death Valley detachment (Serpa and others, 1988). The southwestward dipping reflection is truncated by a prominent sub-horizontal mid-crustal reflection (detachment ?). The Warm Springs fault is terminated by an east dipping reflection that terminates at the southwestward dipping detachment. Major faults are diagrammatically shown. For strike-slip faults, A indicates movement away from viewer and T, towards viewer. H:V = 1:1.

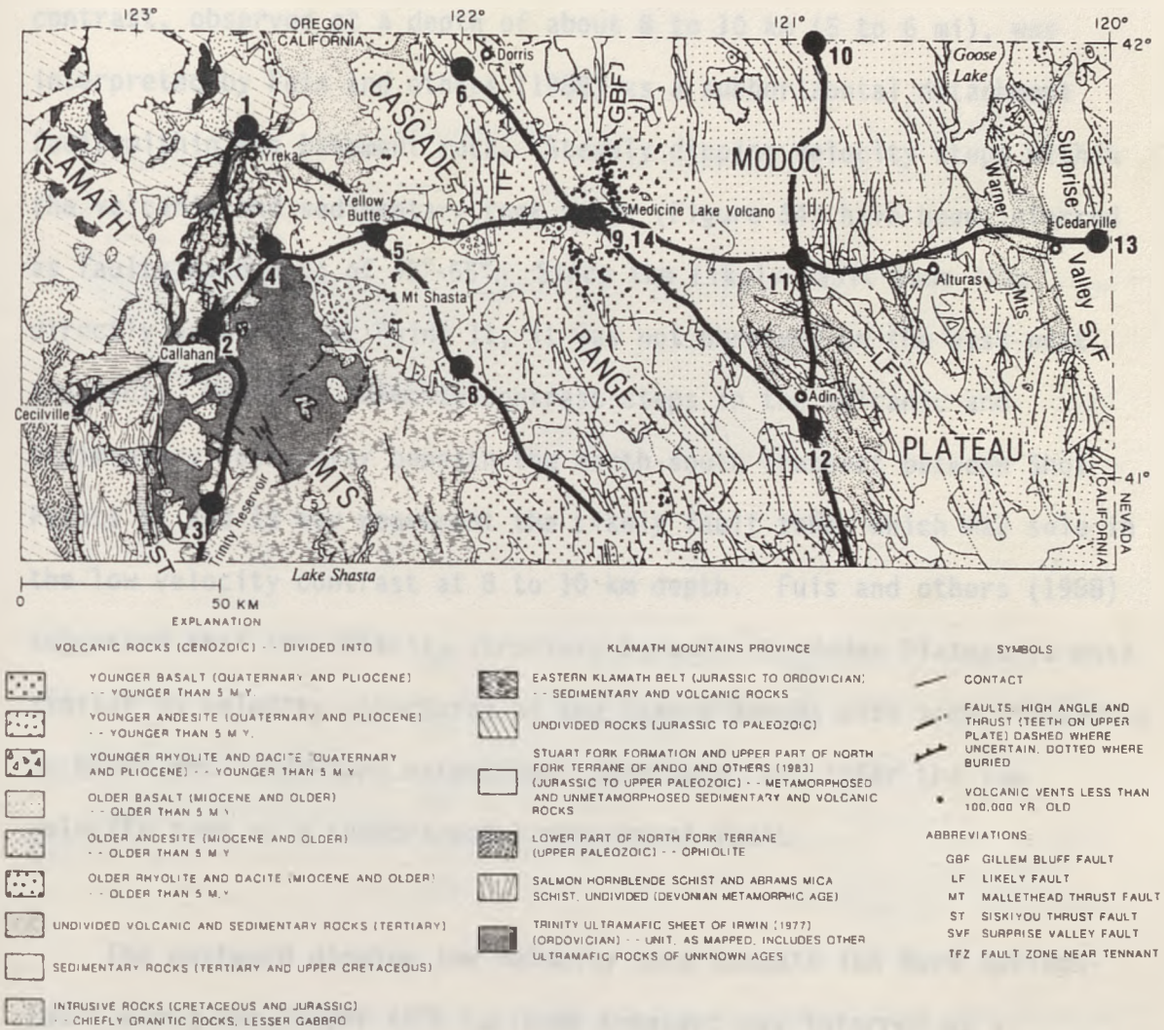

Figure 33. Geologic map of the northeastern California U.S. Geological Survey seismic refraction lines from Figure 2 of Fuis and others (1988). The east-west line from Cecilville to Cedarville, California, provides a cross section of the Modoc Plateau. Shot Point 11 is on the Likely fault zone.

Figure 34 diagrammatically illustrates the inferred structure beneath the Modoc Plateau along the east-west seismic refraction transect in northeastern California. A westward dipping low velocity contrast, observed at a depth of about 8 to 10 km (5 to 6 mi), was interpreted by Fuis and others (1988) as a subhorizontal detachment fault within the basement rock. Steeply dipping velocity steps within the volcanic and sedimentary rock cover (Figure 34) have been inferred as faults with dips of 45°-65°. Since the Likely fault zone lies directly beneath Shot Point 11, it was not observed on the east-west transect. However, velocity contrast steps in the volcanic and sedimentary rock cover beneath the north-south transect between Shot Points 11 and 12 may represent the Likely fault zone, which may sole in the low velocity contrast at 8 to 10 km depth. Fuis and others (1988) suggested that the velocity structure beneath the Modoc Plateau is most similar to velocity structures of the Sierra Nevada with some similarity to Basin and Range-type extensional structure, and infer the low velocity zone as a subhorizontal detachment fault.

The westward dipping low velocity zone beneath the Warm Springs Fault along the COCORP 40°N latitude transect was inferred as a subhorizontal detachment fault (Knuepfer and others, 1987; Lemiszki and Brown, 1988). Moderate dipping faults of the Walker Lane appear to sole in this inferred detachment fault (Figure 33). Similarly, moderate to steeply dipping faults terminate in the inferred westward dipping detachment fault beneath the Modoc Plateau. The inferred subhorizontal

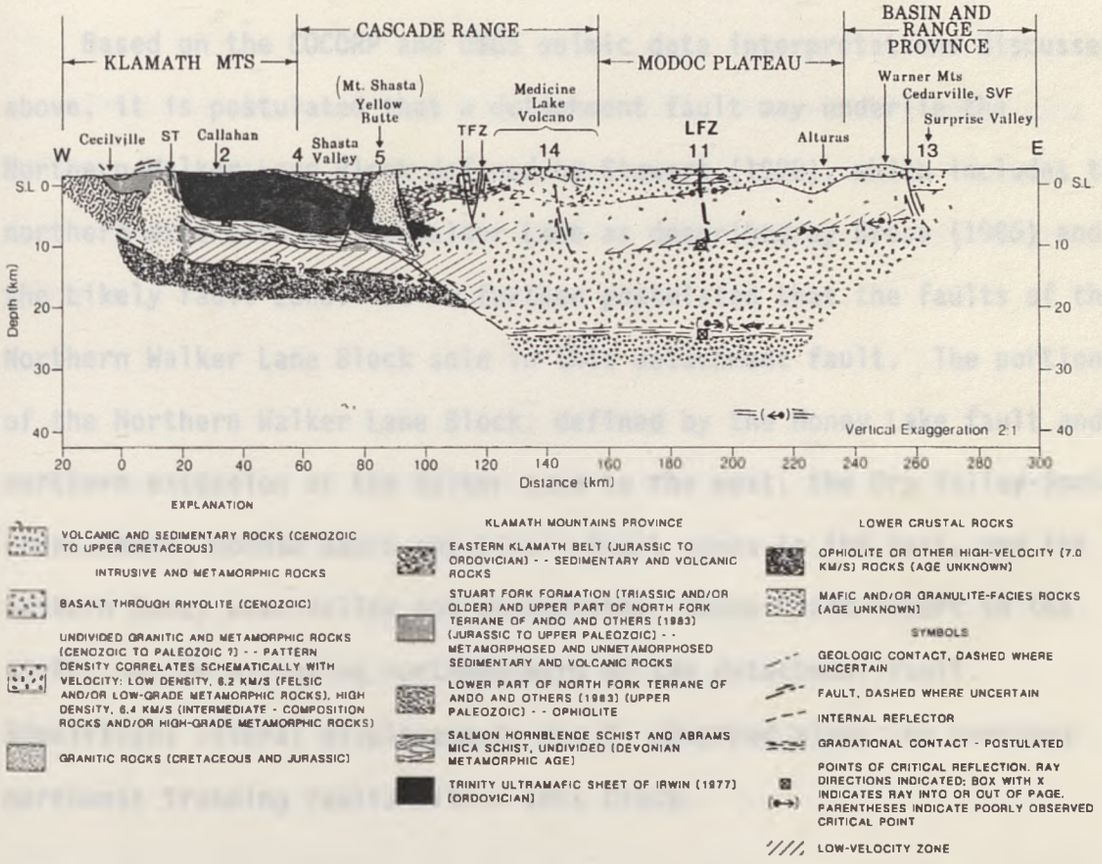

Figure 34. Geologic cross section along the east-west line constructed from velocity-density model (Fig. 5 of Fuis and others, 1988). Klamath Mountains are underlain by stack of oceanic layers. Modoc Plateau is inferred to be underlain, beneath layer of volcanic and sedimentary rocks, by crystalline igneous and metamorphic rocks, constituting roots of magmatic arcs. Cascade Range, in between, is complex suture region, currently being intruded by magma. The northern terminus of the Likely fault zone lies below Shot Point 11 and is not observed in this east-west transect. The dip of the Likely fault zone shown here is inferred from the velocity steps in a north-south transect through Shot Point 11.

detachment at a depth of about 8 to 10 km may be the same low velocity contrast zone inferred as a subhorizontal detachment beneath the Walker Lane on the COCORP 40°N transect, albeit dissimilarities in crustal thickness and rock types inferred from the velocities.

Based on the COCORP and USGS seimic data interpretations discussed above, it is postulated that a detachment fault may underlie the Northern Walker Lane Block defined by Stewart (1988), which includes the northern extension of the Walker Lane as described by Grose (1986) and the Likely fault zone. It is further postulated that the faults of the Northern Walker Lane Block sole in this detachment fault. The portion of the Northern Walker Lane Block, defined by the Honey Lake fault and northern extension of the Walker Lane to the west, the Dry Valley-Smoke Creek Ranch, Bonham Ranch and Likely fault zones to the east, and the eastern Honey Lkae Valley and southwestern Smoke Creek Desert to the south, may be migrating northwestward on the detachment fault. Significant lateral displacements may be absorbed along the numerous northwest trending faults within this block.

The northwestward migration of the Panamint Range block and the formation of the central Death Valley pull-apart in eastern California, and western Nevada, (Stewart, 1983; Serpa and others, 1988) may be analoguos to the Northern Walker Lane Block. Stewart (1983) suggested that the Panamint Range is a structural block which detached from underlying basement rock and was tectonically transported northwestward

along a subhorizontal detachment fault. Interpretations of COCORP profiles in the southern Great Basin (Sepra and others, 1988) have identified the detachment fault postulated by Stewart (1983). Further, Serpa and others (1988) refer to central Death Valley as a pull-apart, formed along the trailing edge of the Panamint Range.

From the above analogy, it is postulated that eastern Honey Lake Valley and southwestern Smoke Creek Desert may be a young pull-apart basin that is forming along the trailing edge of the northwest migrating block within the Northern Walker Lane Block.

CONCLUSIONS

The geologic mapping of this study represents the first detailed Quaternary mapping in the eastern Madeline Plains, California and southwestern Smoke Creek Desert, Nevada. Previous geologic mapping (Bonham, 1969; Gay and Aune, 1958; Lydon and others, 1960) provided regional geologic maps. Dodge (1978) mapped in detail the Quaternary geology of west-central Smoke Creek Desert. This study extends the work of Dodge into southwestern Smoke Creek Desert.

This study delineated and defined: 1) the southern limits of the Likely fault zone in northeastern California, and 2) faults in southwestern Smoke Creek Desert. Sediments about 12,000 and 5,000 years in age provide evidence for late Pleistocene and Holocene surface ruptures on the southeasternmost portion of the Likely fault zone and faults in southwestern Smoke Creek Desert. Two prominent fault zones were mapped in southwestern Smoke Creek Desert. These fault zones are herein informally named the Dry Valley-Smoke Creek Ranch (DV-SCRFZ) and Bonham Ranch (BRFZ) fault zones.

The DV-SCRFZ is a right-oblique-slip fault zone that bounds the western margin of Dry Valley. The DV-SCRFZ bends abruptly about 30° northwest at Smoke Creek and extends to Smoke Creek reservoir, a total fault length of approximately 50 km (31 miles). The fault zone experienced at least two faulting events since uppermost Pleistocene.

The last faulting event resulting in surface rupture (up to 1.1 m) may have been contemporaneous with the last event on the BRFZ. The DV-SCRFZ varies from nearly pure normal displacement in the northerly part of Dry Valley and Smoke Creek Valley to right-oblique slip in the southerly portion of Dry Valley.

The BRFZ is a right-oblique slip fault zone that extends from approximately 12 km north of Buffalo Creek in west-central Smoke Creek Desert to southwesternmost Smoke Creek Desert. It has a total length of at least 48 km, delineated by a nearly through-going fault scarp and several subparallel faults in a broad zone that extends well into Smoke Creek Desert playa. At least two faulting events resulted in surface ruptures, as shown by scarp morphology. Radiometric age dates place the last surface rupture event at 290 ± 60 to 70 years B.P.

The Likely fault zone splays into several faults immediately north of eastern Madeline Plains: Faults D and E (Plate 1) displace deposits equivalent to the Fallon Alloformation (<5,000 years in age) and terminate on the east flank of Observation Peak. Gay and Aune (1958) estimated 2 km of right-slip displacement from offset drainage north of Madeline Plains. Right-slip displacement within eastern Madeline Plains ranges from a few meters to about 150 m.

Uppermost Pleistocene deposits (<12,000 years in age) are displaced by up to 1.7 m of vertical separation by north trending normal faults

that bound the eastern margin of Madeline Plain. These faults extend across the southern Warner Mountains and terminate at the Surprise Valley fault, a Basin and Range extensional fault with at least 1 km vertical displacement (Fuis and others, 1988). The north-south faults that include Fault zone G which bound the eastern margin of Madeline Plains may be conjugate normal faults to the northwest trending Likely fault zone.

Based on the change in fault trends east of the Likely fault zone and structural similarities interpreted from U.S. Geological Survey seismic refraction data (Fuis and others, 1988) and COCORP seismic reflection data (Knuepfer and others, 1987; Lemiszki and Brown, 1988), the Likely fault zone represents the northeastern limit of the northern segment of the Walker Lane defined by Bell (1984), Roberts and Grose (1984) and Grose (1986). The Likely fault zone appears to be a right-step in an otherwise left-stepping tectonic system.

It is proposed that the Pyramid Lake Fault extends into southernmost Smoke Creek Desert. Evidence that supports this extension of the Pyramid Lake Fault includes: 1) right-oblique-slip faults that displace Holocene deposits in the northern Pyramid Lake area (Slemmons, personal communication, 1989), and 2) strike-slip terrain in the Terrace Hills immediately north of Pyramid Lake (Slemmons, personal communication, 1989; Whitney, personal communication, 1989). A small apparent left-slip transfer fault zone at the southernmost end of Smoke

Creek Desert (Bonham, 1969; Slemmons, personal communication, 1989) provides a left-step to the BRFZ. Further, north trending faults in easternmost Honey Lake Valley are consider the extension of the DV-SCRFZ to the Warm Springs fault.

The block defined by the right-step of the Walker Lane to the Likely fault zone on the east and the Honey Lake Fault and northern extension of the Walker Lane on the west may be migrating northwestward along the numerous northwest trending faults within the block. Eastern Honey Lake Valley and southwestern Smoke Creek Desert may represent a young pull-apart basin that is forming along the trailing edge of this block.

In summary, the northern segment of the Walker Lane includes the Likely fault zone. In northeastern California, the Walker Lane trends about N30 -35 W and is delineated by a broad zone (>35 km wide) of right-oblique-slip faults. Grose (1986) terminated the northwestern limit of the Walker Lane in the Medicine Lake Highlands within the Cascade Range province. The northeastern limit of the Walker Lane terminates near Canby, California, in the Modoc Plateau.

REFERENCES

Albers, J.P., 1967, Belt of sigmoidal bending and right-lateral faulting in the western Great Basin: Geological Society of America Bulletin, v.78, p. 143-155.

Allmendinger, R.W., Hauge, T.A., Hauser, E.C., Potter, C.J., Klemperer, S.L., Nelson, K.D., Knuepfer, P., and Oliver, J. 1987, Overview of the COCORP 40°N transect, western United States: The fabric of an orogenic belt: Geological Society of American Bulletin, v.98, no.3, p. 308-319.

Allmendinger, R.W., Sharp, J.W., Von Tish, D., Serpa, L., Brown, L., Kaufman, S., and Oliver, J., 1983, Cenozoic and Mesozoic structure of the eastern Basin and Range province, Utah, from COCORP seismic reflection data: Geology, v. 11, p. 532-536.

Anderson, L.W. and Hawkins, F.F., 1984, Age and recurrence of Holocene surface faulting, Pyramid Lake fault zone, western Nevada: Geological Society of America, Abstracts with Programs, v.16, p. 266.

Armstrong, R.L., 1974, Magmatism, orogenic timing and orogenic diachronism in the Cordillera from Mexico to Canada: Nature, v.247, p. 348-351.

Atwater, T., 1970, Implications of plate tectonics for the Cenozoic tectonic evolution of western North America: Geological Society of America Bulletin, v.81, p. 3513-3536.

Atwater, T and Molner, P., 1973, Relative motion of the Pacific and North American plates deduced from sea-floor spreading in the Atlantic, Indian, and South Pacific oceans, in Kovac, R.L., and Nur, A., eds., Proceedings, conference on tectonic problems of the San Andreas Fault system: Stanford University Publications Geological Science, v.13, p. 136-148.

Axelrod, D.I., 1962, Post-Pliocene uplift of the Sierra Nevada, California: Geological Society of America Bulletin, v.73, p. 183-198.

Bell, E.J., Sanders, C.O., and Slemmons, D.B., 1978, Geologic and geometric analysis of conjugate strike-slip faults and regional strain in the western Basin and Range Province: Geological Society of America, Abstracts with Programs, v.10, p. 95.

Bell, E.J. and Slemmons, D.B., 1979, Recent crustal movements in the central Sierra Nevada-Walker Lane region of California - Nevada: Part II, The Pyramid Lake Right-Slip fault zone segment of the Walker Lane: Tectonophysics, v.52, p. 571-583.

_____, 1982, Neotectonic analysis of the northern Walker Lane, western Nevada and northern California: Geological Society of America, Abstracts with Programs, v.14, p. 148.

Bell, J.D., 1986, Quaternary fault map of the Reno 1° by 2° Quadrangle: U.S. Geological Survey Open File Report 81-981, 62 p.

Benson, L.V., 1978, Fluctuations in the level of pluvial Lake Lahonton during the last 40,000 years: Quaternary Research, v.9, p. 300-318.

Benson, L. and Thompson, R.S., 1987, The physical record of lakes of the great basin, in Ruddiman, W.F. and Wright, H.E., Jr., eds., The geology of North America, Volume K-3, North America and the Adjacent Oceans during the last deglaciation: Geological Society of America Bulletin, p. 246-260

Blake, M.C., Jr., Campbell, R.H., Dibblee, T.W., Jr., Howell, D.G., Nielson, T.H., Normark, W.R., Vedder, J.C., and Silver, E.A., 1978, Neogene basin formation in relation to plate-tectonic evolution of the San Andreas Fault system: American Society of Petrology Bulletin, v.62, p. 344-372.

Bolt, B., and Miller, R.D., 1975, Catalogue of earthquakes in northern California and adjoining areas, 1 January 1910 - 31 December 1972: University of California Berkeley Publications, 567 p.

Bonham, H.F., 1969, Geology and mineral deposits of Washoe and Storey Counties, Nevada: Nevada Bureau of Mines Bulletin 70, 140 p.

Bonham, H.F., and Slemmons, D.B., 1968, Faulting associated with the northern part of the Walker Lane, Nevada: Geological Society of America, Special Paper 101, 290 p.

Bonilla, M.G., Mark, R.K. and Lienkaemper, J.J., 1984, Statistical relations among earthquake magnitude, surface rupture length, and

surface fault displacement: Bulletin of the Seismological Society of America, v.74, p. 2379-2411.

Broecker, W.S. and Orr, P.C., 1958, Radiocarbon chronology of Lake Lahonton and Lake Bonneville: Geological Society of America Bulletin, v.69, p. 1009-1032.

Broecker, W.S. and Kaufman, A., 1965, Radiocarbon chronology of Lake Lahonton and Lake Bonneville II, Great Basin: Geological Society of America Bulletin, v.76, p. 537-566.

Bucknam, R.C. and Anderson, R.E., 1979, Estimation of fault-scarp ages from a scarp-height-slope-angle relationship: Geology, v.7, p. 11-14.

Bull, W.B., Fonseca, J., and Hecker, S., 1984, Detailed geomorphic studies to define late Quaternary fault behavior and Seismic hazard, Central Nevada Seismic Belt: U.S.G.S. Earthquake Hazards Reduction Program Contract No. 21970.

Burchfiel, B.C., and Davis, G.A., 1972, Structural framework and evolution of the southern part of the Cordilleran Oregon, western United States: American Journal of Science, v.272, p. 97-118.

_____, 1975, Nature and controls of Cordilleran orogenesis, western United States: extensions of an earlier synthesis: American Journal of Science, v.275-A, p. 363-396.

Christiansen, R.L., and Lipman, P.W., 1972, Cenozoic volcanism and plate-tectonic evolution of the western United States, II. Late Cenozoic: Royal Society London Transactions, Series A., v.27, p. 249-284.

Churkin, M. Jr., and Eberlein, G.D., 1977, Ancient borderland terrains of the North American Cordillera, correlation and microplate tectonics: Geological Society of America Bulletin, v.88, p. 769-786.

Cole, D.A., Jr., and Lade, P.V., 1984, Influence zones in alluvium over dip-slip faults: Journal of Geotechnical Engineering, ASCE, v.110, no. GT5, Proceedings Paper 18788. p. 599-615

Crowell, J.C., 1974, Origin of Late Cenozoic basins in southern California, in , Dickinson, W.R., ed., Tectonics and Sedimentation: Society of Economic Paleontologists and Mineralogists Special Publication 22, p. 190-204.

Dalrymple, G.B., 1964, Cenozoic chronology of the Sierra Nevada, California: California University Publications Geological Science, v.46, 41 p.

Davis, G.A. and Burchfiel, B.C., 1973, Garlock Fault: An intra-continental transform structure, southern California: Geological Society of America Bulletin, v.84, p.1407-1422.

Davis, J.O., 1977, Quaternary tephrachronology of the Lake Lahonton area, Nevada and California: Ph.D. Dissertation, University of Idaho Graduate School, 150 p.

_____, 1978, Quaternary tephrachronology of the Lake Lahontan area, Nevada and California: University of Nevada Archeological Survey Research Paper 7, 137 p.

_____, 1982, Bits and Pieces: Last 35,000 years in the Lahonton area, in Madsen D. B., and O'Connel, J. F., eds., Man and Environment in the Great Basin: Society of American Archaeologists Papers No. 2, p. 53-75.

_____, 1983, Level of Lake Lahonton during deposition of the Trego Hot Springs tephra about 23,400 years ago: Quaternary Research, v.19, p. 312-324.

_____, 1985, Correlation of Late Quaternary tephra layers in a long fluvial sequence near Summer Lake, Oregon: Quaternary Research, v.23, p. 38-53.

Dickinson, W.R., 1977, Paleozoic plate tectonics and the Evolution of the Cordilleran continental margin, in Armentrout, J.M., Cole, M.R., and Terbest, H. Jr., eds., Cenozoic paleogeography of the western United States: Society of Economic Paleontologists and Mineralogists, Pacific Section, Pacific Coast Paleogeography Symposium 3, p. 1-13.

Dickinson, W.R. and Snyder, W.S., 1978, Plate tectonics of the Laramide Orogeny: Geological Society of America Memoirs 151, p. 355-366.

_____, 1979, Geometry of subducted slabs related to San Andreas Transform: Journal of Geology, v.87, p. 609-627.

Dodge, R.L., 1980, Evaluation of skylab photographs for mapping Quaternary geologic features, west-central Smoke Creek Desert, Nevada: Master Thesis, Colorado School of Mines, 69 p.

Dodge, R.L. and Grose, L.T., 1980, Tectonic and geomorphic evolution of the Black Rock Fault, northwestern Nevada: U. S. Geological Survey, Open-file Report 80-801, p. 494-508.

Dohrenwend, J. C., 1982, Reconnaissance surficial geologic map of the Gabbs-Luning area, west-central Nevada: U.S. Geological Survey, Map MF-1374.

Donath, F.A., 1962, Analysis of Basin Range structure, south-central Oregon: Geological Society of America Bulletin, v.73, p. 1-16.

Duffield, W.A. and McKee, B.H., 1986, Geochronology, structure, and Basin Range tectonism of the Warner Range, northeastern California: Geological Society of America Bulletin, v.97, p. 142-146

Eaton, G.P., Wahl, R.R., Protska, H.J., Mabey, D.R., and Kleinkopf, M.D., 1978, Regional gravity and tectonic Patterns: their relationship to Late Cenozoic epiorogenic and lateral spreading in the western United States, in Stewart, J.H., ed., Cenozoic tectonics and regional geophysics of the western Cordillera: Geological Society of America Memoir 152, p. 51-92.

England, P. and Jackson, J., 1987, Migration of the seismic-aseismic transitions during uniform and nonuniform extension of the continental lithosphere: Geology, v.15, p. 291-294.

Ferguson, H.G. and Muller, S.W., 1949, Structural geology of the Hawthorne and Tonapah Quadrangles, Nevada: U.S. Geological Survey Professional Paper 216, 55 p.

Flint, R.F., 1971, Glacial and Quaternary geology: John Wiley and Sons, Inc., New York, 892 p.

Frei, L.S., 1986, Additional paleomagnetic results from the Sierra Nevada: further constraints on Basin and Range extension and northward displacement in the western United State: Geological Society of America Bulletin, v.97, p. 840-849.

Fuis, G.S., Zucca, J.J., Mooney, W.D., and Milkereit, B., 1987, A geologic interpretation of seismic-refraction results in northeastern California: Geological Society of America Bulletin, v. 98, p.53-65.

Gardner, T.W., Jorgensen, D.W., Shuman, C., and Lemieux, C.R., 1987, Geomorphic and tectonic process rates: effects of measured time intervals: Geology, v.15, p. 259-261.

Gay, T.E., and Aune, Q., 1958, Alturas Sheet of the geologic map of California, 1:250,000: California Division of Mines and Geology Map Sheet.

Grose, L.T.L., 1982, Personal communication

_____, 1895, Volcanotectonic evidence for stress field changes since Late Miocene in Basin and Range - Cascade boundary zone (Walker Lane) of northeastern California: EOS Transactions, American Geophysical Union, vol. 66, no. 46, p. 1091.

_____, 1986, Tectonics of the Walker Lane in NE California and the Honey Lake anomaly: EOS Transactions, American Geophysical Union, vol. 67, no. 47, p. 1211.

_____, 1990, personal communication.

Grose, T.L.T., and McKee, E.H., 1982, Late Cenozoic westward volcanic progression east of Lassen Peak, northeastern California: EOS Transactions, American Geophysical Union, v.63, no.B7, p. 1149.

Hamel, D.S. 1983, Length, style, continuity and displacement of The Battles Well Fault, Mineral County, Nevada: Geological Society of America Abstracts with Programs, v.15.

Hamilton, W., 1978, Mesozoic tectonics of the western United States, in Howell, D.G., and McDougall, K.A., eds., Mesozoic paleogeography of the western United States: Pacific Coast Section, Society of Economic Paleontologist and Mineralogists Pacific Coast Symposium 2, p. 33-7

Hamilton, W., and Meyers, W.B., 1966, Cenozoic tectonics of the western United States: Reviews in Geophysics, v.4, p. 504-549.

Hanks, T.C., Bucknam, R.C., LaJoie, K.R., and Wallace, R.E., 1984, Modification of wave-cut and fault-controlled landforms: Journal of Geophysical Research , v.89, n. 87, p. 5771-5790.

Hanks, T.C. and Wallace, R.E., 1985, Morphological analysis of the Lake Lahonton shoreline and beachfront fault scarps, Pershing County, Nevada: Seismological Society of America Bulletin, v.75, p. 835-846.

Hardyman, R.F., Ekron, E.B., and Byers, F.M., Jr. 1975, Cenozoic strike-slip, normal, and detachment faults in the northern part of the Walker Lane, west-central Nevada: Geological Society of America Abstracts with Programs, v. 7, n. 7, p. 110.

Hill, D.P., 1982, Contemporary block tectonics: California and Nevada: Journal of Geophysical Research, v. 87, n. B7, p. 5433-5450.

Holtz, R.D. and Kovacs, W.D., 1981, An introduction to geotechnical engineering: Prentice-Hall, Inc., Englewood Cliffs, New Jersey, 733 p.

Hooke, R. 1965, Processes on arid-region alluvial fans: Journal of Geology, v. 75, p. 438-460.

Hoover, D.L., Swadley, W.C. and Gordon, A.J., 1981, Correlation characteristics of surficial deposits with a description of

surficial stratigraphy in the Nevada Test Site region: U.S. Geological Survey Open-File Report 81-512.

Keller, E.A., 1986, Investigations of active tectonics: Use of surficial earth processes, in Wallace, R.E., panel chairman, Studies in Geophysics, Active Tectonics: National Academy Press, Washington, D.C., p. 136-147.

Kistler, R.W., Robinson, A.C. and Fleck, R.J., 1980, Mesozoic right lateral faults in eastern California: Geologic Society of America, Abstracts with Programs, v. 12, p. 115.

Klemperer, S.L., Hauge, T.A., Hauser, E.C., Oliver, J.E. and Potter, C.J., 1988, The Moho in the northern Basin and Range Province, Nevada, along the COCORP 40°N seismic-reflection transect: Geological Society of America Bulletin, v. 97, n. 5, p. 603-618.

Knuepfer, P.L.K., Lemiszki, P.J., Hauge, T.A., Brown, L.D. Kaufman, S., and Oliver, J.E., 1987, Crustal structure of the Basin and Range-Sierra Nevada transition from COCORP deep seismic-reflection profiling: Geological Society of America Bulletin, v. 98, n. 4, p. 488-4

Lade, P.V., and Cole, D.A., Jr., 1984, Ground rupture zones in alluvium over dip-slip faults: Proceedings of The 21st Annual Engineering Geology and Soils Engineering Symposium, April 1984, p. 29-44.

Lade, P.V., Cole, D.A., Jr., and Cummings, D., 1984a, Influence zones in alluvium over dip-slip faults: Journal of Geotechnical Engineering, v. 110, n. 5, p. 599-615.

_____, 1984b, Multiple failure surfaces over dip-slip faults: Journal of Geotechnical Engineering, v. 110, n. 5, p. 616-627.

Lawrence, R.D., 1976, Strike-slip faulting terminates the Basin and Range Province in Oregon: Geological Society of America Bulletin, v. 87, p. 846-850.

Lemiski, P.J., and Brown, L.D., 1988, Variable crustal structure of strike-slip fault zones as observed on deep seismic reflection profiles: Geological Society of America Bulletin, v.100, p. 665-676.

Lydon, P.A., Gay, T.E., and Jennings, C.W., 1960, Westwood Sheet of the geologic map of California, 1:250,000: California Division of Mines and Geology Map Sheet.

Lynn, H. B., Hale, L. D., and Thompson, G. A., 1981, Seismic reflections from basal contacts of batholiths: Journal of Geophysical Research, v. 86, p. 10,633-10,638.

Menard, H. W., 1974, Geology, resources, and society, an introduction to earth science: W. H. Freeman and Company, San Francisco, CA, 621 p.

Mohler, Amy S., 1980, Earthquake/earth tide correlation and other features of the Susanville, California, earthquake sequence of June - July, 1976: Seismological Society of America Bulletin, v. 70, n. 5, p. 1583-1593.

Molinari, M.P., 1983, Wrench fault tectonics of the southeast margin of the central Walker Lane, west central Nevada: Geological Society of America, Abstracts with Programss with Programs, v. 15, p. 384.

Morrison, R.B., 1961, Lake Lahonton stratigraphy and history in the Carson Desert (Fallon) area, Nevada: U.S. Geological Survey Professional Paper 424-D, p. D111-D114.

_____, 1964, Lake Lahonton: Geology of the southern Carson Desert, Nevada: U.S. Geological Survey Professional Paper 401, 156 p.

_____, 1965, Quaternary of the Great Basin, in Wright, H.E., Jr. and Frye, D.G., eds., The Quaternary of the United States: Princeton, New Jersey, Princeton University Press, p. 265-291.

Morrison, R.B. and Frye, J.C., 1965, Correlation of the middle and Late Quaternary successions of the Lake Lahonton, Lake Bonneville, Rocky Mountain (Wasatch Range), southern Great Plains and Eastern Midwest area: Nevada Bureau of Mines Report 9, 45 p.

Morrison, R.B. and Davis, J.O., 1984, Quaternary stratigraphy and archeology of the Lake Lahonton area: A re-assessment in western geological excursions: Geological Society of America and University of Nevada, Reno, v. 1, p. 252-281.

McClay, K.R. and Ellis, P.G., 1987, Geometries of extensional fault systems developed in model experiments: Geology, v. 15, n. 4, p. 341-344.

McMurdie, P.S., 1983, Modoc-Cascade study for northern California: Geothermal Resources Council Bulletin, v. 12, n. 7, p. 26.

Nash, D.B., 1980, Morphologic dating of degraded normal fault scarps: Journal of Geology, v. 88, p. 353-360.

_____, 1984, Morphologic dating of fluvial scarps and fault scarps near west Yellowstone, Montana: Geological Society of America Bulletin, v. 95, p. 1413-1424.

_____, 1986, Morphologic dating and modeling degradation of fault scarps, in Wallace, R. E., panel chairman, Studies in Geophysics, Active Tectonics: National Academy Press, Washington, D.C., p. 181-194.

Nettleton, W.D., and Witty, J.E., Nelson, R.E., and Hawley, J.W., 1975, Genesis of argillic soils of the desert areas of the southwestern United States: Soil Science Society of America Proceedings, v.39, p.919-926.

Nielson, R.L., 1965, Right lateral strike-slip faulting in the Walker Lane, west-central Nevada: Geological Society of America Bulletin, v. 76, p. 1301-1308.

Nielson, T.H. and McKee, 1979, Paleogene paleogeography of the western United States, in Armentrout, J.M., Cole, M.R., and Terbest, H. Jr., eds., Cenozoic paleogeography of the western United States: Society of Economic Paleontologists and Mineralogists, Pacific Coast Section Paleogeography Symposium 3, p. 257-275.

Nielson, T.H. and Stewart, J.H., 1980, The Antler Orogeny, mid-Paleozoic tectonism in western North America: Geology, v.8, p. 298-302.

Noble, D.C., 1972, Some observations on the Cenozoic volcano-tectonic evolution of the Great Basin, western United States: Earth and Planetary Science Letters, v. 17, p. 142-152.

Pakiser, L.C., 1964, Gravity, volcanism, and structure in the southern Cascade Range, California: Geological Society of America Bulletin, v. 75, p. 611-620.

Pease, R.W., 1965, Modoc County - a geographic time continuum on the California volcanic table land: California University Publications in Geography, v. 17, 304 p.

_____, 1969, Normal faulting and lateral shear in northeastern California: Geological Society of America Bulletin, v. 80, p. 715-720.

Peterson, F.F., 1981, Landforms of The Basin and Range Province defined for soil survey: Nevada Agricultural Experiment Station, University of Nevada-Reno Technical Bulletin 28, 53 p.

Poole, F.G., 1974, Flysch deposits of Antler Forkland Basin, western United States, in Dickinson, V.R., ed., Tectonics and

sedimentation: Society of Economic Paleontologists and Mineralogists, Special Publication, n. 22, p. 58-82.

Potter, C.J., Liu, C., Huang, J., Zheng, L., Hauge, T. A., Allmendinger, R. W., Oliver, J. E., Kaufman, S., and Brown, L., 1987, Crustal structure of north-central Nevada: Results from COCORP deep seismic profiling: Geological Society of America Bulletin, v. 98, p. 330-337.

Profett, J.M., Jr., and Profett, B.H., 1976, Stratigraphy of the Tertiary ash-flow tuffs in the Yerington District, Nevada: Nevada Bureau of Mines and Geology Report 27, 29 p.

Rich, E.I., and Steele, W.C., 1974, Geologic structures in northeastern California as detected from ERTS-1 satellite imagery: Geology, v.2, p. 166-169.

Ritter, D.F., 1979, Alluvial fans and stream morphology, in Buesch, D., ed., Geomorphic applications in engineering geology: Association of Engineering Geologists, Southern California Section, p. 21-45.

Roberts, C.T., and Grose, T.L.T., 1982, Late Cenozoic extensional strain rates and directions in the Honey Lake-Eagle Lake region, northeastern California: EOS Transactions, American Geophysical Union, v. 63, n. 45, p. 1107.

_____, 1984, Structural boundary between the Sierra Nevada and Cascade provinces, northeastern California: Geological Society of America, Abstracts with Programs, v. 16, n. 6, p. 636.

Ryall, A.S., Slemmons, D.B., and Gedney, L.D., 1966, Seismicity, tectonism and surface faulting in the western United States during historic time: Seismological Society of America Bulletin, v. 56, n. 5, p. 1105-1135.

Ryall, A.S., and Van Wormer, J.D., 1980, Sierra Nevada-Great Basin boundary zone: earthquake hazard related to structure, active tectonic Processes and anomalous patterns of earthquake occurrence: Seismological Society of America Bulletin, v. 70, p. 1557-1572.

Sbar, M.L., 1982, Delineation and interpretation of seismotectonic domains in western North America: Journal of Geophysical Research, v. 87, n. B5, p. 3919-392.

Schilling, J.H., 1965, Isotopic age determinations of Nevada rocks: Nevada Bureau Mines Report 10, 72 p.

Schumm, S.A., 1965, Quaternary paleohydrology, in Wright, H.E., Jr. and Frye, D.G., eds., The Quaternary of the United states: Princeton, New Jersey, Princeton University Press, p. 783-794.

Serpa, L., De Voogd, B., Wright, L., Oliver, J., Hauser, E., and Troxel, B., 1988, Structure of the central Death Valley pull-apart basin and vicinity from COCORP profiles in the southern Great Basin: Geological Society of America Bulletin, v. 100, p. 1437-1450.

Shawe, D.R., 1965, Strike-slip control of Basin-Range structure indicated by historic faults in western Nevada: Geological Society of America Bulletin, V. 76, p. 1361-1378.

Silberling, N.J., 1973, Geologic events during Permian-Triassic time along the Pacific margin of the United States, in Logan, A., and Hills, L. V., eds., The Permian and Triassic systems and their mutual boundary, Calgary, Alberta, Canada: Alberta Society of Petroleum Geologists Memoir 2, p. 345-362.

Slemmons, D.B., 1977, State-of-the-art for assessing earthquake hazards in the United States; faults and earthquake magnitude: U.S. Army Engineer Waterways Experiment Station Miscellaneous Paper S-73-1, Report 6, 166p.

_____, 1989, personal communication.

Slemmons, D.B., Bodin, P., and Zhang, X., 1989, Determination of earthquake size for active faults: Proceedings of International Seminar on Seismc Zonation, Guang-zhou, China, p. 157-169.

_____, 1981, A procedure for analyzing fault-controlled lineaments and the activity of faults: in O'Leary D.W., and Earle, J.L., eds, Proceedings of the Third International Conference on Basement Tectonics, n. 3, p. 33-49.

_____, 1982, Determination of design earthquake magnitudes for microzonation: Proceedings of the Third International Earthquake Microzonation Conference, Volume I of III, p. 119-130.

Slemmons, D.B., and Chung, D.H., 1982, Maximum Credible Magnitudes for the Calaveras and Hayward fault zones, California: Proceedings of The Conference on Earthquake Hazards in the Eastern San Francisco Bay Area: California Division of Mines and Geology, Special Paper 62, p. 115-124.

_____, and dePolo, C.M., 1986a, Evaluation of active faulting and associated hazards, in Wallace, R. E., panel chairman, Studies in Geophysics, Active Tectonics: National Academy Press, Washington, D.C., p. 45-62.

_____, 1986b, Determination of earthquake size: Proceedings of Conference XXXIX: U.S. Geological Survey Open-File Report, p. 181-196.

Slemmons, D.B., Van Wormer, D., Bell, E.J., and Silverman, M.L., 1979, Recent crustal movements in the Sierra Nevada-Walker Lane region of California-Nevada: Part I, rate and style of deformation: Tectonophysics, v. 52, p. 561-570.

Smith, G.I. and Street-Perrott, F.A., 1983, Pluvial lakes of the western United states, in Wright, H.E.,Jr., ed., Late Quaternary environments of the United States, in Porter, S.C., ed., The Late Pleistocene, Volume 1: Minneapolis, Minnesota, University of Minnesota Press, p. 190-211.

Snyder, C.T., Hardyman, G., and Zdenek, F.F., 1964, Pleistocene lakes in the Great Basin: United States Geological Survey Miscellaneous Geologic Investigations Map I-416.

Snyder, W.S., Dickinson, W.R. and Silverman, M.L., 1976, Tectonic implications of space-time patterns of Cenozoic magmatism in the western United States: Earth and Planetary Science Letters, v. 32, n. 1, p. 91-106.

Speed, R.C., 1977, Island-arc and other paleogeographic terrains of the late Paleozoic age in the western Great Basins, in Stewart, J.H., Stevens, C.H., and Fritsche, A.E., eds., Paleozoic paleogeography of the western United States: Society of Economic Paleontologists and Mineralogists, Pacific Section, Pacific Coast Paleogeography Symposium 1, p. 349-362.

Stewart, J. H., 1971, Basin and Range structure: A system of horsts and grabens produced by deep-seated extension: Geological Society of America Bulletin, v. 82, p. 1019-1044.

_____, 1978, Basin and Range structure in western North America, A Review, in Smith, R. B. and Eaton, G. P., eds., Cenozoic Tectonics and Regional Geophysics of the Western Cordillera: Geological Society of America Memoir 152, p. 1-32.

_____, 1980, Geology of Nevada: Nevada Bureau of Mines and Geology, Special Publication No. 4, 136 p.

_____, 1983a, Extensional tectonics in the Death Valley area, California: Transport of the Panamint Range structural block 80 km northwestward: Geology, v. 11, p. 153-157.

_____, 1983b, Cenozoic structure and tectonics of the northern Basin and Range Province, California, Nevada, and Utah, in the role of heat in the development of energy and mineral resources in the northern

Basin and Range Province: Geothermal Resources Council Special Report No.13, p. 25-40.

_____, 1988, Tectonics of the Walker Lane belt, western Great Basin: Mesozoic and Cenozoic deformation in a zone of fault, in Ernst, W. G., ed., Metamorphism and crustal evolution of the western United States (Rubey Volume VII): Englewood Cliffs, NJ, Prentice-Hall, p. 685-713.

_____, Albers. J.P., and Pool, F.G., 1968, Summary of regional evidence for right-lateral displacement in the western Great Basin: Geological Society of America Bulletin, v. 79, n. 10, p. 1407-1413.

_____, 1970, Summary of regional evidence for displacement in the western Great Basin, Reply: Geological Society of America Bulletin, v. 81, p. 2175-2180.

Tchalenko, J.S., 1970, Similarities between fault zones of different magnitudes: Geological Society of America Bulletin, v. 81, p. 1625-1640.

Terzaghi, K. and Peck, R.B., 1967, Soil mechanics in engineering practice: John Wiley and Sons, Inc., New York, 729 p.

Thompson, G.S. and White, D.E., 1964, Regional geology of the Steamboat Springs area, Washoe County, Nevada: U.S. Geological Survey Professional Paper 458-A.

Valastro, S., Jr., Davis, E.M., and Varela, A., 1978, University of Texas radiocarbon dates XII, Radiocarbon No. 2: American Journal of Science, v. 20, n. 2, p. 245-273.

Vetter, U.R., 1984, Focal mechanisms and crustal stress patterns in western Nevada and eastern California: Annales Geophysica, v. 2, p. 699-710.

Vetter, U.R., and Ryall, A.S., 1983, Systematic change of focal mechanism with depth in the western Great Basin: Journal of Geophysical Research, v. 88, n.b10, p. 8237-8250.

Wallace, A.B., 1975, Geology and mineral deposits of the Pyramid District, southern Washoe County, Nevada: University of Nevada, Reno, Ph.D. Thesis, 197 p.

Wallace, R.E., 1977, Profiles and ages of young fault scarps: Geological Society of America Bulletin, v. 88, p. 1267-1288.

_____, 1978a, Geometry and rates of change of fault generated range fronts, north-central Nevada: U.S. Geological Survey Journal of Research, v.6, no.5, p. 637-650.

_____, 1980a, Tectonic analysis of active faults: U.S. Geological Survey Semi-Annual Technical Report 9900-01270, October 1, 1979 - March 31, 1980, Section H-5, p. 3.

Wernicke, B., 1981, Low-angle normal faults in the Basin and Range Province: Rappe Tectonics in an Extending Orogen: Nature, v. 291, n. 5817, p. 645-648.

_____, and Burchfiel, B.C., 1982, Modes of extensional tectonics: Journal of Structural Geology, v. 4, n. 2, p. 105-115.

Whitney, R.A., 1980, Structural - tectonic analysis of northern Dixie Valley, Nevada: Master of Science Thesis, University of Nevada, Reno, 65 p.

_____, 1987, personal communication.

_____, 1989, personal communication.

Wise, D.U., 1963, An outrageous hypothesis for the tectonic pattern of the North American Cordillera: Geological Society of America Bulletin, v. 74, p. 357-362.

Wright, L., 1976, Late Cenozoic fault patterns and stress fields in the Great Basin and westward displacement of the Sierra Nevada Block: Geology, v. 4, n. 8, p. 489-494.

Ziony, J.I., and Yerkes, R.F., 1985, Evaluating earthquake and surface-faulting potential, in Ziony, J. I., ed., Evaluating earthquake hazards in the Los Angeles region - an earth-science perspective: U.S. Geological Survey Professional Paper 1360, p. 43-91.

Zoback, M.L., and Thompson, G.A., 1978, Basin and Range rifting in northern Nevada: clues from a mid-Miocene rift and its subsequent offset: Geology, v. 6, p. 111-116.

_____, and Zoback, M.D., 1980, Faulting patterns in north-central Nevada and strength of the Crust: Journal of Geophysical Research, v. 85, n. B1, p. 275-284.

Zoback, M.D., Zoback, M.L., Mount, V. S., Suppe, J., Eaton, J. P., Healy, J. H., Oppenheimer, D., Reasenberg, P., Jones, L., Raleigh, C. B., Wong, I. G., Scotti, O., and Wentworth, C., 1987, New evidence on the state of stress of the San Andreas fault system: Science, n. 111, v. 238, p. 1105-1111.

APPENDIX A

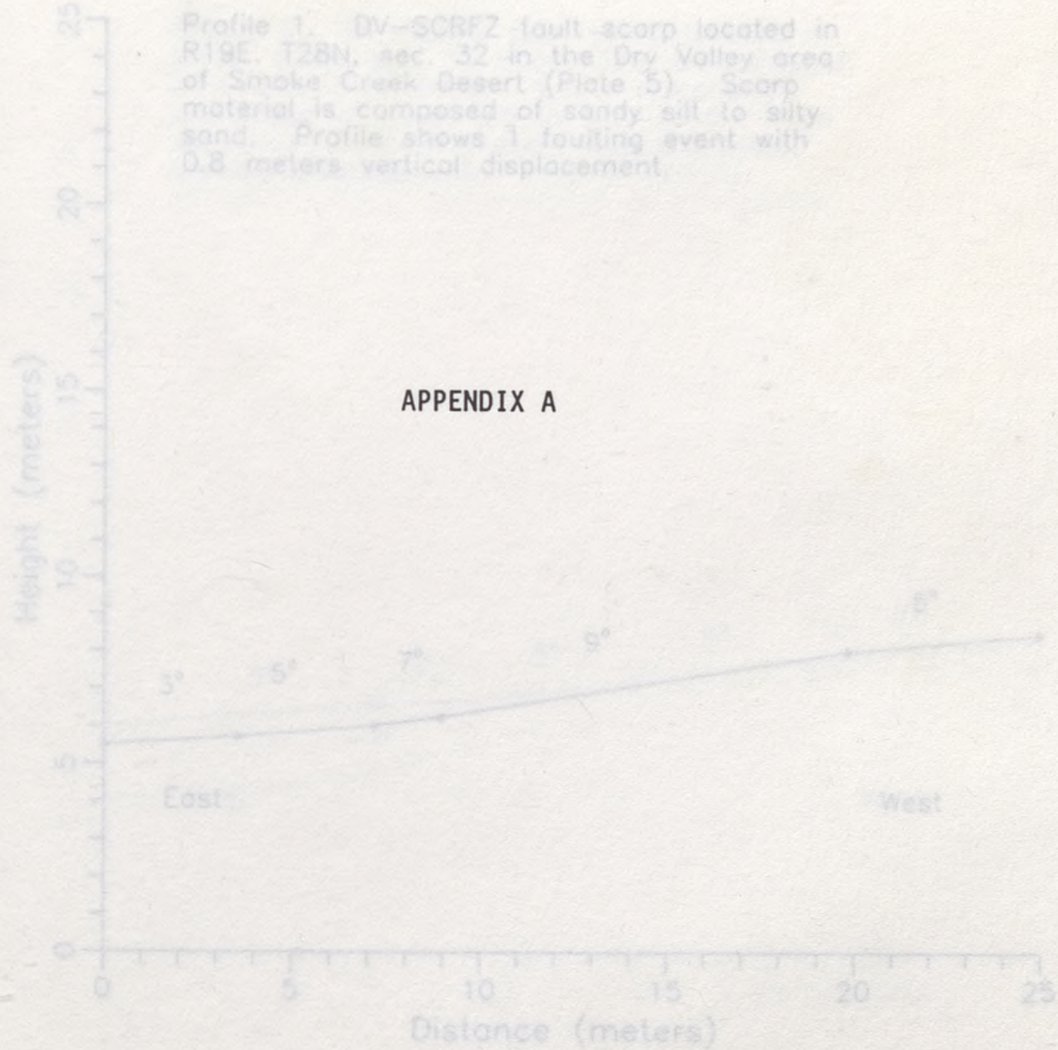

Profile 1. DV-SCRFZ fault scarp located in R19E, T28N, sec. 32 in the Dry Valley area of Smoke Creek Desert (Plate 5). Scarp material is composed of sandy silt to silty sand. Profile shows 1 faulting event with 0.8 meters vertical displacement.

Profile 1. DV–SCRFZ fault scarp located in R19E, T28N, sec. 32 in the Dry Valley area of Smoke Creek Desert (Plate 5). Scarp material is composed of sandy silt to silty sand. Profile shows 1 faulting event with 0.8 meters vertical displacement.

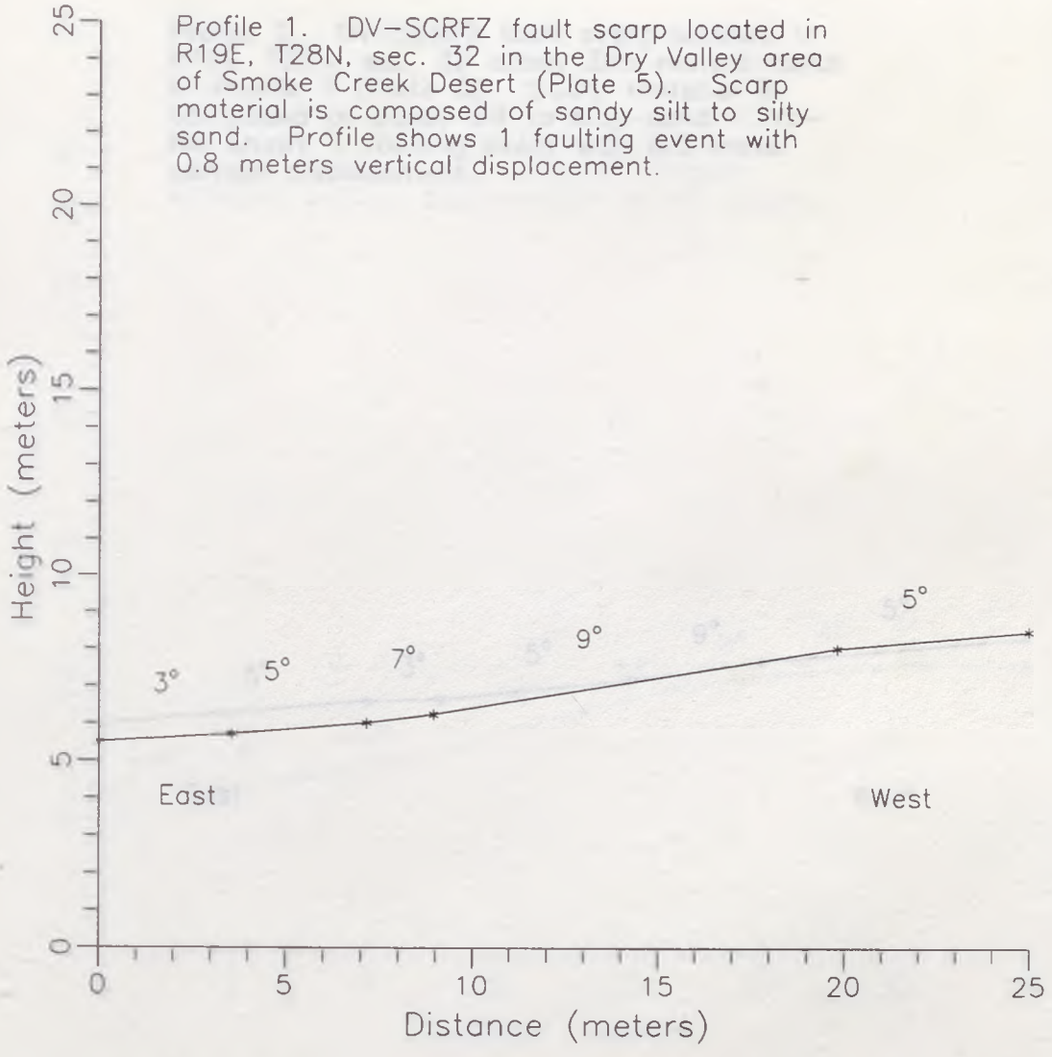

Profile 2. DV–SCRFZ fault scarp located in R19E. T28N, sec. 32 about 396 meters north of Profile 1 (Plate 5). Scarp material is composed of sandy silt to silty sand. Profile shows 1 faulting event with 0.5 meter vertical displacement.

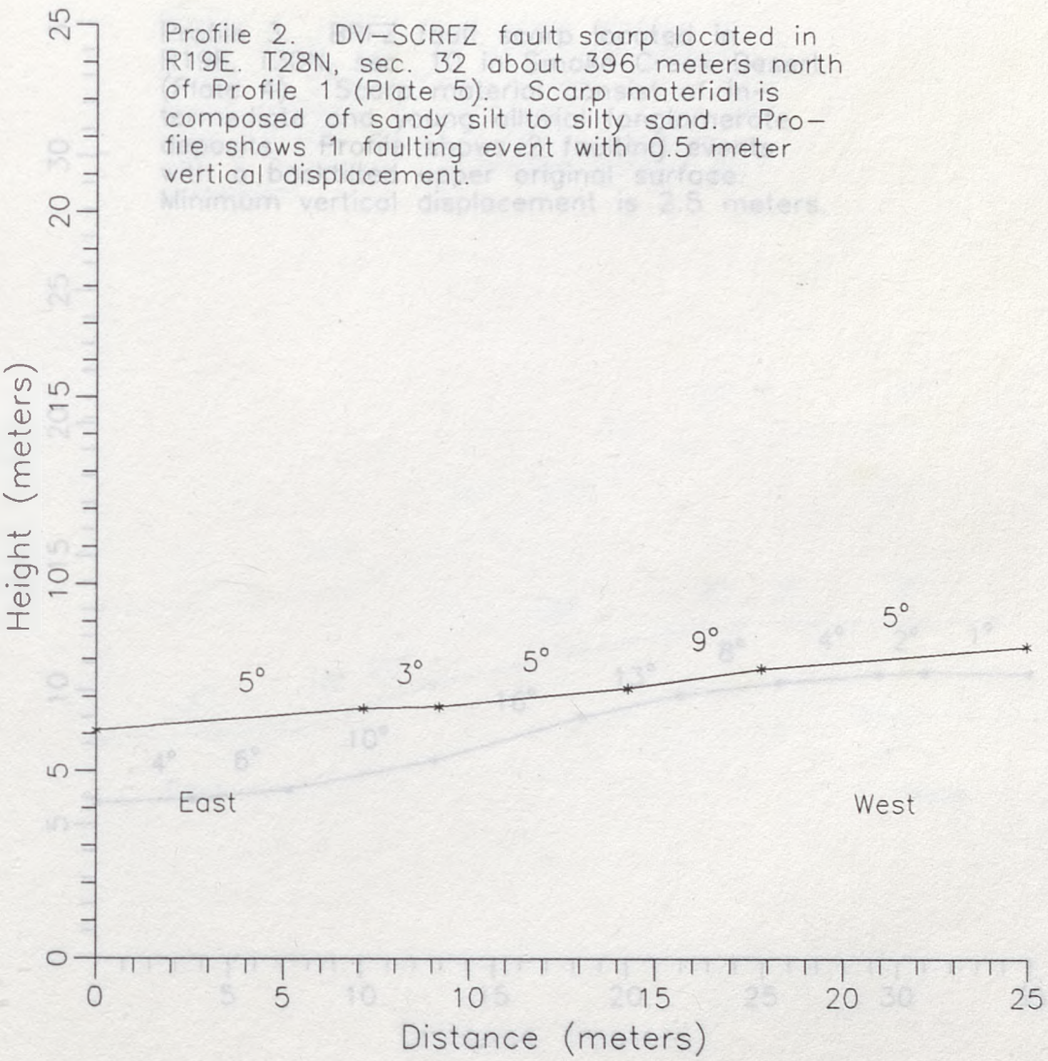

Profile 3. BRFZ fault scarp located in R19E, T30N, sec. 10 in Smoke Creek Desert (Plate 4). Scarp material consist of intermediate and young alluvial fanglomerate deposits. Profile shows 2 faulting events with a backtilted upper original surface. Minimum vertical displacement is 2.5 meters.

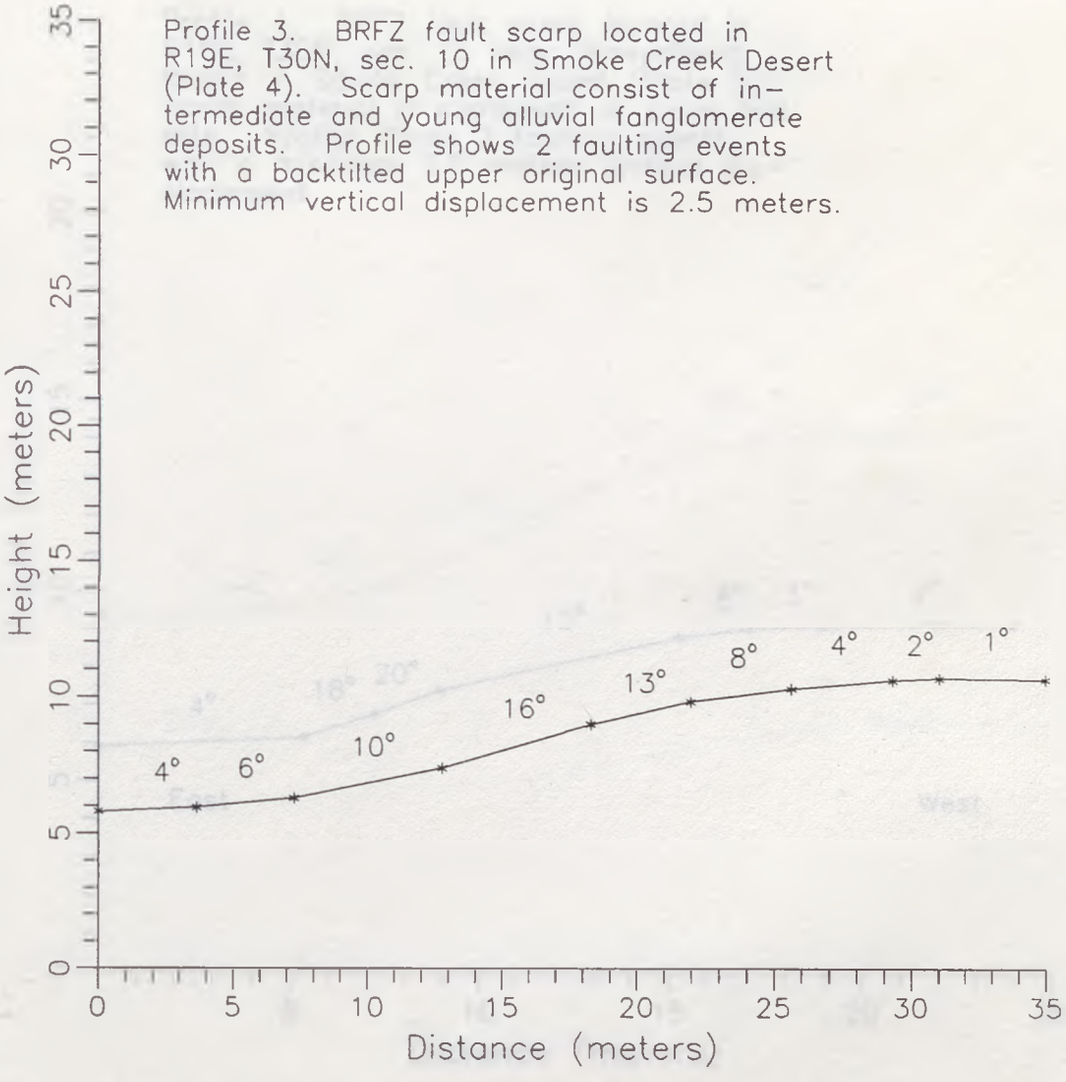

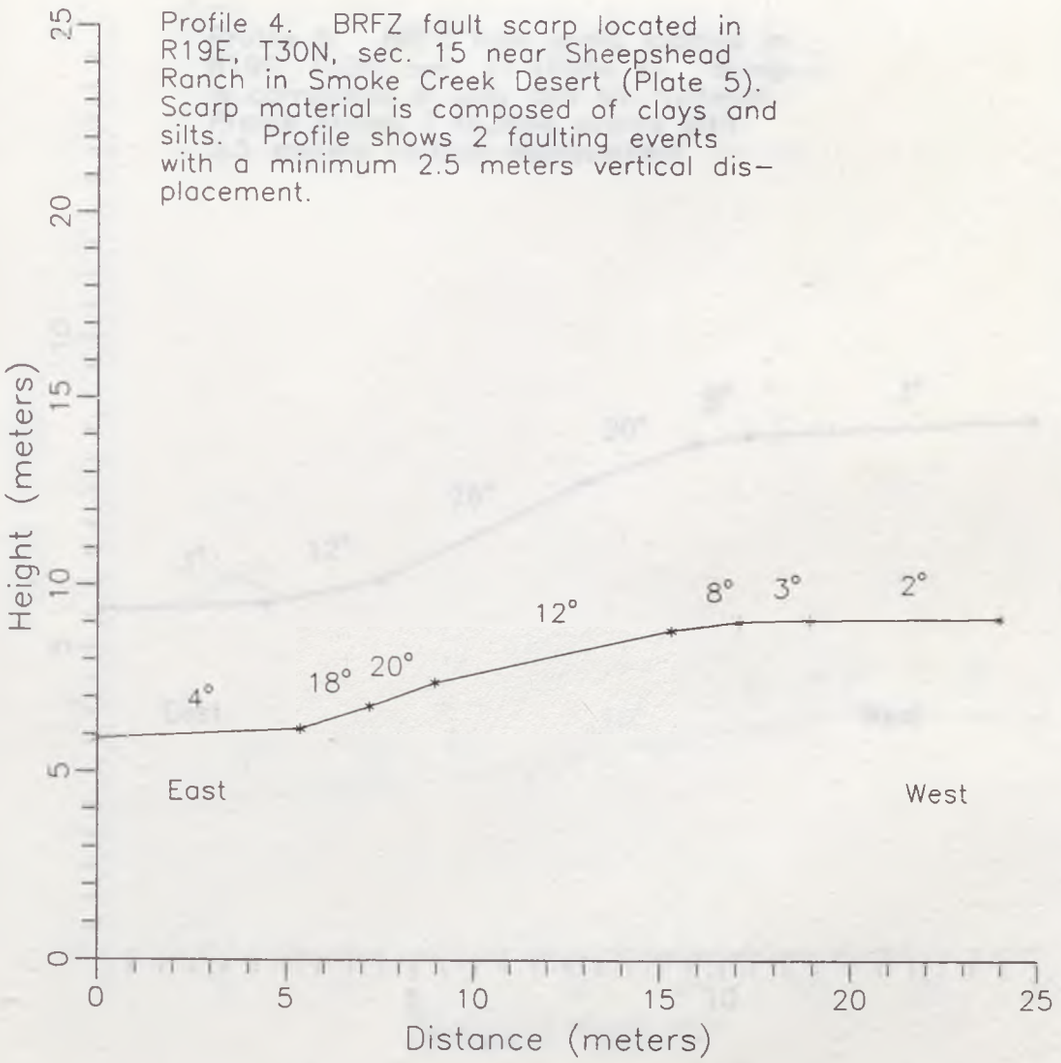

Profile 4. BRFZ fault scarp located in R19E, T30N, sec. 15 near Sheepshead Ranch in Smoke Creek Desert (Plate 5). Scarp material is composed of clays and silts. Profile shows 2 faulting events with a minimum 2.5 meters vertical dis-placement.

Profile 5. BRFZ fault scarp located in R19E, T30N, sec. 21 (Plate 4). Scarp is composed of clay and silt material. Profile shows 2 faulting events with 2.5 meters vertical displacement.

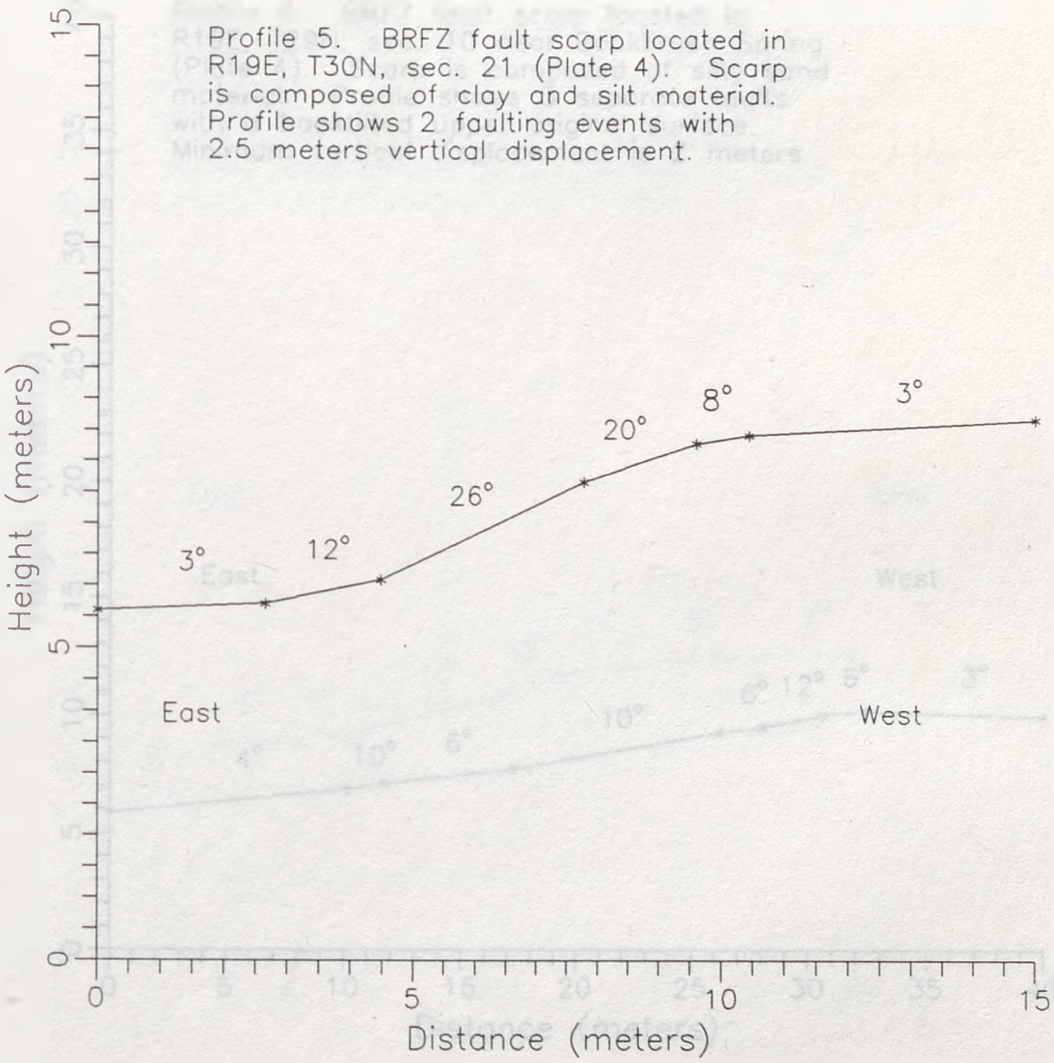

Profile 6. BRFZ fault scarp located in R19E, T29N, sec. 10 near Buckbrush Spring (Plate 4). Scarp is composed of silty sand material. Profile shows 3 separate faults with a backtilted upper original surface. Minimum vertical displacement is 2 meters.

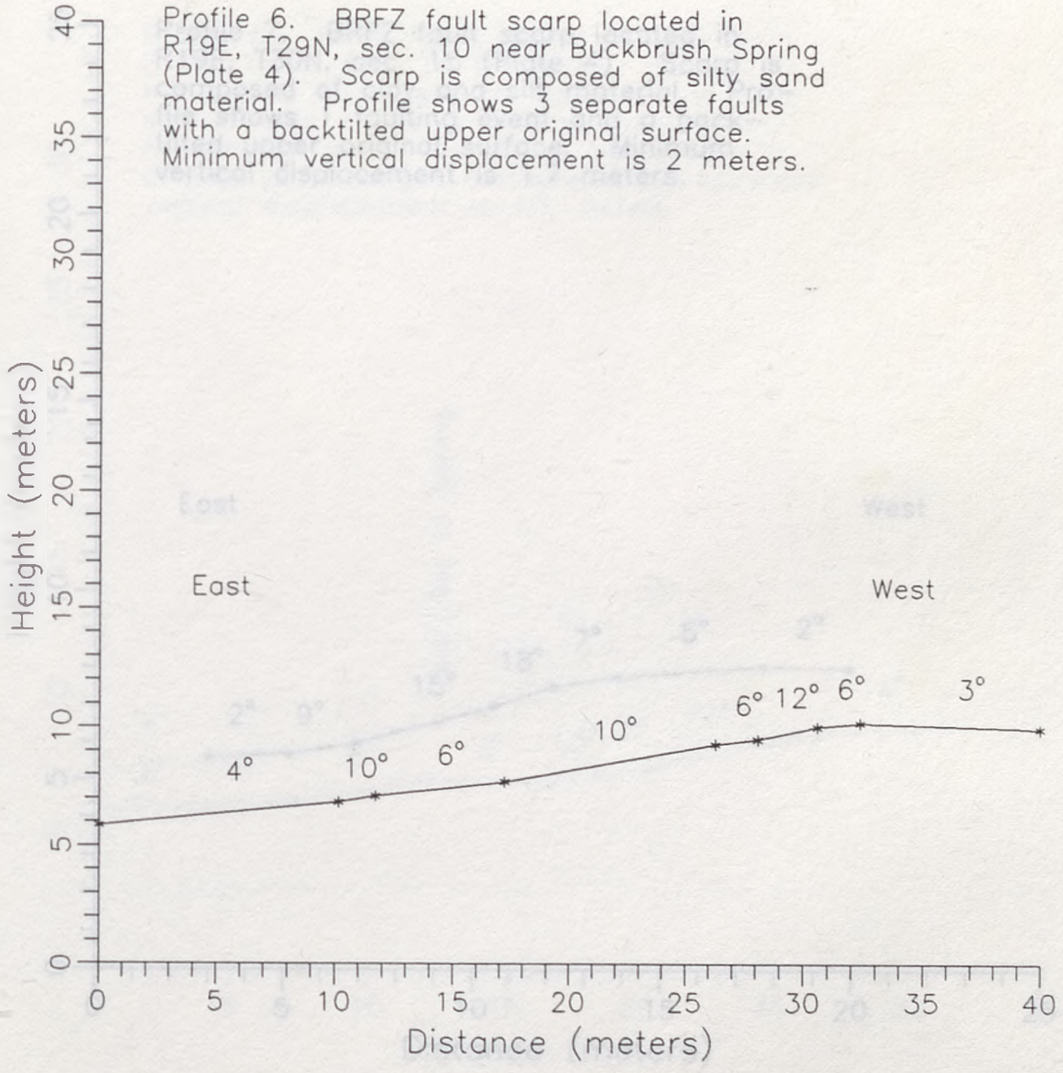

Profile 7. BRFZ fault scarp located in R19E, T30N, sec. 15 (Plate 4). Scarp is composed of clay and silt material. Profile shows 1 faulting event and a back-tilted upper original surface. Minimum vertical displacement is 1.7 meters.

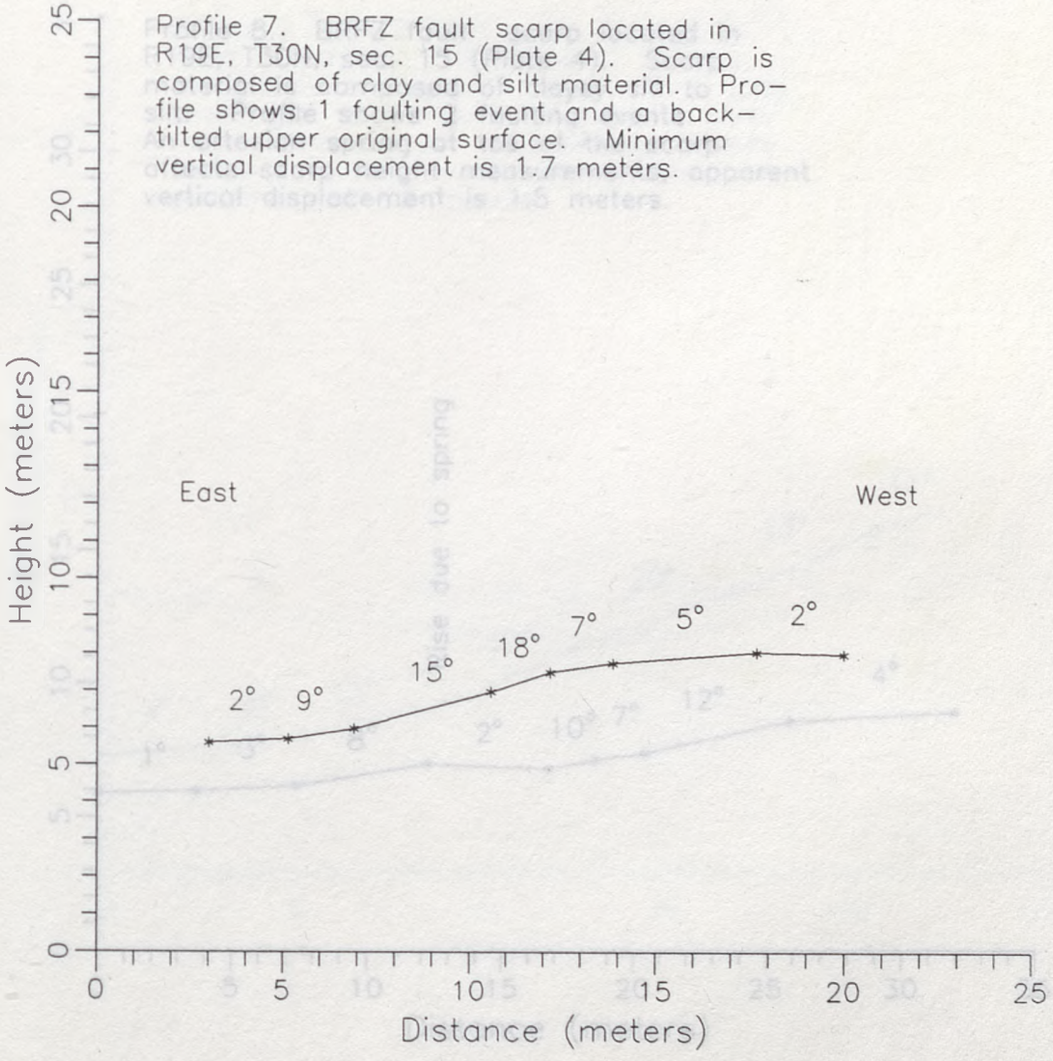

Profile 8. BRFZ fault scarp located in R19E, T30N, sec. 15 (Plate 4). Scarp material is composed of clayey silt to silt. Profile shows 2 faulting events. An artesian spring at toe of the scarp affects scarp height measurements, apparent vertical displacement is 1.5 meters.

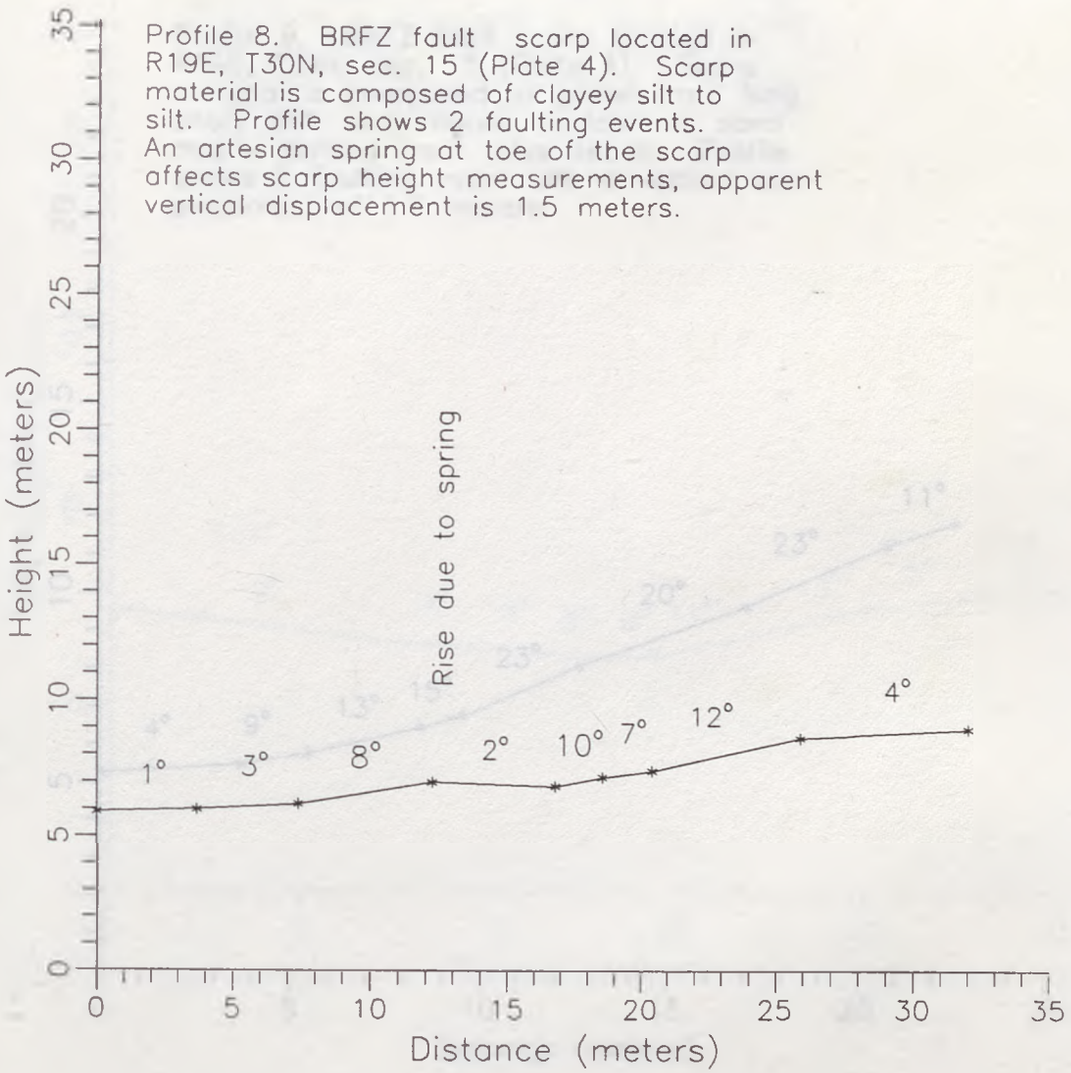

Profile 9. BRFZ fault scarp located in R19E, T29N, sec. 15 (Plate 4). Scarp material is composed of gravel from long shore drift and angular boulders in sand matrix derived from talus debris. Profile shows 2 faulting event with a vertical displacement of 1.5 meters.

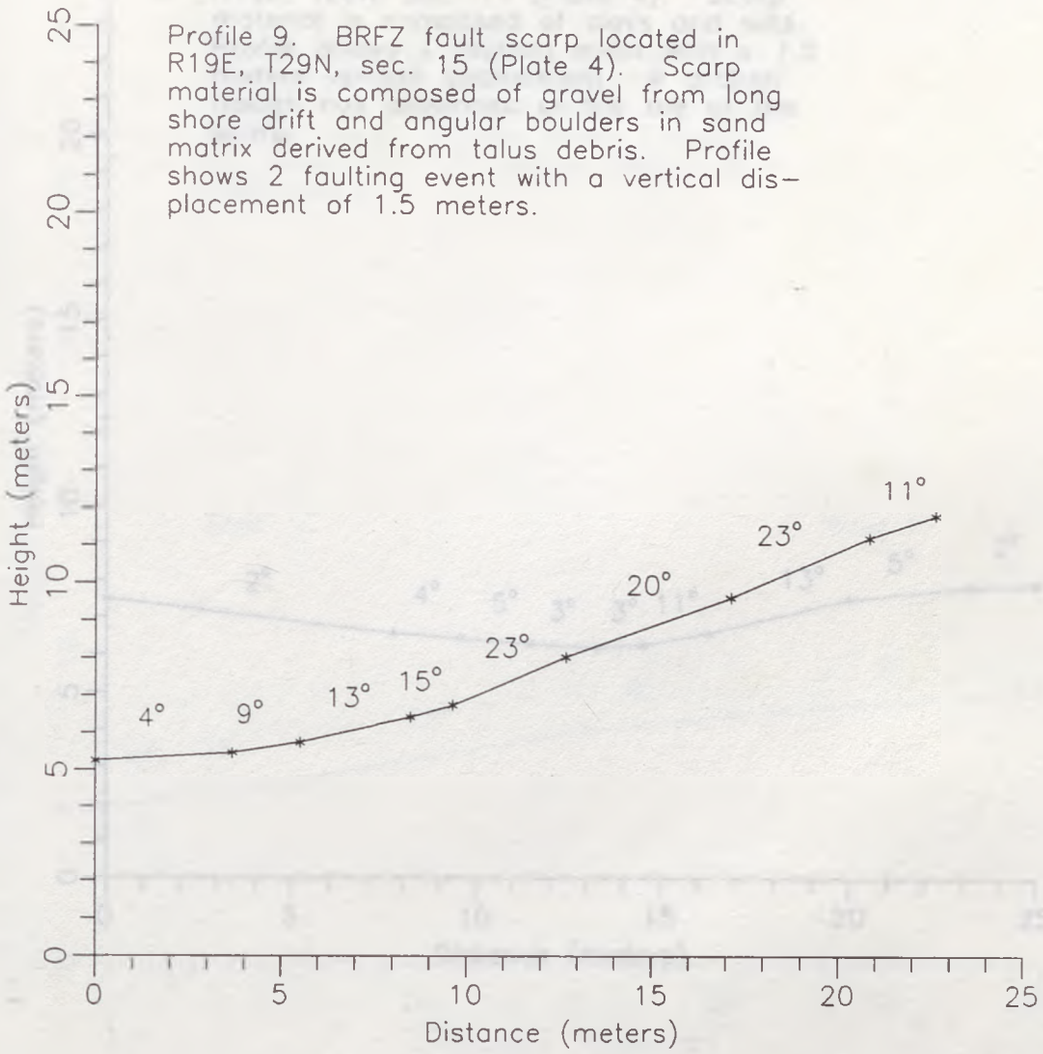

Profile 10. BRFZ fault scarp located in R19E, T29N, sec. 11 (Plate 4). Scarp material is composed of clays and silts. Profile shows 1 faulting event with a 1.5 meters vertical displacment. A graben trough has developed at the toe of the scarp.

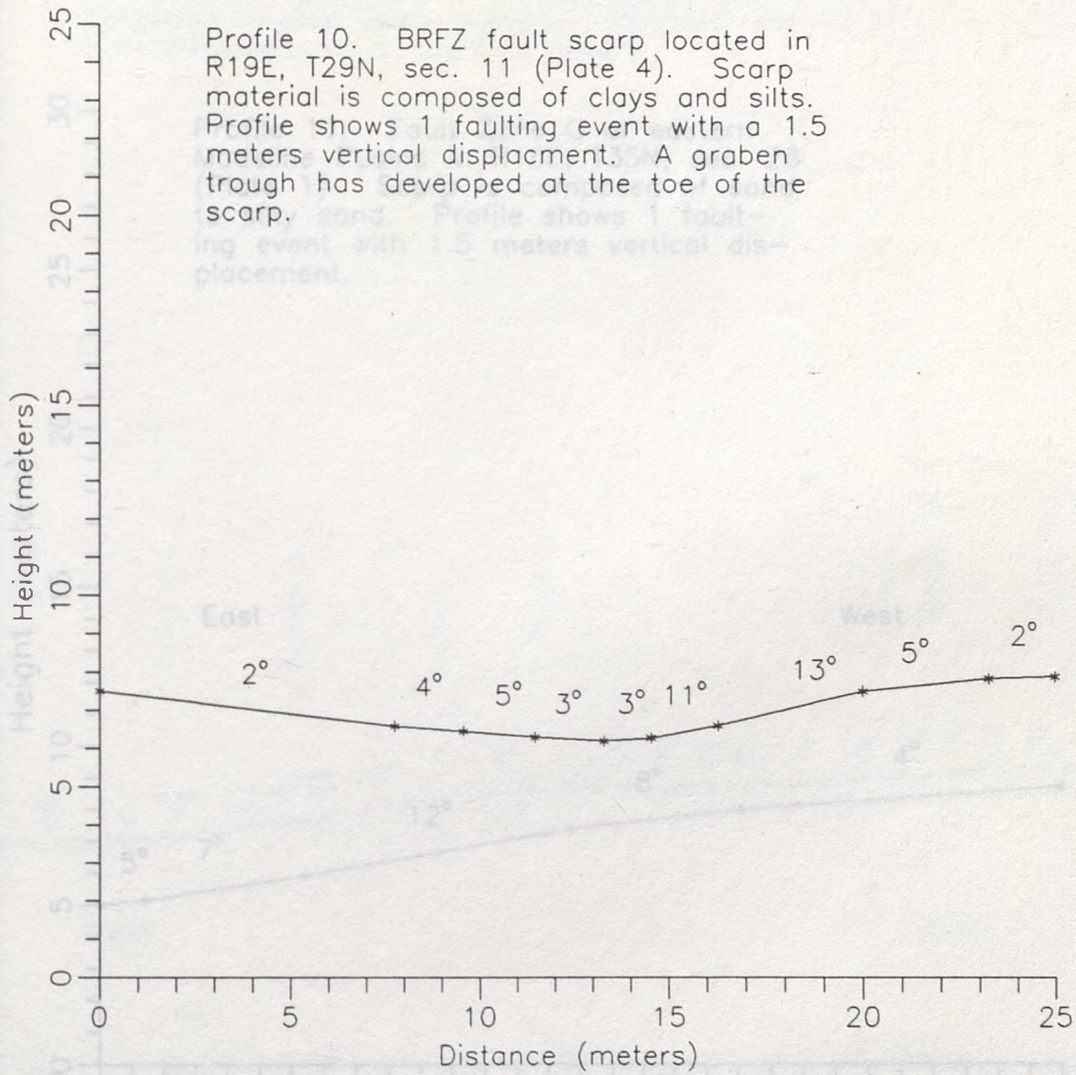

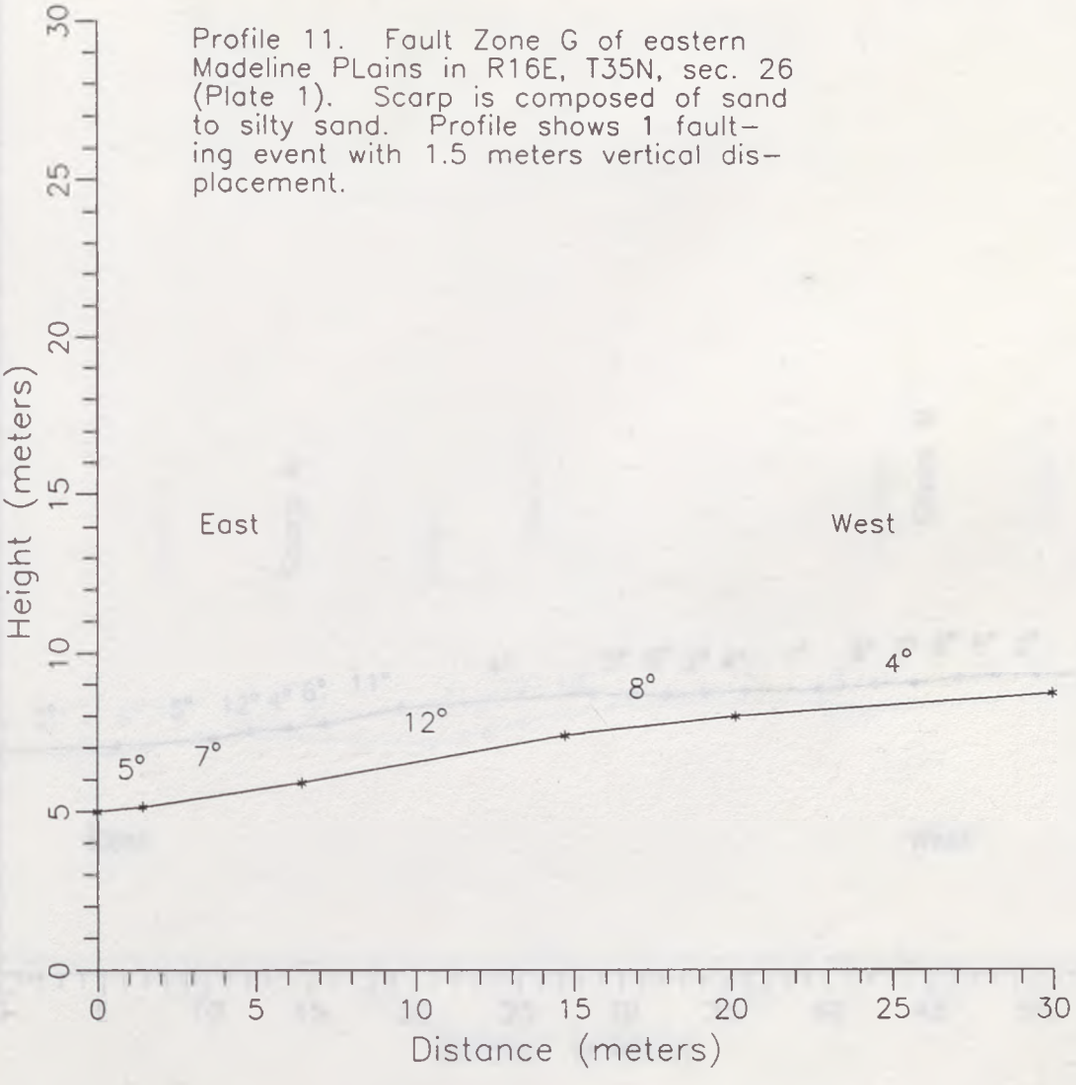

Profile 11. Fault Zone G of eastern Madeline PLains in R16E, T35N, sec. 26 (Plate 1). Scarp is composed of sand to silty sand. Profile shows 1 faulting event with 1.5 meters vertical displacement.

Profile 12. BRFZ fault scarp located in R19E, T28N, sec.13 (Plate 5). Scarp is composed of silty sand sandy silt. Profile shows 2 fault scarps and a backtilted original upper surface. Minimum vertical displacement is about 3 meters.

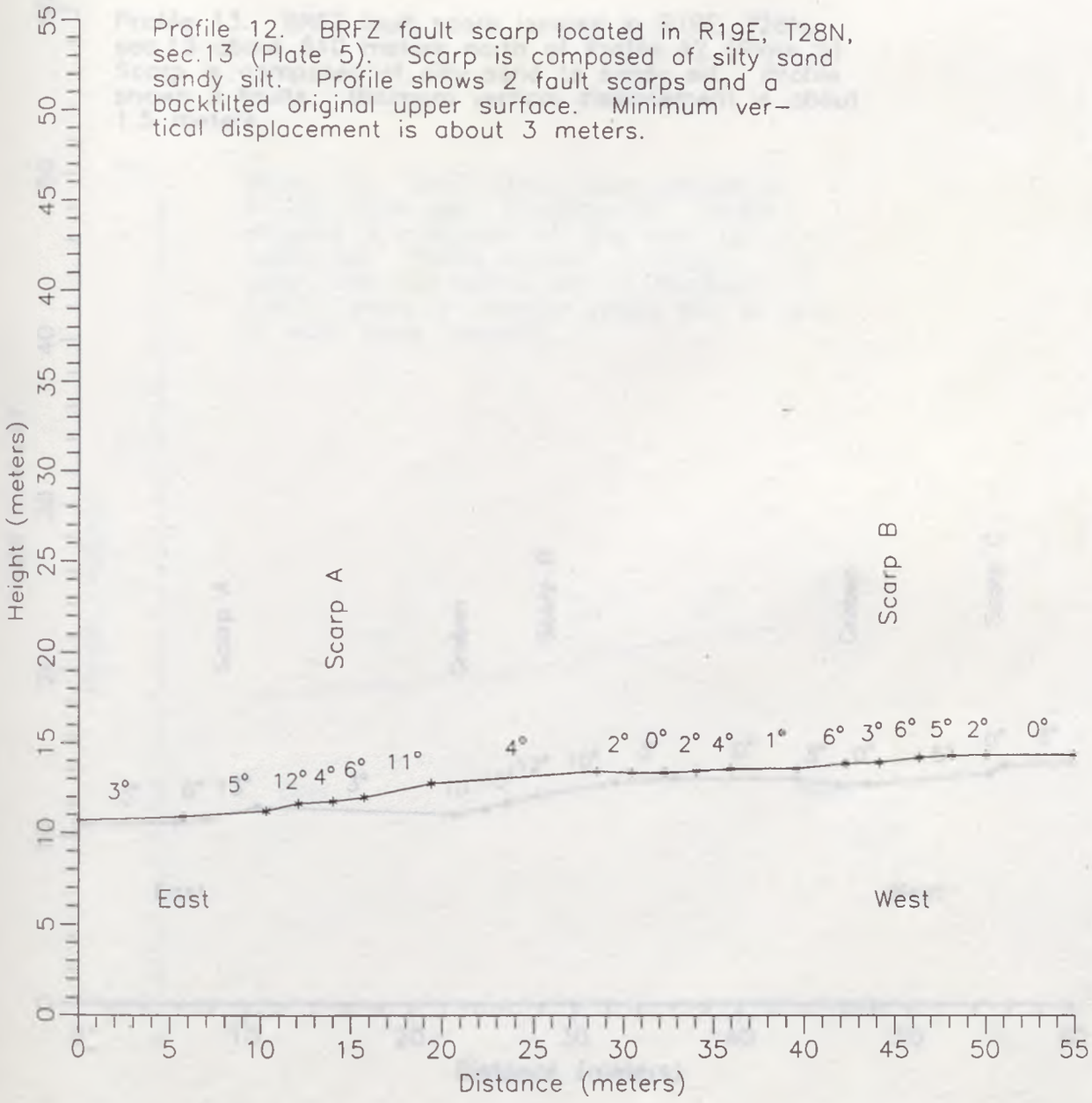

Profile 13. BRFZ fault scarp located in R19E, T28N, sec.13 about 610 meters north of Profile 12 (Plate 5). Scarp is composed of silty sand to sandy silt. Profile shows 3 faults. Minimum vertical displacement is about 1.5 meters.

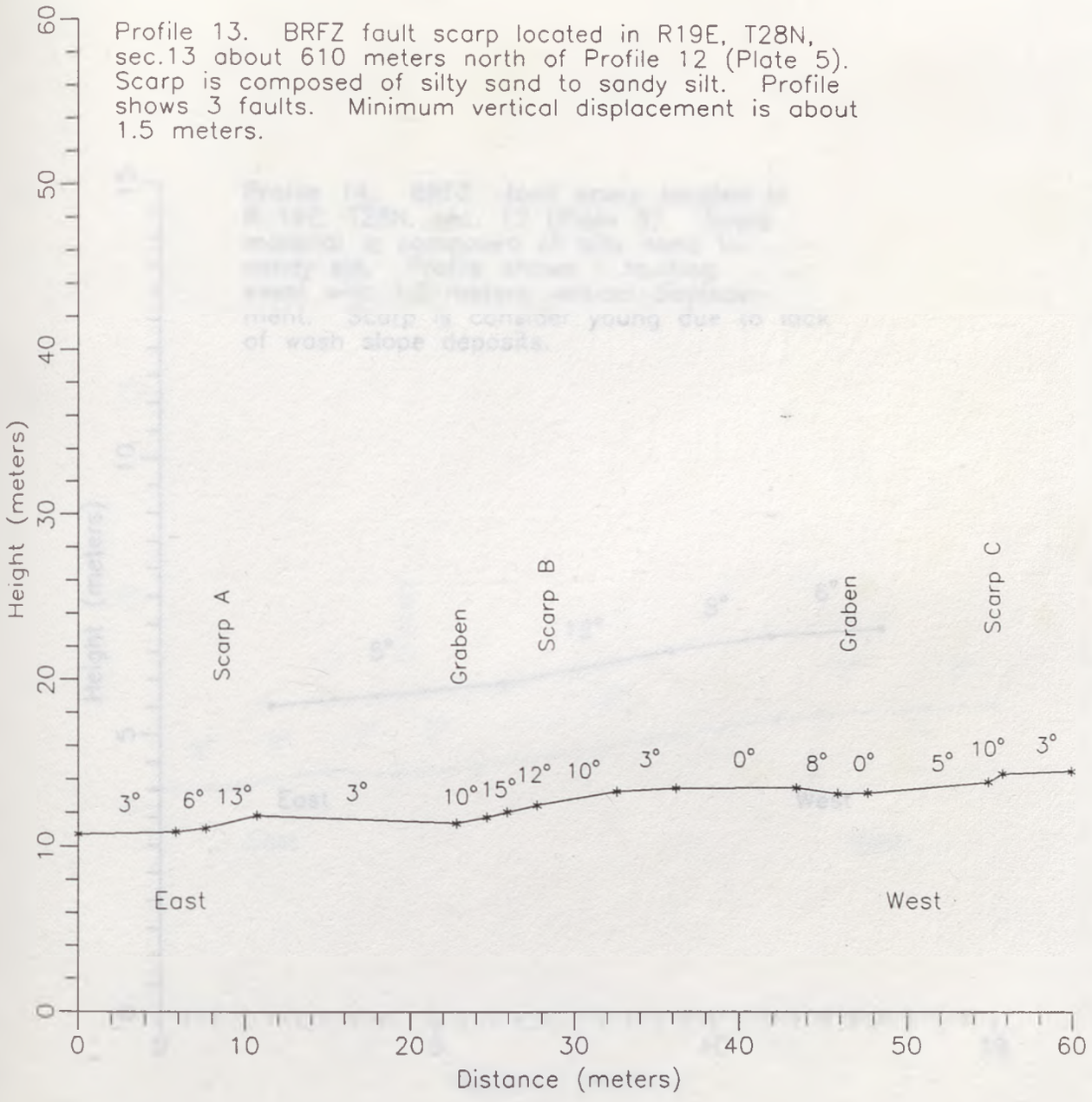

Profile 14. BRFZ fault scarp located in R 19E, T28N, sec. 12 (Plate 5). Scarp material is composed of silty sand to sandy silt. Profile shows 1 faulting event with 1.2 meters vertical displacement. Scarp is consider young due to lack of wash slope deposits.

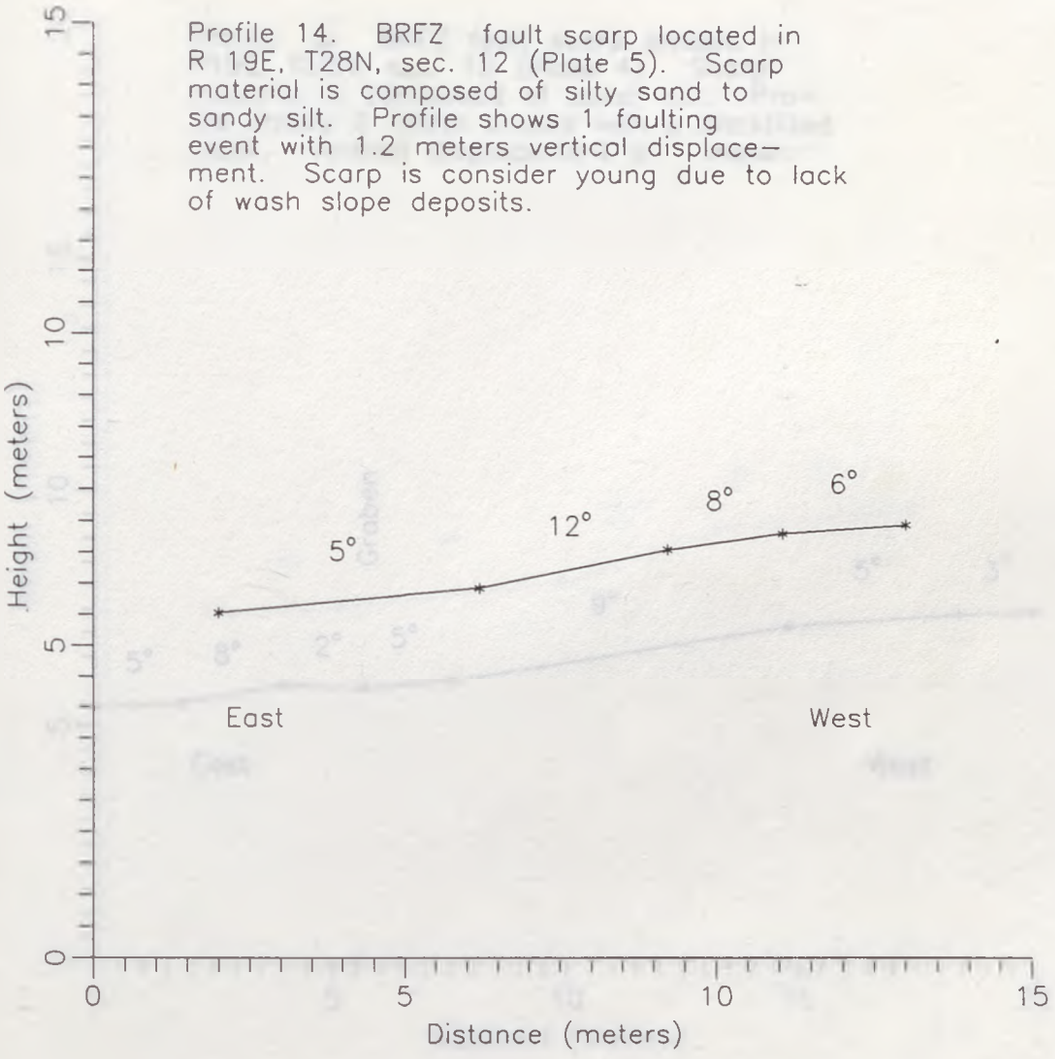

Profile 15. BRFZ fault scarp located in R19E, T30N, sec. 12 (Plate 4). Scarp material is composed of sandy silt. Profile shows 2 faults breaks with a backtilted block. Vertical displacement is 1 meter.

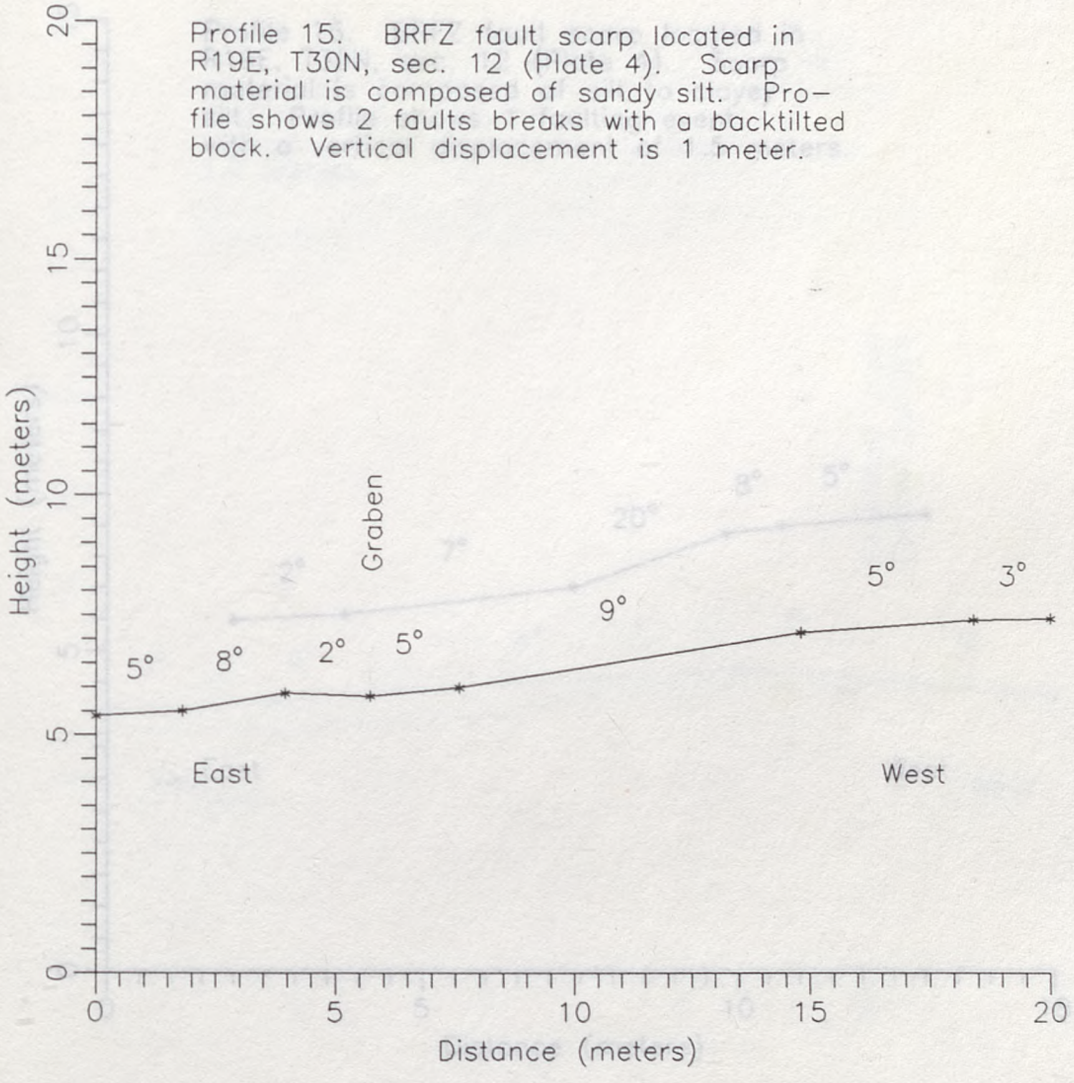

Profile 16. BRFZ fault scarp located in R19E, T30N, sec. 12 (Plate 4). Scarp material is composed of silt to clayey silt. Proflie shows 1 faulting event with a vertical displacement of 1.5 meters.

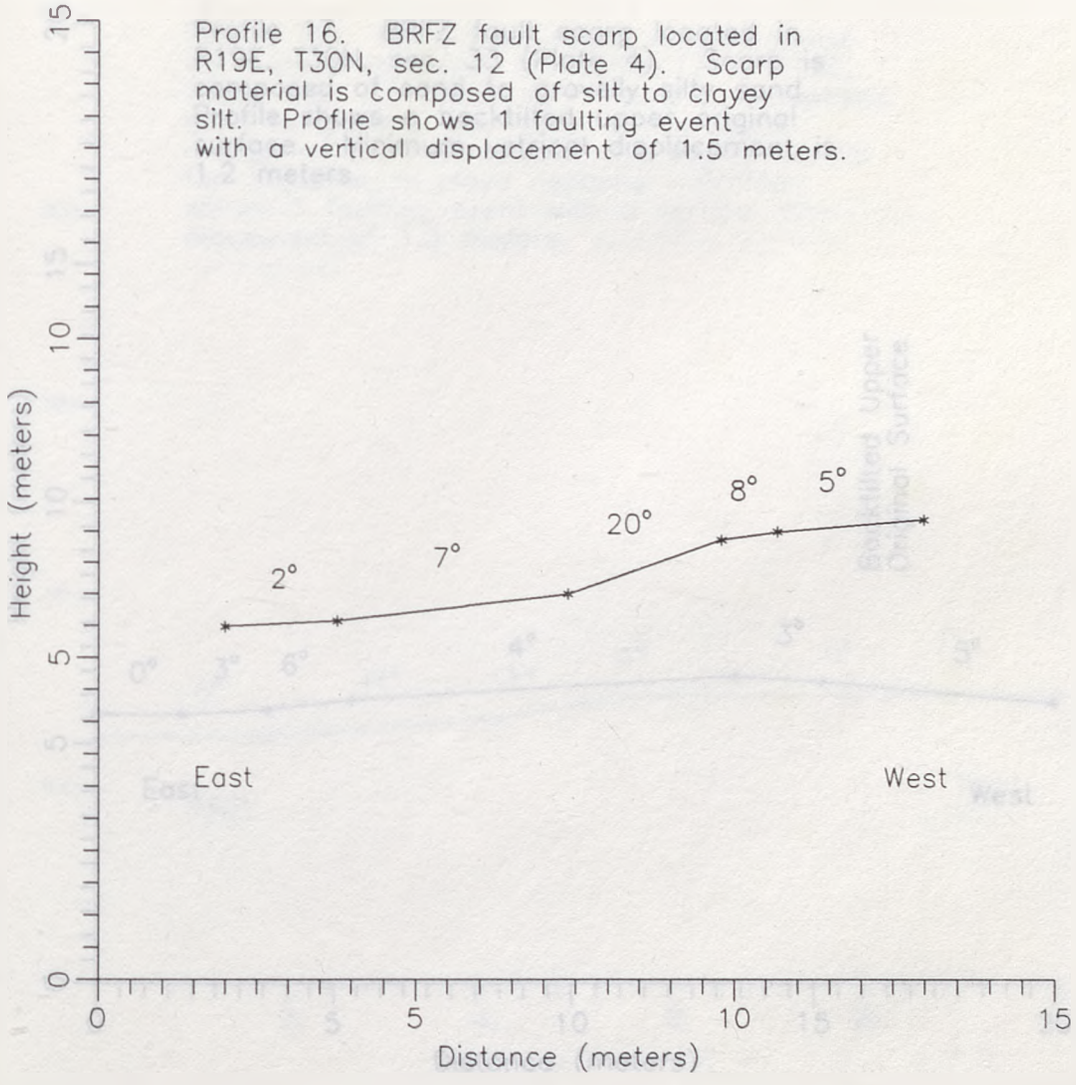

Profile 17. BRFZ fault scarp located in R19E, T30N, sec. 33 (Plate 4). Scarp is composed of sand to gravelly silty sand. Profile shows a backtilted upper original surface. Minimum vetrical displacement is 1.2 meters.

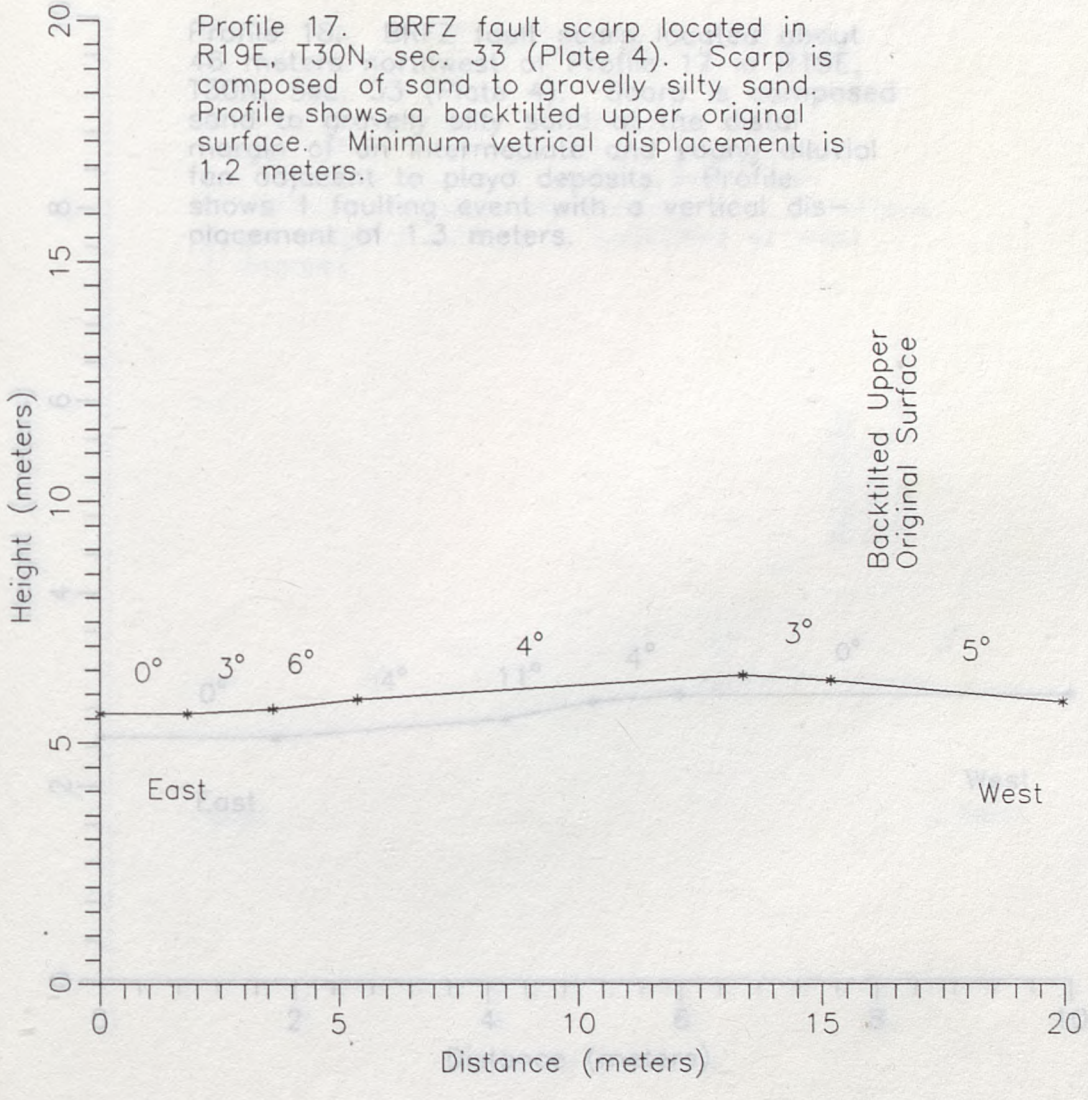

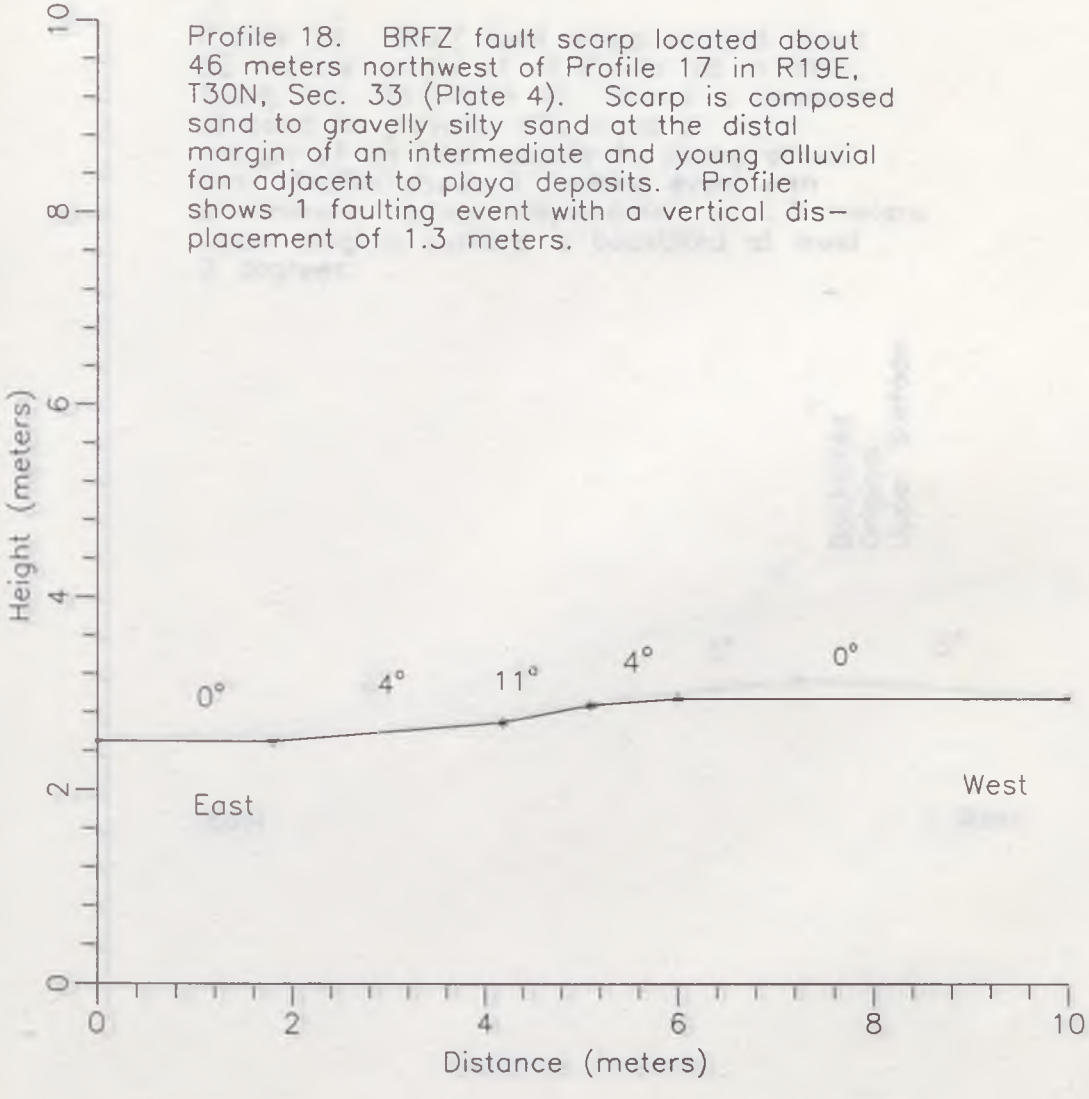

Profile 18. BRFZ fault scarp located about 46 meters northwest of Profile 17 in R19E, T30N, Sec. 33 (Plate 4). Scarp is composed sand to gravelly silty sand at the distal margin of an intermediate and young alluvial fan adjacent to playa deposits. Profile shows 1 faulting event with a vertical dis-placement of 1.3 meters.

Profile 19. BRFZ fault scarp located about 92 meters northwest of Profile 18 in R19E, T30N, sec. 28 (Plate 4). Scarp is composed of sand to gravelly, silty sand at distal margin of an intermediate to young alluvial fan. Profile shows 1 faulting event with a minimum vertical displacement of 1.8 meters. Upper original surface is backtilted at least 3 degrees.

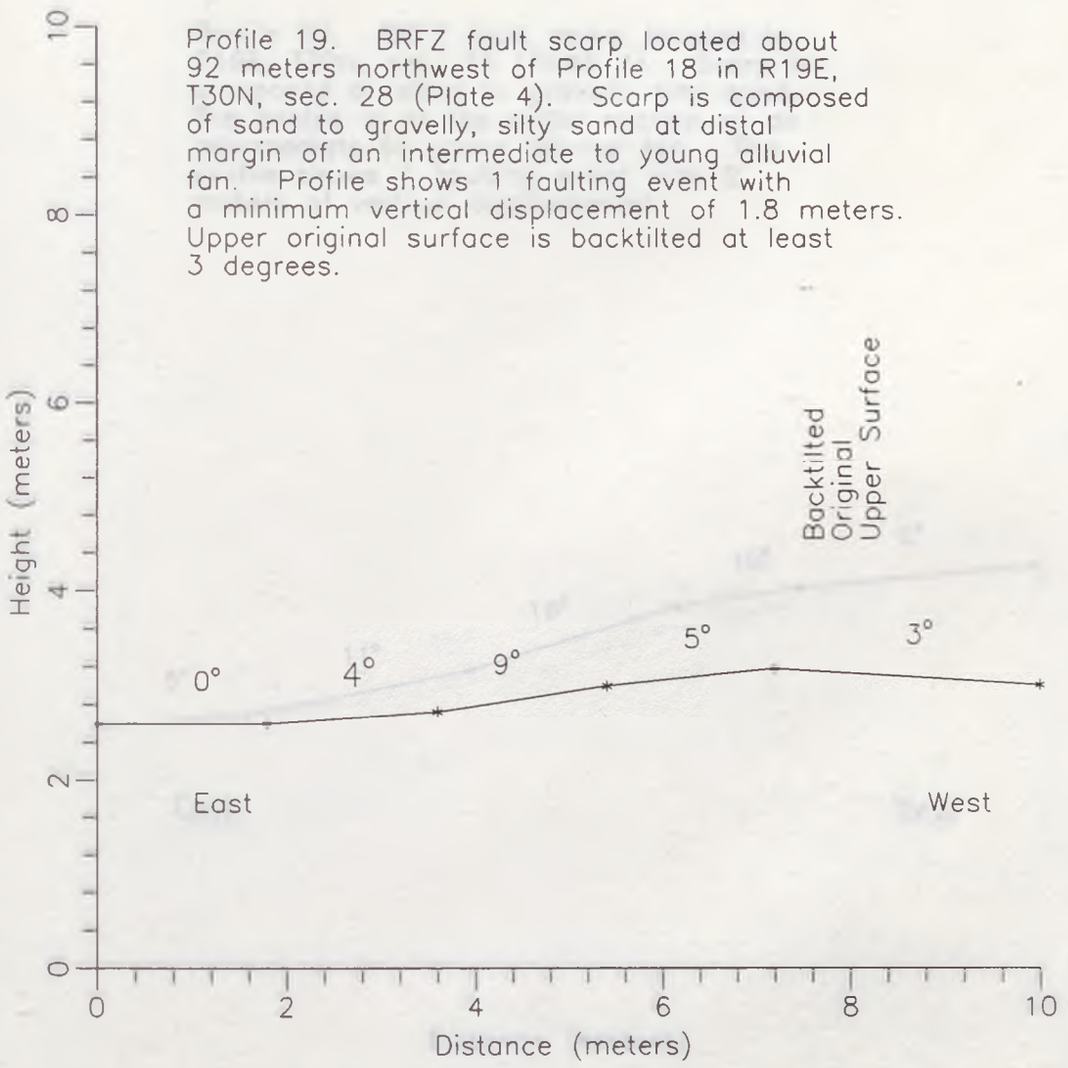

Profile 20. BRFZ fault scarp located in R19E, T30N, sec. 34 (Plate 4). Scarp is composed of sand to gravelly silty sand. The profile is at the distal margin of an intermediate to young alluvial fan. The profile shows 1 faulting event with 2 meters of vertical displacement.

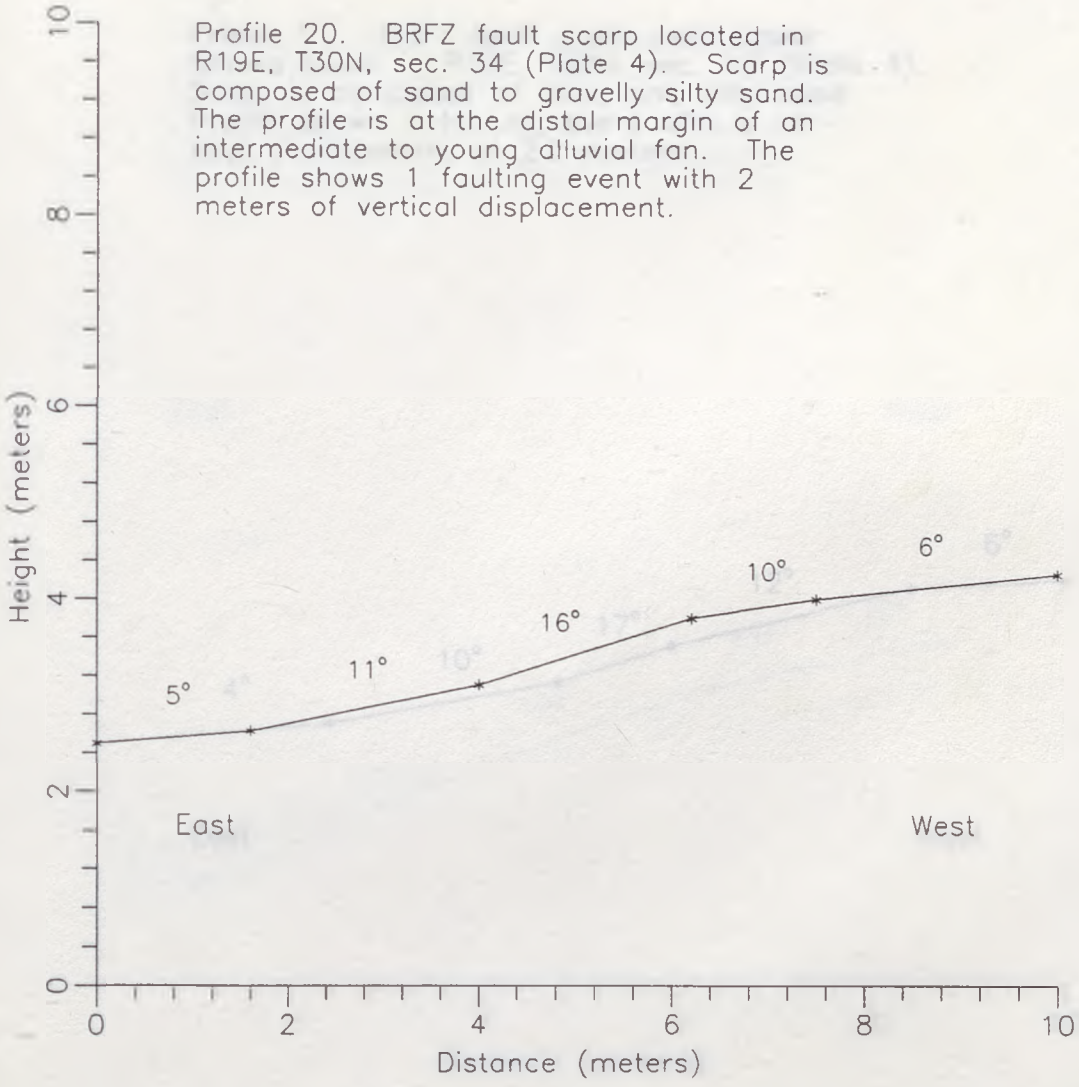

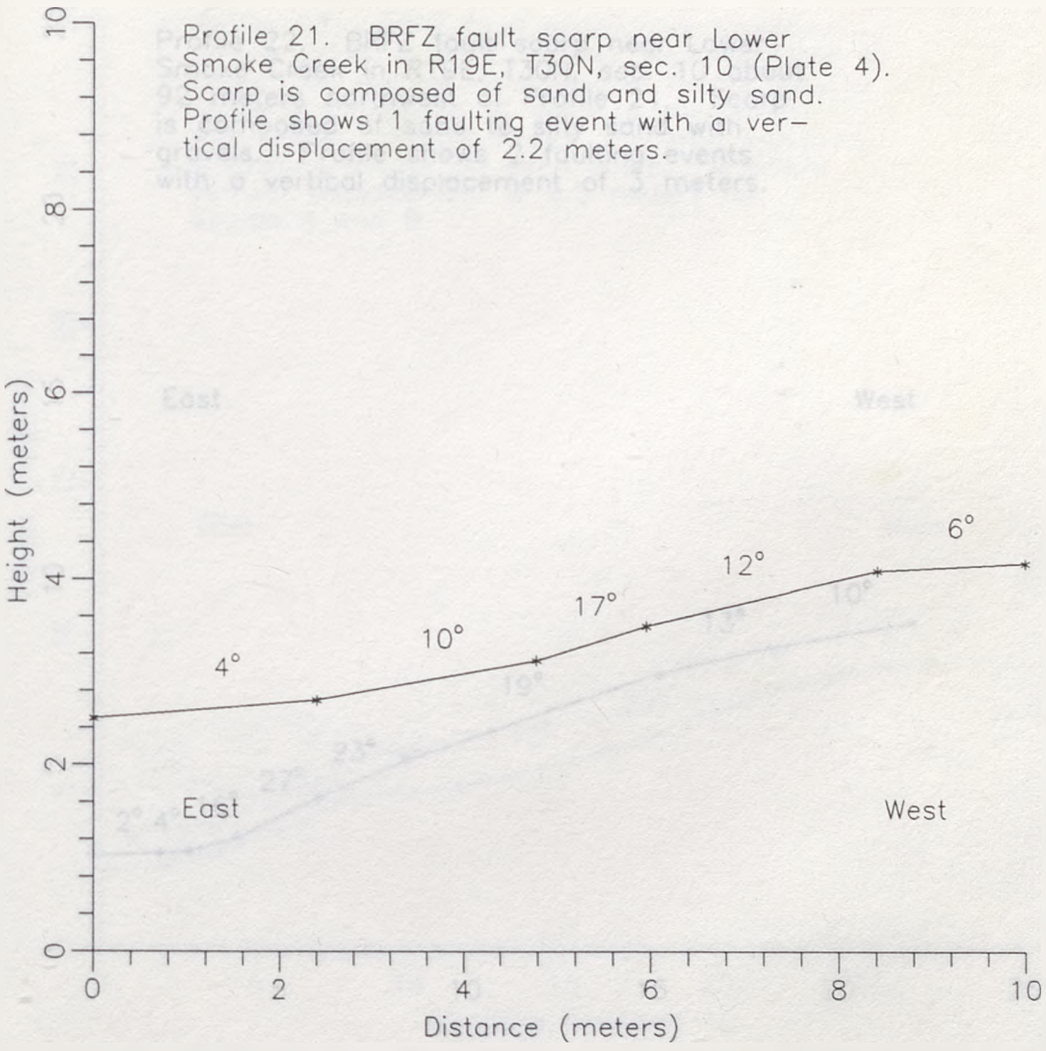

Profile 21. BRFZ fault scarp near Lower Smoke Creek in R19E, T30N, sec. 10 (Plate 4). Scarp is composed of sand and silty sand. Profile shows 1 faulting event with a vertical displacement of 2.2 meters.

Profile 22. BRFZ fault scarp near Lower Smoke Creek in R19E, T30N, sec. 10 about 92 meters northwest of Profile 21. Scarp is composed of sand to silty sand with gravels. Profile shows 2 faulting events with a vertical displacement of 3 meters.

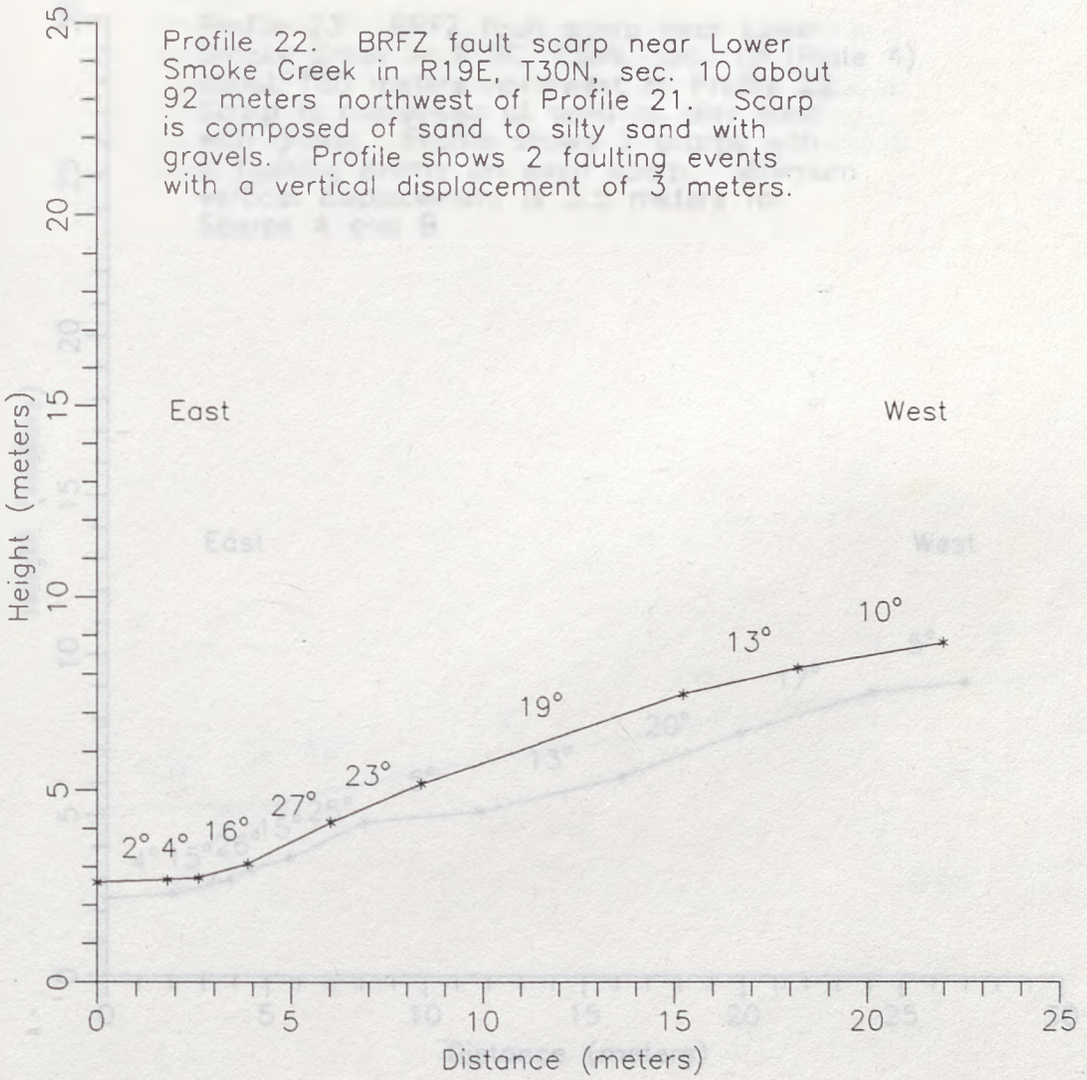

Profile 23. BRFZ fault scarp near Lower Smoke Creek in R19E, T30N, Sec. 10 (Plate 4) about 150 meters northwest of Proflie 22. Scarp is composed of sand to silty sand with gravel. Profile shows 2 scarps with 2 faulting events on each scarp. Minimum vertical displacement is 3.5 meters for Scarps A and B.

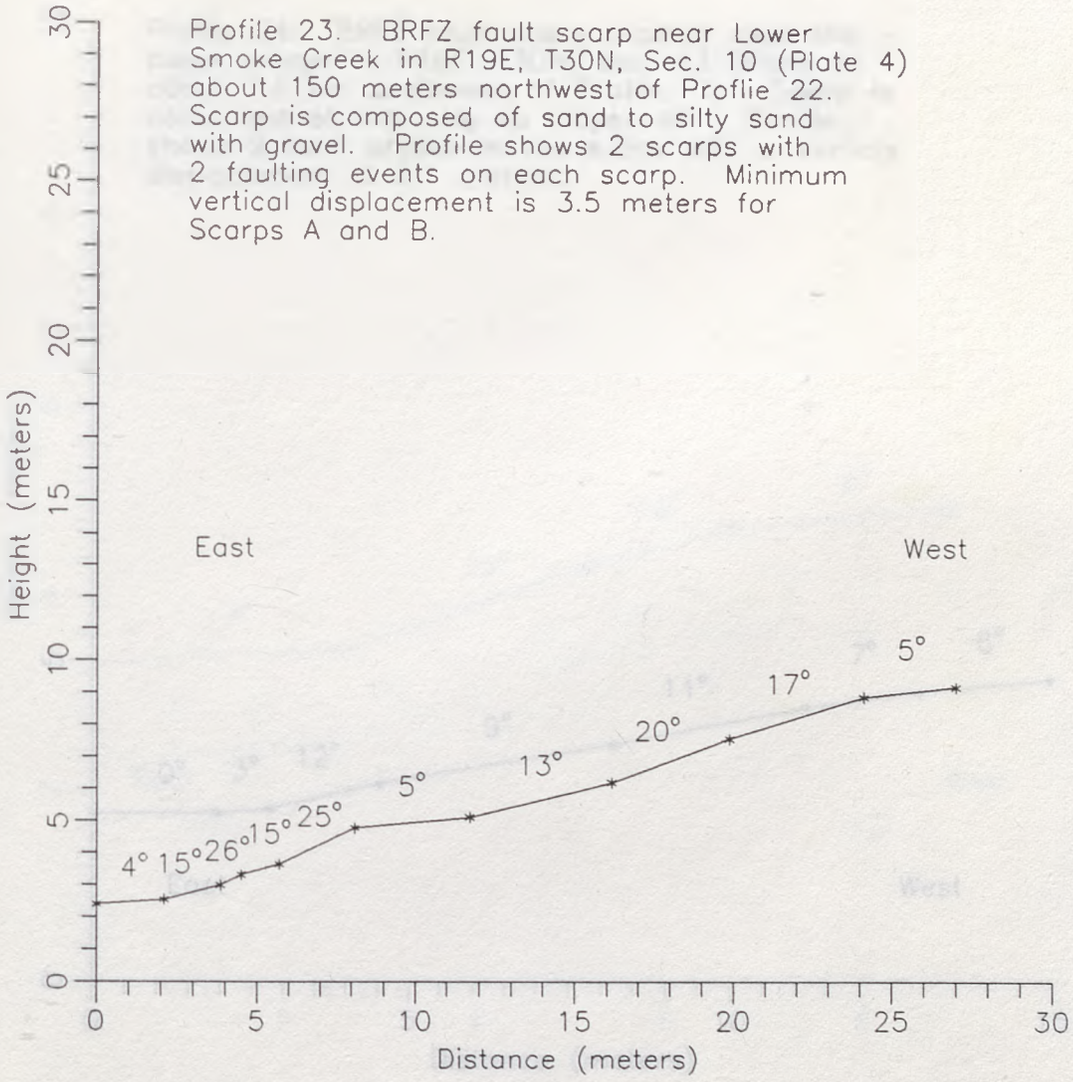

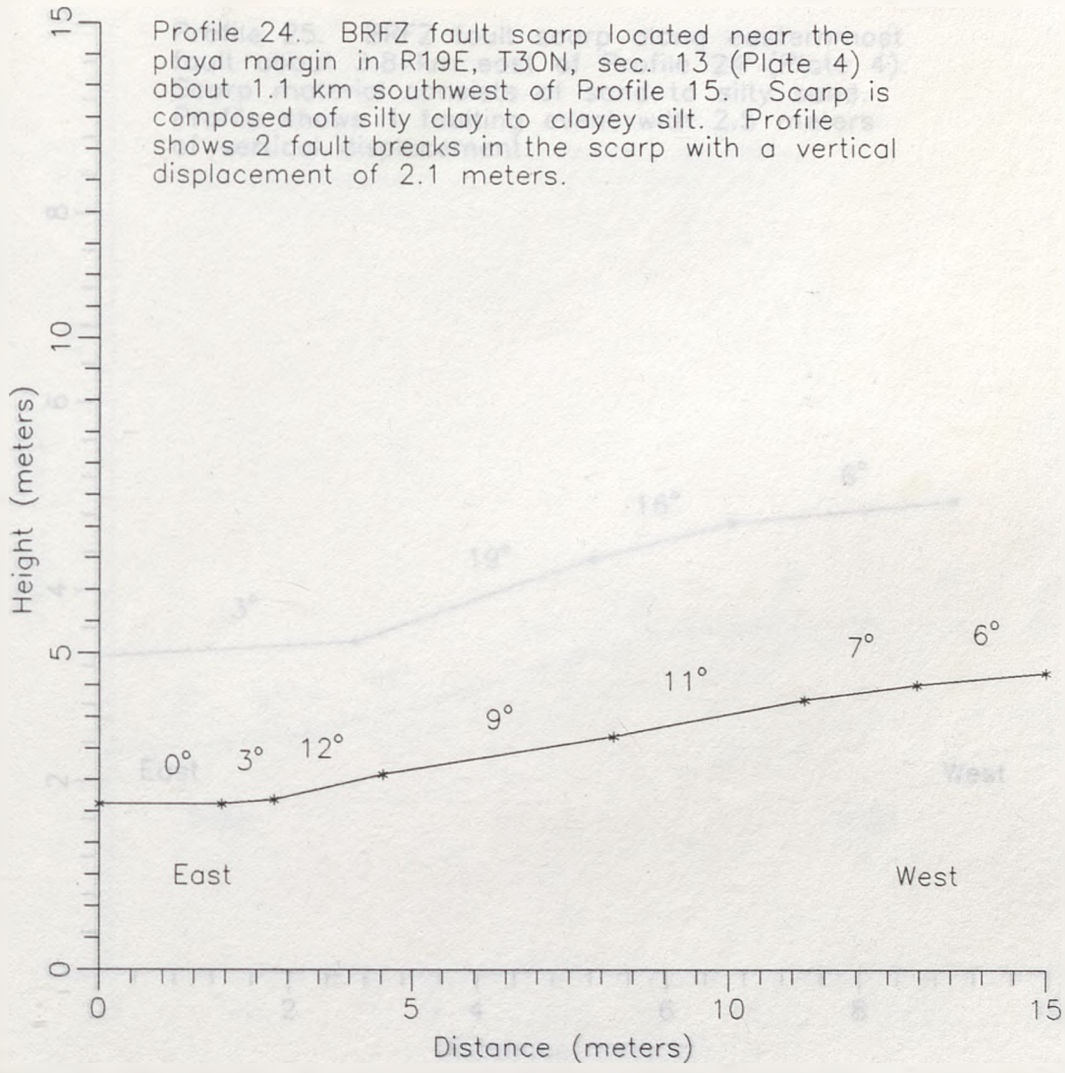

Profile 24. BRFZ fault scarp located near the playa margin in R19E, T30N, sec. 13 (Plate 4) about 1.1 km southwest of Profile 15. Scarp is composed of silty clay to clayey silt. Profile shows 2 fault breaks in the scarp with a vertical displacement of 2.1 meters.

Profile 25. BRFZ fault scarp along easternmost fault about 3.8 km east of Profile 24 (Plate 4). Scarp material consists of sand to silty sand. Profile shows 1 faulting event with 2.5 meters of vertical displacement.

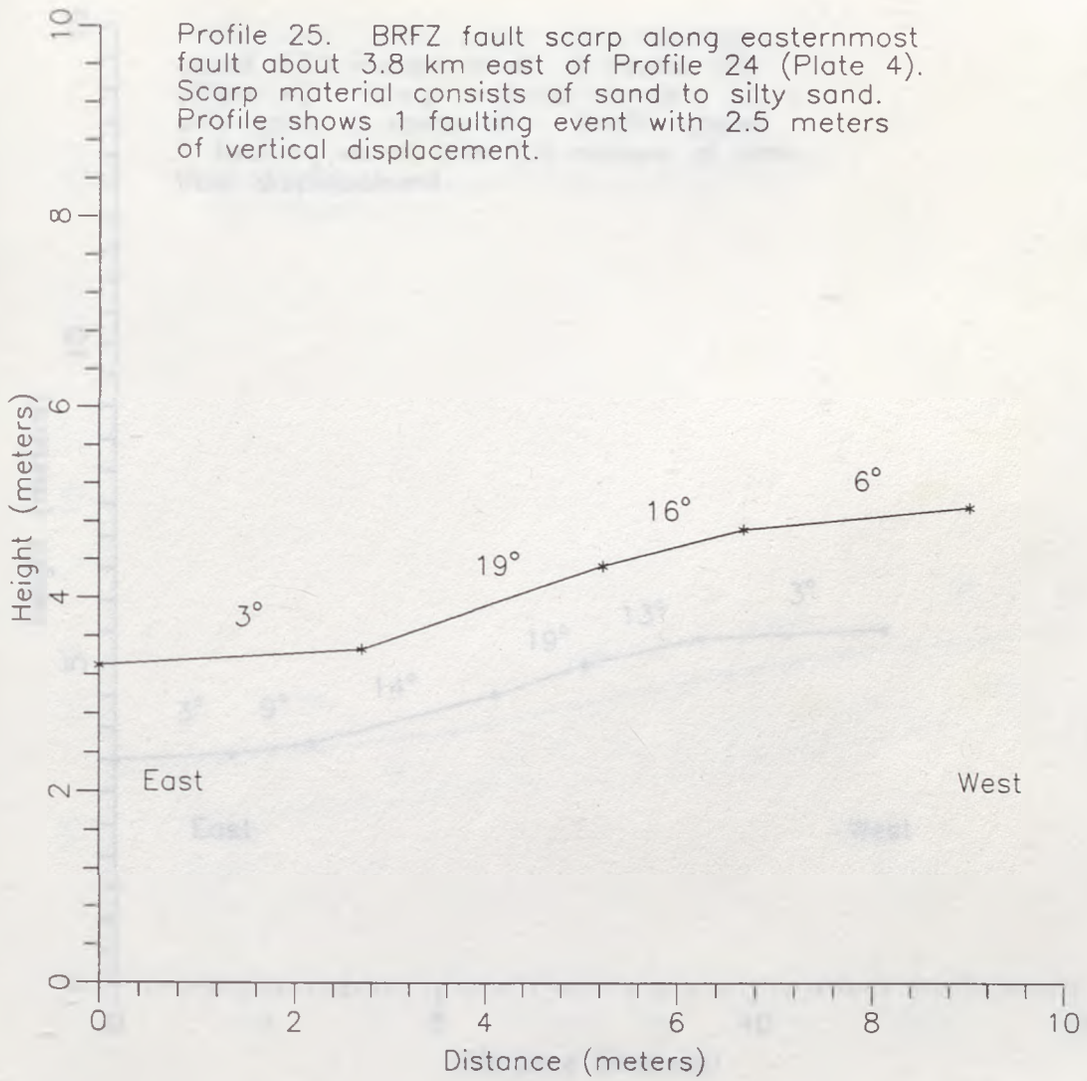

Profile 26. BRFZ fault scarp located about 530 meters north of Profile 25 (Plate 4). Scarp material consists of silty sand to sandy silt. Profile shows 1 faulting event with 2.9 meters of vertical displacement.

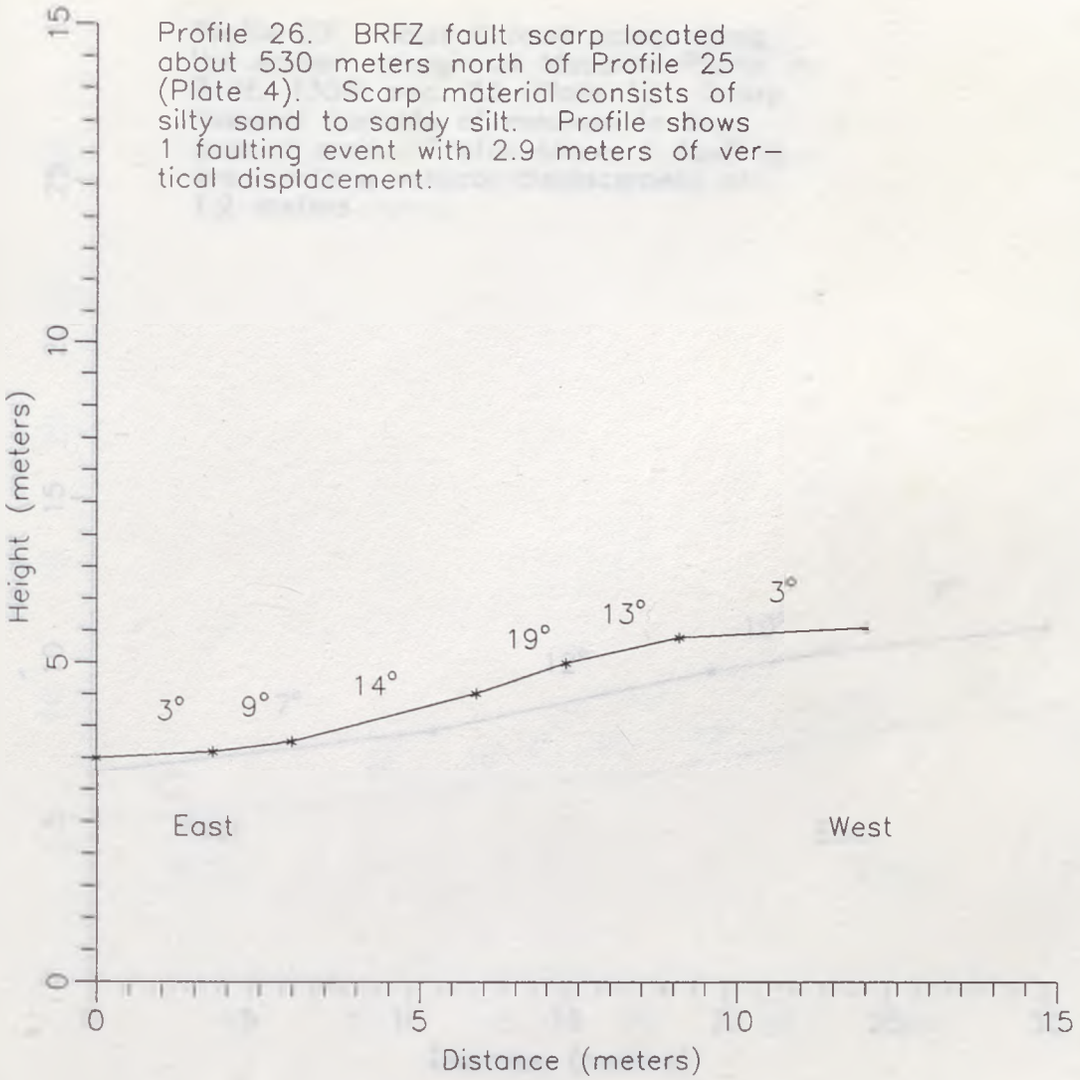

Profile 27. Fault G fault scarp along the eastern margin of Madeline Plains in R16E, T35N, sec. 23 (Plate 1). Scarp material consists of medium to fine grained sand. Profile shows 1 faulting event with a vertical displacement of 1.2 meters.

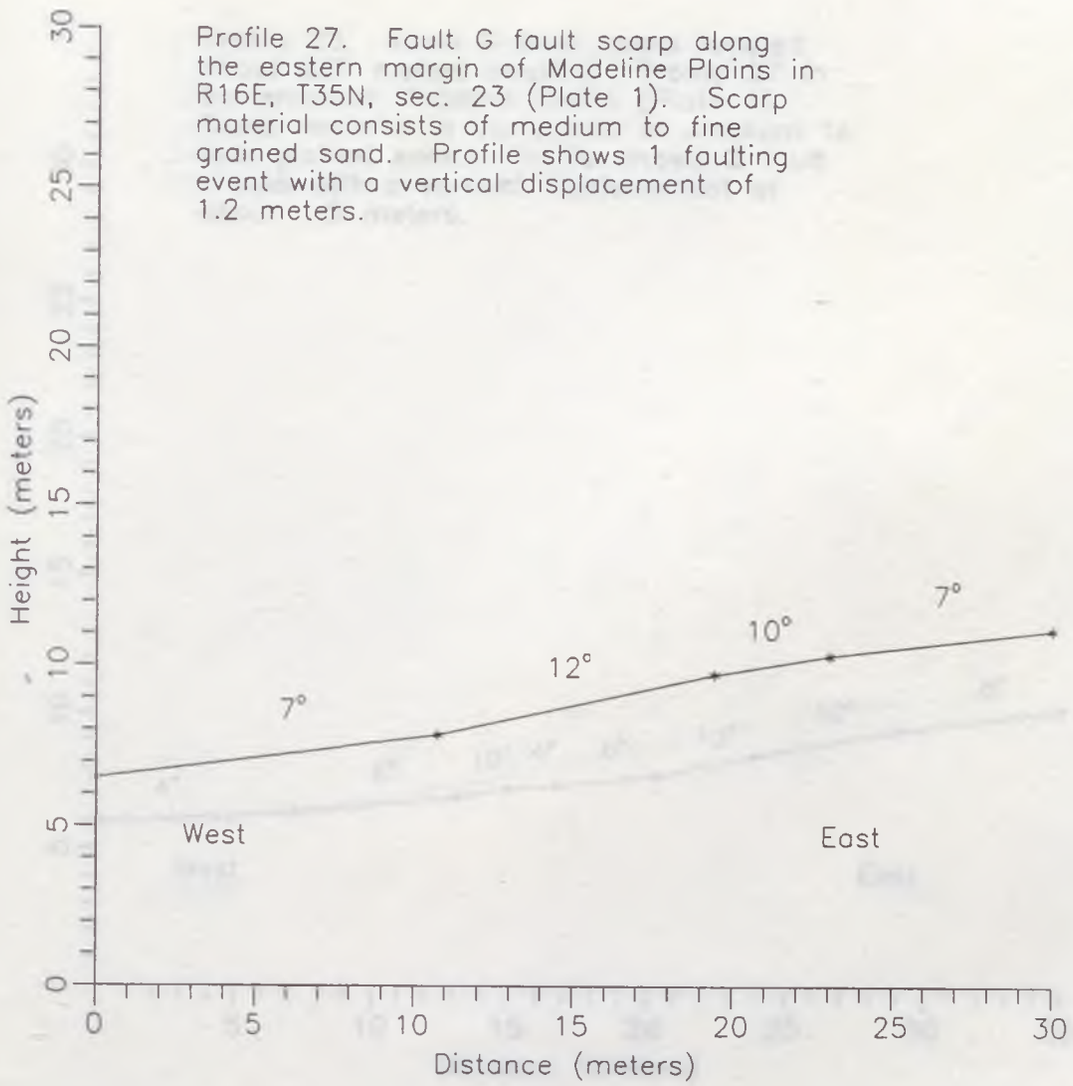

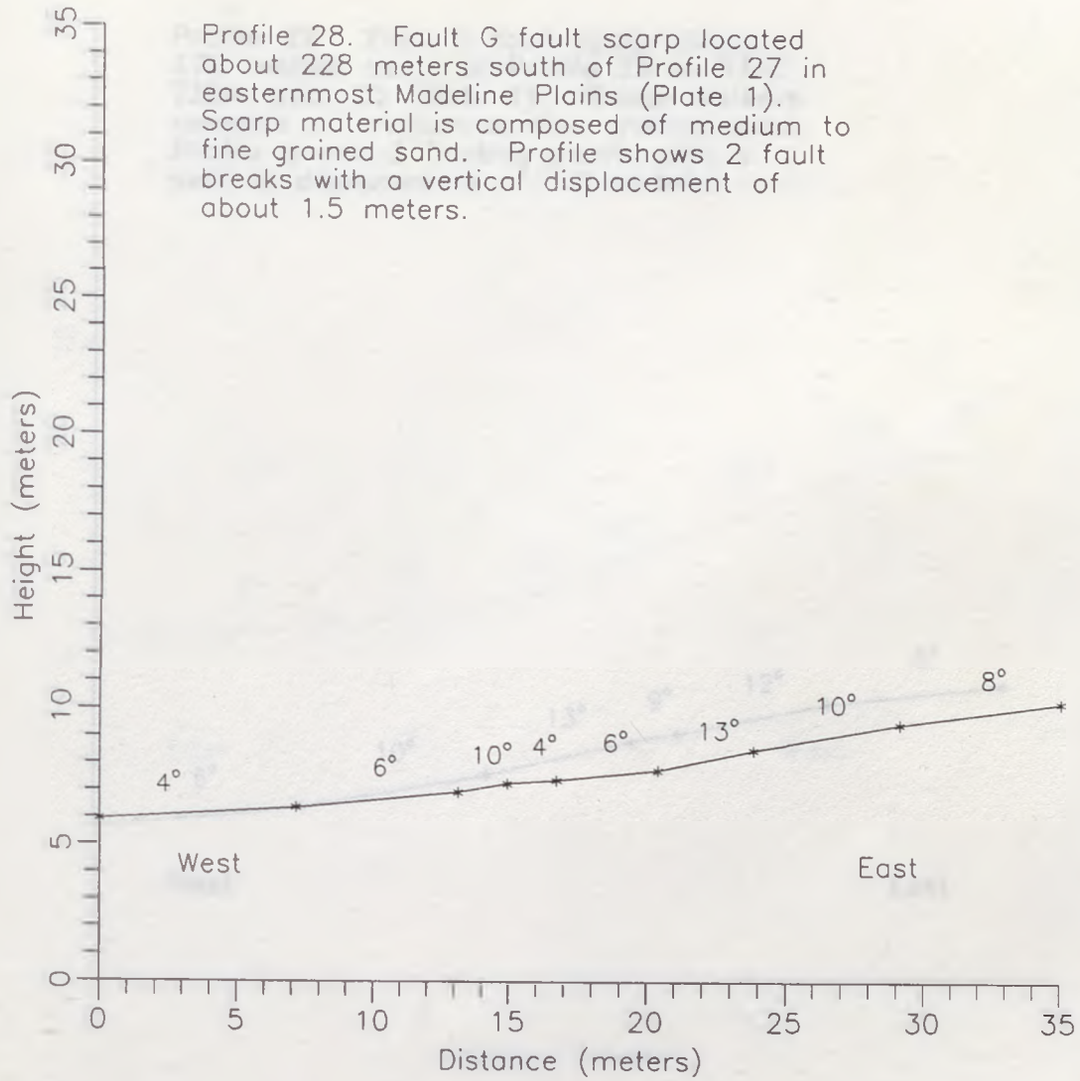

Profile 28. Fault G fault scarp located about 228 meters south of Profile 27 in easternmost Madeline Plains (Plate 1). Scarp material is composed of medium to fine grained sand. Profile shows 2 fault breaks with a vertical displacement of about 1.5 meters.

Profile 29. Fault G fault scarp about 170 meters south of Profile 28 in R16E, T35N, sec. 23 (Plate 1). Scarp material consists of medium to fine grained sand. Profile shows 2 faulting events with a vertical displacement of 1.3 meters.

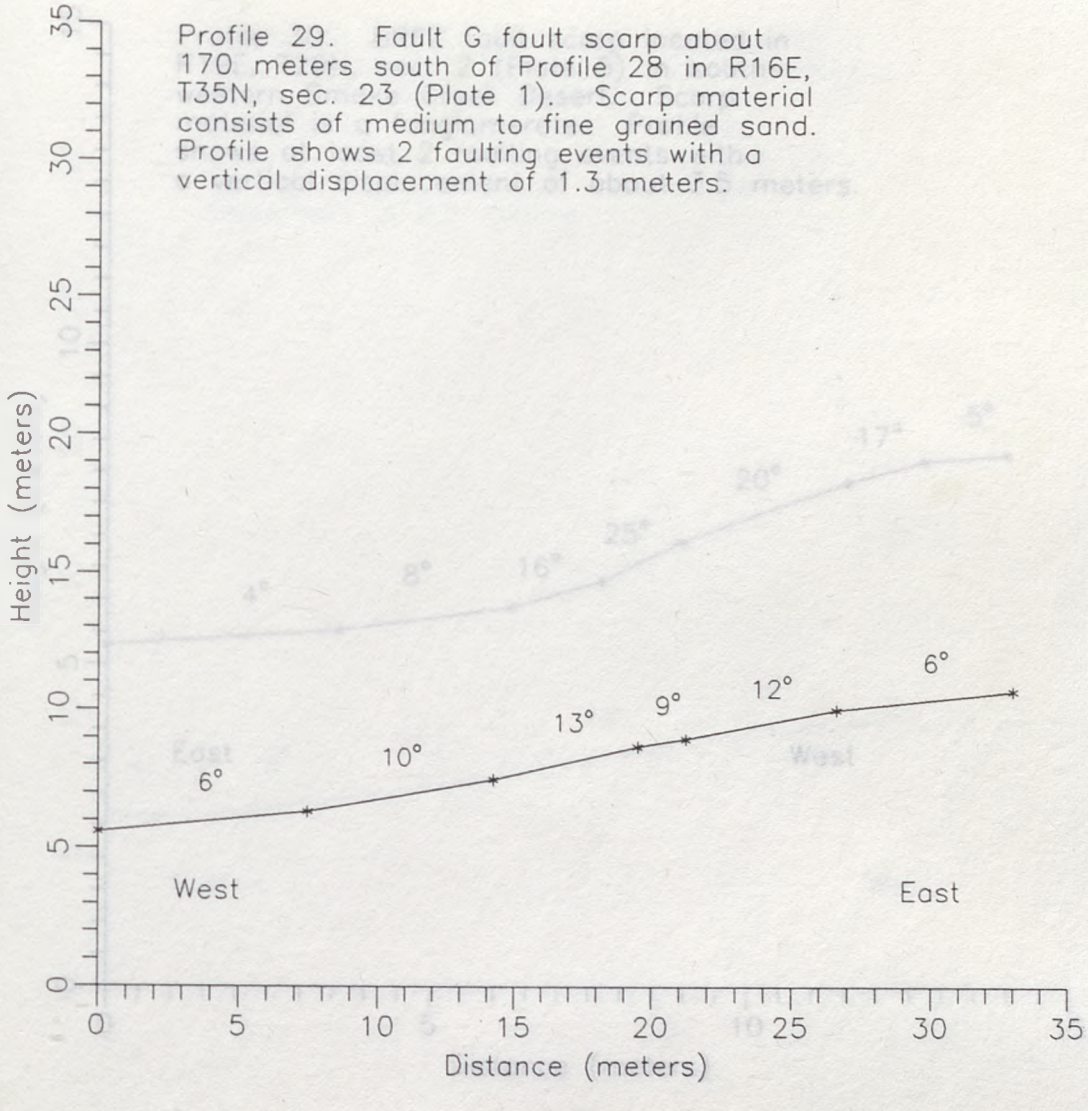

Profile 30. BRFZ fault scarp located in R19E, T29N, sec. 2 (Plate 5) in southwestern Smoke Creek Desert. Scarp material is a fanglomerate. Profile shows at least 2 faulting events with a vertical displacement of about 3.5 meters.

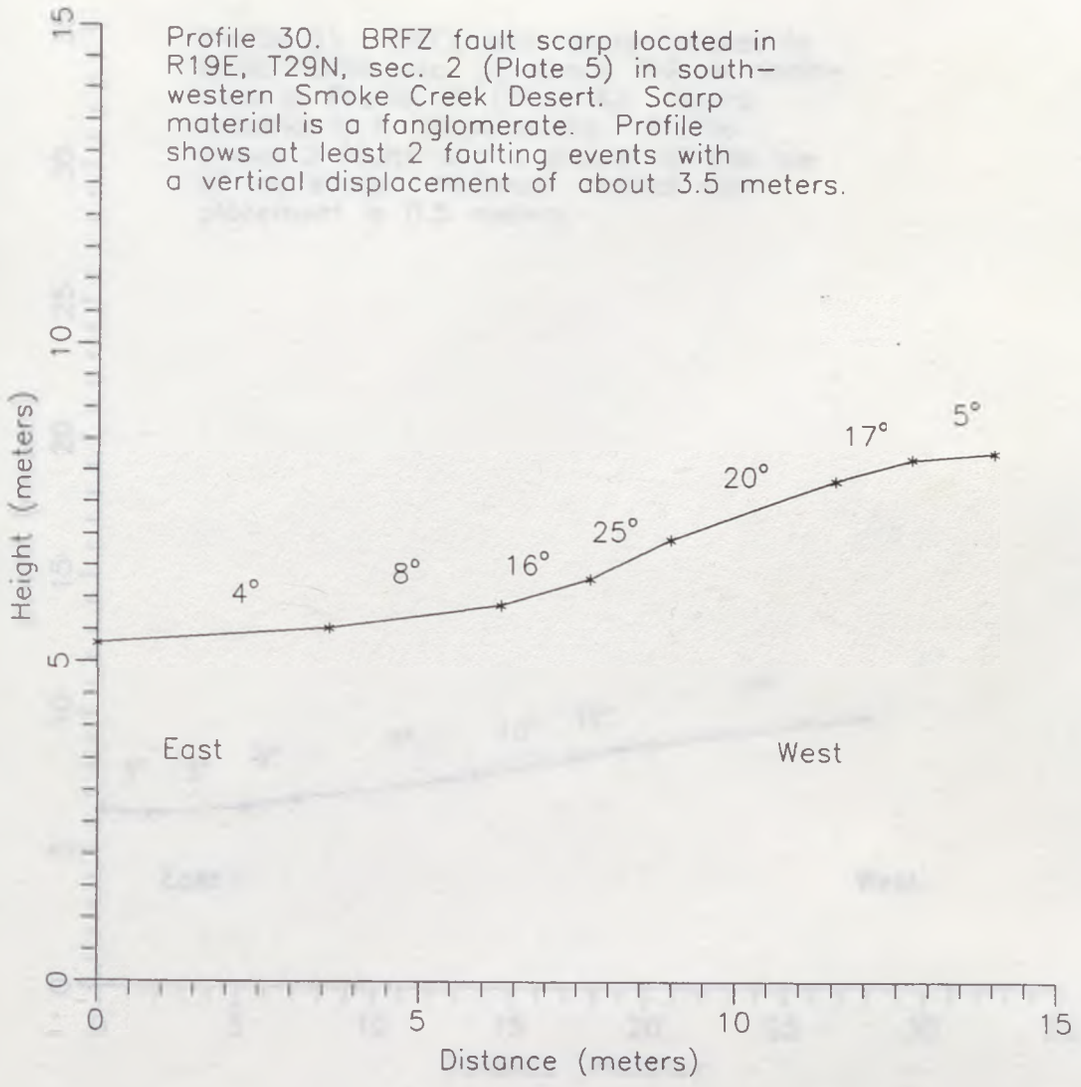

Profile 31. BRFZ fault scarp located in R19E, T30N, sec. 35 about 762 m northwest of Profile 30 (Plate 4). Scarp material is a fanglomerate. Profile shows 2 faults and a graben at the toe of the scarp. Minimum vertical displacement is 0.5 meters.

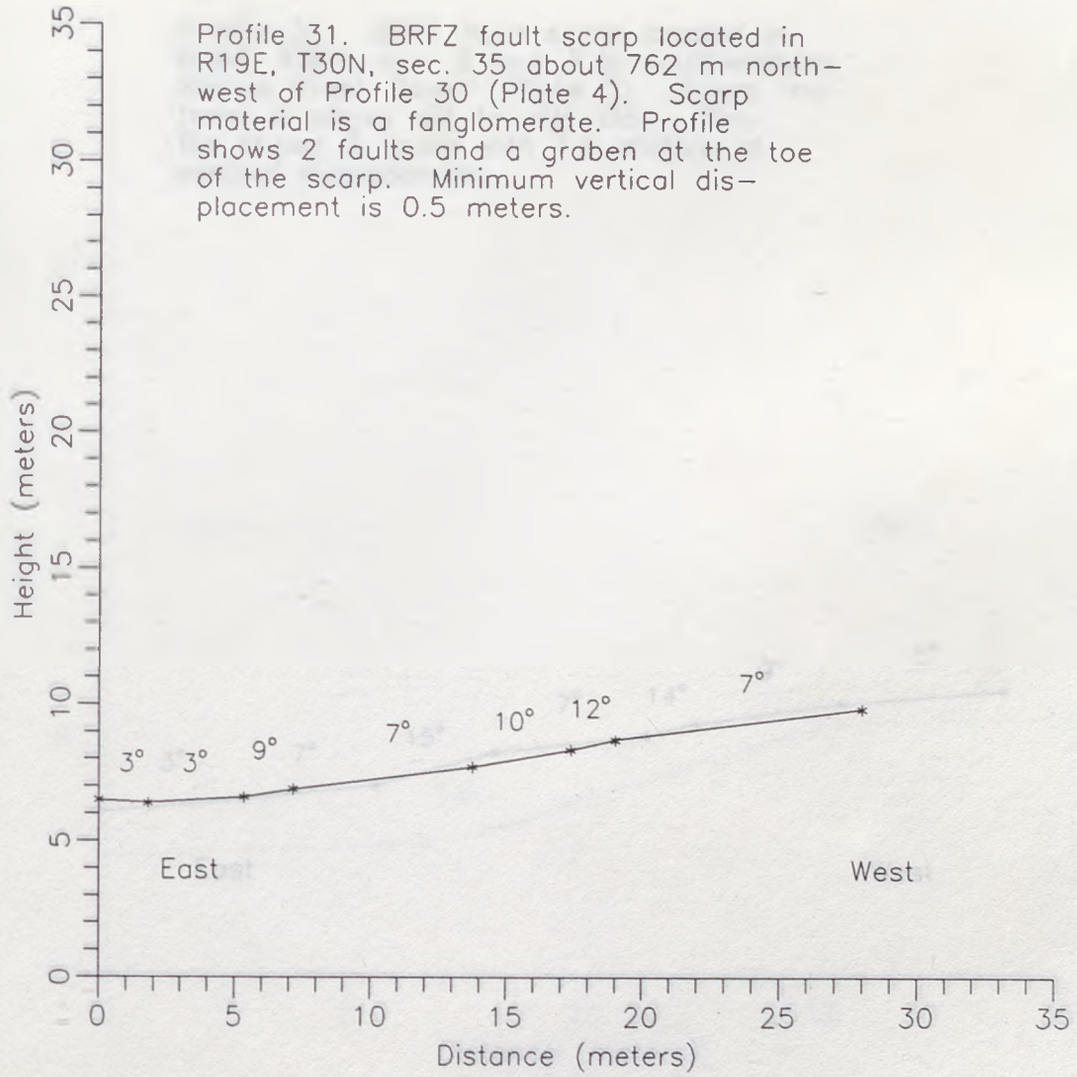

Profile 32. BRFZ fault scarp located in R19E, T30N, sec. 2 and 3 in southwestern Smoke Creek Desert (Plate 3). Scarp material is clayey silt to silty clay. Profile shows 2 faults with 1.6 meters of vertical displacement.

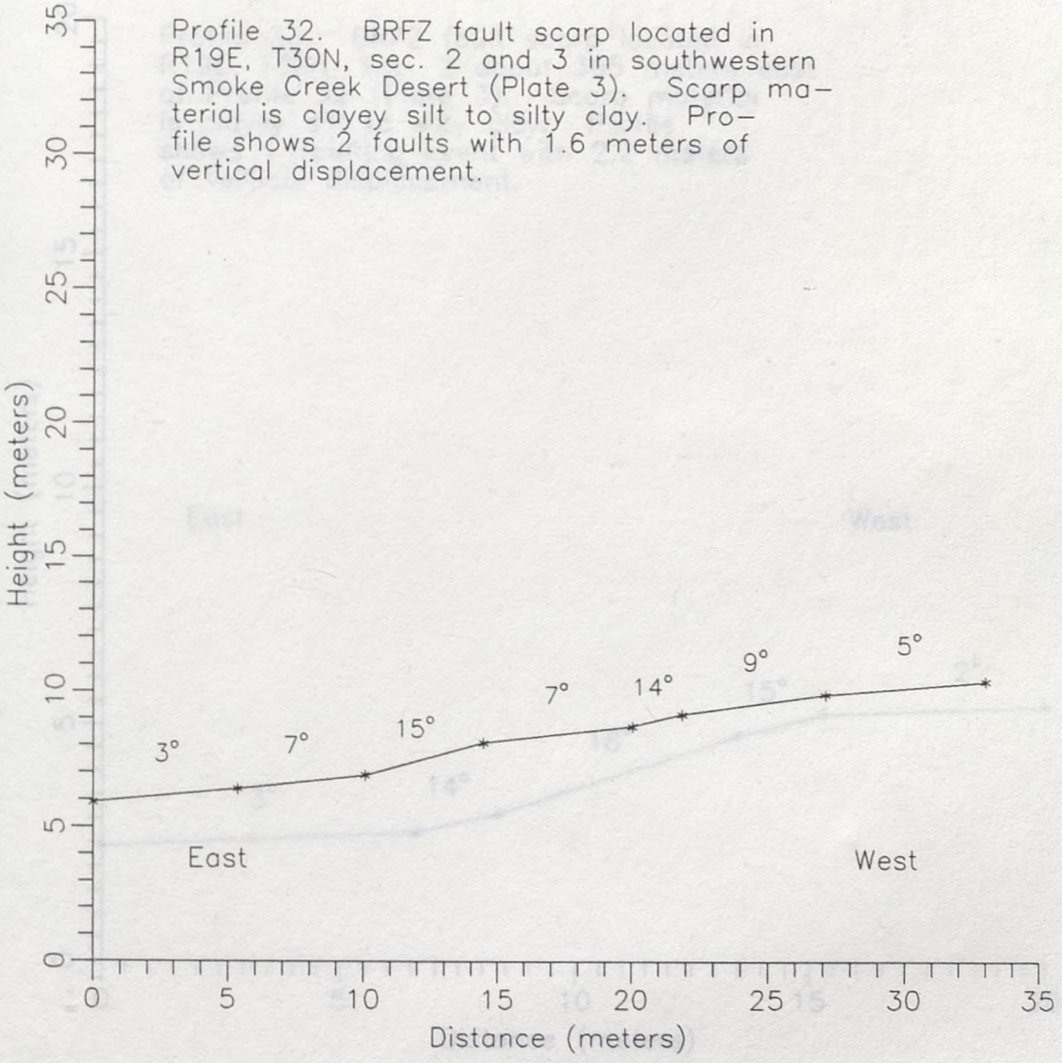

Profile 33. BRFZ fault scarp located in R19E, T30N, Sec. 2 about 365 meters east of Profile 32 (Plate 3). Scarp material is clayey silt to silty clay. Profile shows 1 faulting event with 2.2 meters of vertical displacement.